

**Molecular and Cellular Analysis of the  
“Adenylyl Cyclase” Exotoxins from *Bacillus anthracis* and  
*Bordetella pertussis***

**Dissertation**

zur Erlangung des Doktorgrades der Naturwissenschaften (Dr. rer. nat.)  
der Naturwissenschaftlichen Fakultät IV – Chemie und Pharmazie –  
der Universität Regensburg



vorgelegt von  
**Corinna Spangler**  
aus Osterhofen/Deggendorf  
2010

Die vorliegende Arbeit entstand unter der Leitung von Herrn Prof. Dr. R. Seifert und Herrn Prof. Dr. O. Wolfbeis im Zeitraum von November 2006 bis Januar 2009 am Institut für Analytische Chemie, Chemo- und Biosensorik und am Institut für Pharmakologie und Toxikologie der Naturwissenschaftlichen Fakultät IV – Chemie und Pharmazie – der Universität Regensburg und zwischen Februar 2009 und März 2010 am Institut für Pharmakologie der Medizinischen Hochschule Hannover.

Das Promotionsgesuch wurde eingereicht am 07. April 2010.

Das Kolloquium findet am 11. Juni 2010 statt.

Prüfungsausschuss:

|                            |                  |
|----------------------------|------------------|
| Prof. Dr. Armin Buschauer  | (Vorsitzender)   |
| Prof. Dr. Roland Seifert   | (Erstgutachter)  |
| Prof. Dr. Otto Wolfbeis    | (Zweitgutachter) |
| Prof. Dr. Jens Schlossmann | (Drittprüfer)    |

Krise ist ein produktiver Zustand.  
Man muss ihr nur den Beigeschmack  
der Katastrophe nehmen.

Max Frisch

## **Danksagung**

Zum Gelingen dieser Arbeit haben viele Menschen beigetragen durch wertvolle Ratschläge, wissenschaftliche Diskussionen, tatkräftige Unterstützung und einer gehörigen Portion Geduld.

Ein besonderer Dank gilt Herrn Prof. Roland Seifert für seinen unerschütterlichen Optimismus, die wissenschaftlichen Diskussionen und Anregungen und das Vertrauen, das er in mich gesetzt hat. Herr Seifert, Sie waren immer in der Lage, mich zu motivieren, und haben mir zahlreiche Möglichkeiten eröffnet.

Außerdem gilt mein Dank Herrn Prof. Otto Wolfbeis und Herrn Dr. Michael Schäferling für die wissenschaftlichen Diskussionen und die tatkräftige Unterstützung in Sachen Fluoreszenzanalytik. Ich habe an Ihrem Lehrstuhl viel lernen dürfen!

Edeltraud Schmid und Annette Stanke danke ich für die Unterstützung in allen Lebenslagen, v.a. beim Umzug von Regensburg nach Hannover und den damit verbundenen Schwierigkeiten.

Weiterhin möchte ich Herrn Prof. Volkhard Kaefer dafür danken, dass er mich an den Massenspektrometern hat arbeiten lassen. Ich habe Deinen Input und die Diskussionen mit Dir sehr genossen. Annette Garbe, Heike Burhenne, Kerstin Beste, und Ina Hackbarth gebührt mein aufrichtiges Dankeschön für die Einführung und praktische Unterweisung am MS und ihre Geduld mit mir, wenn ich Fragen zu oder Probleme mit den Geräten hatte.

Dr. Sabine Wolter und Dr. Detlef Neumann möchte ich für die Einweisung und Unterstützung im Primerdesign danken, Herrn Oliver Dittrich-Breiholz für die Durchführung der Microarrays.

Juliane von der Ohe hat mir tatkräftig zur Seite gestanden, mir die Tücken und Tricks der Zellkultur näher gebracht und mir gezeigt, wie RNA- und DNA-Präparationen durchgeführt werden. Durch die Unterstützung bei der Real-Time PCR hast Du mir außerdem sehr geholfen. Vielen Dank dafür!

Herrn Prof. Frieder Kees gilt mein Dank für die Einführung in die Enzymreinigung und die Erläuterungen und Diskussion in der praktischen Durchführung.

Weiterhin danke ich Dr. Daniel Ladant von der Unité de Biochimie des Interactions Macromoléculaires am Institut Pasteur, Paris und Dr. Wei-Jen Tang vom Ben-May Institute for Cancer Research der University of Chicago für die Bereitstellung von Enzymen und Plasmiden sowie für die wissenschaftliche Kooperation und die anregenden Diskussionen.

Doris Burger, Melanie Hübner, Heike Mader, Elisabeth Schinner, Rebecca Scholz, Mark-Steven Steiner, Katrin Uhlmann und Ulrike Voigt möchte ich für die netten

Kaffeerunden, Spieleabende und außerdienstlichen Aktivitäten danken, die den Laboralltag aufgefrischt und mir wieder Mut und Motivation für neue Herausforderungen gegeben haben.

Allen Mitarbeitern und Kollegen des Instituts für Analytische Chemie, Chemo- und Biosensorik und des Instituts für Pharmakologie und Toxikologie der Universität Regensburg sowie des Instituts für Pharmakologie der Medizinischen Hochschule Hannover möchte ich für die angenehme Arbeitsatmosphäre, die tatkräftige Hilfe, wo sie nötig war, und die für alle Probleme offenen Ohren danken. Ich wurde an allen Instituten nett aufgenommen und habe dort gerne gearbeitet. Herzlichen Dank an alle!

Ein weiterer Dank geht an die Deutsche Forschungsgemeinschaft (DFG) für die finanzielle Unterstützung der Entwicklung des Fluoreszenzassays.

Ein ganz besonderes Dankeschön geht an meine Eltern, Rosemarie und Josef Schiller, die mir viele Freiräume gegeben aber auch Grenzen gesetzt haben. Sie haben mir mein Studium ermöglicht, mich durch intensive Gespräche und Diskussionen in meinen Entscheidungen bestärkt und mich durchs Leben begleitet. Sie haben in allen Lebenslagen hinter mir gestanden, auch wenn es manchmal schwer fiel. Ohne Euch wäre das hier nicht möglich gewesen! Vielen, Vielen Dank!

Ein weiterer ganz persönlicher Dank gilt meinem Mann Christian, der mit mir durch Studium und Promotion ging und mich auf einzigartige Weise unterstützt und gestärkt hat. Er hat meinen Frust ertragen, wenn es grade nicht vorwärts ging, meine strapazierten Nerven in Zeiten des Wartens und meine überschäumende Freude, wenn es dann doch funktionierte. Du warst, bist und bleibst mein Fels in der Brandung! Danke!

# Table of Contents

|   |               |
|---|---------------|
| <b>1. Introduction</b>  | <b>1</b>      |
| <b>1.1. Mammalian Adenylyl Cyclases</b>   | <b>1</b>      |
| 1.1.1. Structure and Topology of Adenylyl Cyclase Isoforms  | 1             |
| 1.1.2. Tissue Distribution and Regulation   | 2             |
| 1.1.3. Physiology and Pathology of ACs  | 4             |
| 1.1.4. Pharmacology   | 5             |
| <b>1.2. Bacterial Adenylyl Cyclase Toxins</b>   | <b>7</b>      |
| 1.2.1. <i>Bacillus anthracis</i> , the Causative Agent of Anthrax   | 7             |
| 1.2.2. <i>Bordetella pertussis</i> , the Etiological Pathogen of Whooping Cough                                       | 9             |
| 1.2.3. Adenylyl Cyclase Toxins EF and CyaA: a Comparison  | 10            |
| 1.2.4. Fluorescent Nucleotide Derivatives and Their Interaction with AC Toxins  | 15            |
| <b>1.3. Cyclic nucleotides – Small Molecules in Signal Transduction</b>   | <b>17</b>     |
| <b>1.4. Detection and Quantitation Methods for Nucleotides</b>  | <b>19</b>     |
| 1.4.1. Luminescent Lanthanide Complexes for the Determination of Nucleotides  | 19            |
| 1.4.2. Determination and Quantitation Methods for Cyclase Reactions   | 23            |
| <b>1.5. References</b>  | <b>30</b>     |
| <br><b>2. Aim of Work</b>   | <br><b>41</b> |
| <br><b>3. A Fluorimetric Assay for Real-time Monitoring of Adenylyl Cyclase Activity Based on Terbium Norfloxacin</b> | <br><b>42</b> |
| <b>3.1. Abstract</b>  | <b>42</b>     |
| <b>3.2. Introduction</b>  | <b>42</b>     |
| <b>3.3. Materials and Methods</b>   | <b>44</b>     |
| 3.3.1. Edema Factor (EF)  | 44            |
| 3.3.2. Protein Purification   | 45            |
| 3.3.3. Microwell-Plate Based Fluorescence Assays  | 45            |
| 3.3.4. Reagents   | 45            |
| 3.3.5. Enzyme-Activity Assays Using TbNflx as Indicator   | 46            |
| <b>3.4. Results</b>   | <b>47</b>     |

|             |   |           |
|-------------|---|-----------|
| 3.4.1.      | Calibration Plots for the AC System and Enzyme Toxicity of TbNflx                                       | 47        |
| 3.4.2.      | Specificity of TbNflx Response  | 48        |
| 3.4.3.      | Monitoring of Enzyme Activity   | 49        |
| 3.4.4.      | Screening of EF Inhibitors  | 50        |
| 3.4.5.      | Determination of $V_o^{\max}$ and $K_M$   | 52        |
| 3.4.6.      | Validation of Fluorescence Assay by a Radiometric Assay Using $[\alpha\text{-}^{32}\text{P}]\text{ATP}$ | 53        |
| 3.4.7.      | Calculation and Illustration of ATP Turnover  | 53        |
| 3.4.8.      | Z-Factor  | 54        |
| <b>3.5.</b> | <b>Discussion</b>   | <b>55</b> |
| <b>3.6.</b> | <b>References</b>   | <b>57</b> |

|             |  |           |
|-------------|--|-----------|
| <b>4.</b>   | <b>Cytidylyl Cyclase Activity of Bacterial and Mammalian “Adenylyl” Cyclases</b> | <b>60</b> |
| <b>4.1.</b> | <b>Abstract</b>  | <b>60</b> |
| <b>4.2.</b> | <b>Introduction</b>  | <b>60</b> |
| <b>4.3.</b> | <b>Materials and Methods</b>   | <b>62</b> |
| 4.3.1.      | Chemicals  | 62        |
| 4.3.2.      | Enzyme and Membrane Preparations   | 63        |
| 4.3.3.      | Nucleotidyl Cyclase Assays   | 63        |
| 4.3.4.      | Cell Culture   | 64        |
| 4.3.5.      | Extraction of cNMPs from Cells   | 65        |
| 4.3.6.      | RNA-Extraction   | 65        |
| 4.3.7.      | Microarray-Based mRNA Expression Analysis  | 65        |
| 4.3.8.      | Real-Time PCR (RT-PCR)   | 66        |
| 4.3.9.      | Quantitation of Cyclase Reactions  | 67        |
| 4.3.10.     | Quantitation of Cell Extracts  | 68        |
| 4.3.11.     | Analysis of Data   | 69        |
| <b>4.4.</b> | <b>Results</b>   | <b>70</b> |
| 4.4.1.      | Nucleotidyl Cyclase Activity of CyaA-N and EF                                    | 70        |
| 4.4.2.      | Effects of CyaA Holotoxins and EF in Intact Cells                                | 74        |
| 4.4.3.      | cCMP Formation by Mammalian ACs  | 80        |
| <b>4.5.</b> | <b>Discussion</b>  | <b>81</b> |
| <b>4.6.</b> | <b>References</b>  | <b>84</b> |

|                                      |           |
|--------------------------------------|-----------|
| <b>5. Summary</b>                    | <b>89</b> |
| 5.1. Summary in English              | 89        |
| 5.2. Summary in German               | 90        |
| <b>6. Curriculum Vitae</b>           | <b>92</b> |
| <b>7. Abstracts and Publications</b> | <b>93</b> |



## 1. Introduction

A large number of enzymatically catalyzed reactions are related to the conversion of ATP. Adenylyl cyclases (ACs) convert ATP to cyclic adenosine 3',5'-monophosphate (cAMP) and pyrophosphate (PP<sub>i</sub>). The small molecule cAMP was found to be a second messenger in mammalian cells. In mammals, ten different isoforms of ACs are known, nine of which are membrane-bound. Invasive microorganisms have exploited the dependence of mammals on the second messenger cAMP and synthesize highly active cyclase toxins or produce activators for host ACs in order to subvert host defense mechanisms.<sup>1,2</sup>

Apart from the already known cyclic nucleotides cAMP and cGMP, the existence of other cyclic nucleotides *in vivo* like cyclic cytidine 3',5'-monophosphate (cCMP) has been discussed since the 1970s, but could never be proven definitely. The existing cyclic nucleotide 3',5'-monophosphate (cNMP) detection and quantitation methods contributed to this controversy as they are for the most part cross-reactive, non-selective and not sufficiently sensitive.<sup>3,4,5</sup>

### 1.1. Mammalian Adenylyl Cyclases

#### 1.1.1. Structure and Topology of Adenylyl Cyclase Isoforms

In mammalian tissue nine membrane-bound AC (mAC) isoforms have been identified with a tenth soluble form that has distinct catalytic and regulatory properties, resembling cyanobacterial and mycobacterial enzymes. The soluble AC (sAC) possesses a highly conserved catalytic core compared to mAC, although there are significant differences in its primary sequence.<sup>6,7</sup>

The nine membrane-bound ACs have a highly complex membrane topology and exhibit a striking sequence homology in the primary structure of the catalytic core. Hydrophobic amino acid residues are arranged in two sets of six adjacent transmembrane spans separated by a large hydrophilic loop.<sup>8</sup> The proposed structure contains a short variable N-terminus, followed by the first set of six transmembrane helices, a large cytoplasmic domain consisting of 360-390 amino acids (C1), the second set of transmembrane helices and a second cytoplasmic domain (C2) with 255-330 amino acids (Fig. 1.1).<sup>6,7,8</sup>

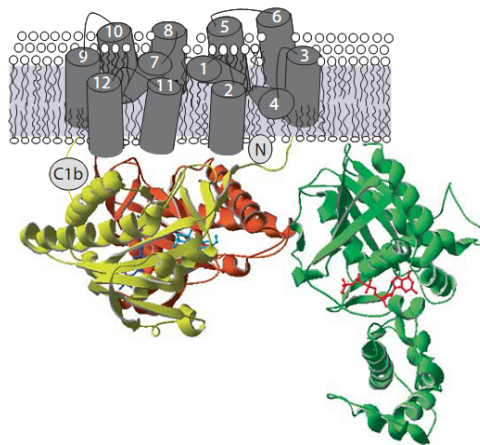


**Fig. 1.1.** Adenylyl cyclase structure taken from Sadana *et al.*<sup>7</sup> Crystal structure of the cytoplasmic domains of AC in complex with GTP $\gamma$ S-Gs $\alpha$ , the activator forskolin (FSK) and the P-site inhibitor, 2',5'-dideoxy-3'ATP. Depicted are C1 (yellow), C2 (red), Gs $\alpha$  (green), FSK (cyan) and P-site inhibitor (dark blue). Transmembrane domains have been modeled from 12-membrane spanning transporters.<sup>7</sup>

The domains C1 and C2 form the catalytic core of ACs and are both required for catalytic activity. The mixture of the soluble VC1 and IIC2 domains, which lack the transmembrane spans, results in regulatory properties similar to the full-length membrane bound enzyme.<sup>1</sup> Two highly conserved aspartic acid residues within the catalytic core coordinate two catalytic metal ions at conserved topological locations. Both are probably engaged with Mg<sup>2+</sup> in the cell, although they show specificity for both Mn<sup>2+</sup> and Zn<sup>2+</sup>. The divalent cations are crucial for AC activity.<sup>9</sup>

### 1.1.2. Tissue Distribution and Regulation

The activation of membrane-bound ACs in mammalian cells is mediated by G-proteins, which in turn are regulated by G-protein-coupled receptors (GPCRs). Binding of hormones, neurotransmitters or sensory signals to cell surface receptors initiates the G-protein signaling cascade. G-proteins are membrane-associated heterotrimeric proteins composed of a GDP-bound  $\alpha$ -subunit and a  $\beta\gamma$ -heterodimer. Receptor activation promotes GDP release and replacement by GTP in G-proteins. GTP induces a conformational change in G-proteins leading to the activation and dissociation of G $\alpha$  from the  $\beta\gamma$ -subunit. ACs are regulated by G $\alpha$ - as well as from G $\beta\gamma$ -subunits in an AC isoform- and G-protein-dependent manner. G-proteins return to their inactive state by the intrinsic GTPase activity of the G $\alpha$ -subunit.<sup>2,8,9,10</sup>

sAC and sAC-like ACs are the only enzymes known that are regulated directly and specifically by bicarbonate. Bicarbonate probably increases AC activity by facilitating the transition from the open to the closed form during catalysis. However, the bicarbonate binding site in sACs remains unknown. sACs are additionally activated by the presence of Ca<sup>2+</sup> ions increasing the affinity for the substrate ATP. The K<sub>M</sub> of sACs reside in the millimolar

range and, therefore, is unusually high for an AC. However, it is speculated that sACs react to changing ATP concentrations in whole cells or compartments and may act as an ATP sensors.<sup>6</sup>

The large number of AC isoforms raises the question as to why ten specific isoforms are needed and what specific functional role each one plays in the organism. Part of the specificity is defined by the tissue distribution which has been largely unraveled by PCR analysis due to low expression of ACs and lack of specific antibodies.<sup>7,9,11</sup>

**Table 1.1.** Tissue distribution, physiological function and regulatory properties of mammalian ACs as reviewed by Tang *et al.*<sup>12</sup> and Sadana *et al.*<sup>7</sup>

| AC isoform | Distribution  | Associated function  | Regulation   |
|------------|---|--|--|
| AC 1       | Brain, adrenal gland  | Learning, memory, synaptic plasticity, opiate withdrawal   | G <sub>sα</sub> ↑, G <sub>iα</sub> ↓, G <sub>oα</sub> ↓, G <sub>βγ</sub> ↓, PKC(↑), CaM↑, FSK↑ |
| AC 2       | Brain, skeletal muscle, lung  | Synaptic plasticity, arrest of cell proliferation  | G <sub>sα</sub> ↑, G <sub>βγ</sub> ↑, PKC↑, FSK↑   |
| AC 3       | Olfactory epithelium, pancreas, brain, heart, lung, testis                    | Olfaction, sperm function, locomotor activity, food, consumption, leptin insensitivity <sup>13</sup> | G <sub>sα</sub> ↑, G <sub>βγ</sub> ↓, PKC(↑), CaM↑, FSK↑                                       |
| AC 4       | Widespread  | Depression, suicidal tendencies <sup>14</sup> , photoreception <sup>15</sup>                         | G <sub>sα</sub> ↑, G <sub>βγ</sub> ↑, PKC↓, FSK↑   |
| AC 5       | Heart, striatum, kidney, liver, lung, testis, brain, skeletal muscle, adrenal | Cardiac contraction, motor coordination, drug dependency, pain                                       | G <sub>sα</sub> ↑, G <sub>βγ</sub> ↑, G <sub>iα</sub> ↓, G <sub>zα</sub> ↓, PKA↓, PKC↑, FSK↑   |
| AC 6       | Heart, kidney, liver, lung, brain, testis, skeletal muscle, adrenal           | Cardiac contraction  | G <sub>sα</sub> ↑, G <sub>βγ</sub> ↑, G <sub>iα</sub> ↓, G <sub>zα</sub> ↓, PKA↓, FSK↑         |
| AC 7       | Widespread  | Ethanol dependency, depression   | G <sub>sα</sub> ↑, G <sub>βγ</sub> ↑, PKC↓, FSK↑   |
| AC 8       | Brain, lung, pancreas, testis, adrenal  | Memory, learning, synaptic plasticity, drug withdrawal   | G <sub>sα</sub> ↑, G <sub>iα</sub> ↓, CaM↑, FSK↑   |
| AC 9       | Widespread  | Learning, memory   | G <sub>sα</sub> ↑, PKC↑  |
| sAC        | Testis and detected in all tissues  | Fertilization, sperm capacitation  | Ca <sup>2+</sup> ↑, HCO <sub>3</sub> <sup>-</sup> ↑  |

↑,↓ symbolize stimulation or inhibition, respectively

mACs are classified according to their regulatory properties and functionality and are subdivided into four distinct families. The Ca<sup>2+</sup>-calmodulin (CaM)-sensitive ACs are isoforms 1, 3 and 8, whereas ACs 2, 4 and 7 are stimulated by G<sub>βγ</sub>. Sensitivity to inhibition by Ca<sup>2+</sup> and G<sub>oi</sub> applies to ACs 5 and 6. AC 9 comprises the last family of membrane-bound isoforms and

is not subject to activation by the diterpene forskolin (FSK) from *Coleus forskohlii*, but is regulated by calcineurin.<sup>7,1</sup>

Phosphorylation of ACs by protein kinase A (PKA) or C (PKC) represents feedback regulations within the signal transduction cascade. PKA serves as feedback inhibitor of ACs 5 and 6, whereas PKC may display either stimulatory or inhibitory effects. In case of stimulatory PKC phosphorylation highly synergistic effects with  $G_{\alpha}$  subunits may be observed. This especially holds true for sensitization of AC 2 and 7 for  $G_{s\alpha}$  (see Table 1.1).<sup>7</sup>

### 1.1.3. Physiology and Pathology of ACs

The majority of the data on the physiology of ACs has been obtained by overexpression studies using cell transfection or transgenic animals and by gene disruption studies exploiting genetic knockout animals and the identification of natural gene mutations leading to a loss-of-function or gain-of-function phenotype.

It was reported that two-point mutations in the promotor region of the AC 3 gene in rats may be causing a decrease in glucose-induced insulin production in spontaneously diabetic mice. Furthermore, AC 3-deficient mice fail in several olfaction-based behavioral tests and lack electro-olfactogram responses. Additionally, the mouse model indicates AC 3 as important parameter for the growth of arterial smooth muscle cells.<sup>1,11</sup> Novel results link AC 3 to physical activity, food consumption, and leptin-insensitivity and, therefore, weight control. A Swedish study in obese men found that polymorphisms in AC 3 were present. These data could be confirmed by male and female AC 3 knock-out mice that were about 40% and 70%, respectively, heavier than the control group.<sup>13</sup>

CaM-regulated ACs play a crucial role in learning and memory. Double knockout mice deficient in AC 1 and AC 8 exhibit neither long-term memory nor late long-term potentiation. Infusion of the AC activator FSK into the hippocampus of these mice restores normal function of the brain. Single knockout animals are normal in these functions but display other neurological defects.<sup>1,11</sup>

AC 5 and 6 are predominant in the heart. In heart failure, the level of AC 6 decreases while that of AC 5 remains the same. When overexpressing AC 6 in murine hearts increased sensitivity to epinephrine and an enhanced cardiac function is retained and thus, heart function in murine cardiomyopathy can be improved. However, overexpression of AC 5 leads to myocardial damage through cellular degeneration and fibrosis over the lifetime of the animal, whereas AC 5 knock-out mice have an increased lifespan of approx. 30%.<sup>7,11</sup>

Mutations found in the human genome causing constitutively active receptors – yielding permanently active ACs – have been found in familial male precocious puberty/testotoxicosis, overactive thyroid adenomas, non-autoimmune autosomal dominant

hyperthyroidism and Jansen-type metaphyseal chondrodysplasia. McCune-Albright syndrome, endocrine tumors and testotoxicosis may be ascribed to a more prevalent mutation in  $G_{s\alpha}$  resulting in a constitutively active G-protein.<sup>1,10</sup>

Inactivating mutations of G-proteins may lead to Albright hereditary osteodystrophy including reduced melanocortin signaling in hypothalamus, impaired parathyroid-hormone-related peptide signaling in chondrocytes, resistance to various hormones, obesity, short stature, subcutaneous ossifications and mental or developmental deficits. An unusual form of pseudohypoparathyroidism underlies reduced AC activity suggesting the presence of inactivating mutations in ACs.<sup>1,10</sup>

ACs play a prominent role in model systems for drug abuse, dependency and withdrawal. Cells chronically treated with opiates exhibit supersensitive AC activity – *via* upregulated ACs, PKA and cAMP-responsive element binding protein (CREB) – upon stimulation after withdrawal of the drug. Supersensitization is observed for AC isoforms 1, 5, 6 and 8. Interestingly, chronic opioid abuse leads to relative desensitization of ACs 2, 4 and 7. The mechanisms underlying this form of sensitization, however, remain obscure.<sup>7,1,2,11</sup>

#### 1.1.4. Pharmacology

Although there are not yet approved drugs for ACs on the market, several small molecules are known to modulate the activity of ACs. The diterpene FSK activates the synthetic AC construct VC1:IIC2 and all membrane-bound AC isoforms except for AC 9. FSK binds to the second site structurally related to the active site in mACs and thereby, induces rearrangement of the domains to the active conformation. AC 9 is presumably insensitive to activation by FSK and derivatives due to an amino acid change (Ser 1112 → Ala, Leu 1082 → Tyr)<sup>16</sup> in this binding pocket.<sup>1,6,7,11</sup>

P-site inhibitors represent a major class of AC inhibitors which are in general non-selective towards specific isoforms. P-site inhibitors are typically adenosine derivatives acting un- or noncompetitively. They are more potent on the activated form of ACs in comparison to the basal state by stabilizing a product-like transition state together with  $PP_i$ . Some very potent P-site inhibitors may also bind in the absence of  $PP_i$ .<sup>6,7,1,11</sup> However, AC 5 selective P-site inhibitors could be identified amongst AC 2-, AC 3-, and AC 5-overexpressing insect cells. These selective inhibitors comprise classic P-site inhibitors like 2',5'-dideoxy adenosine and a new class of effectors containing an adenine ring joined by a metal chelating hydroxamic acid linker forming a  $Mg^{2+}$  complex in the active site of the enzyme like 1*R*,4*R*-3-(6-aminopurin-9-yl)-cyclopentane-carboxylic acid hydroxymide (PMC 6) (see Fig. 1.2.).<sup>17</sup>

2'(3')-*O*-(*N*-Methylanthraniloyl)-(MANT)- and 2',3'-*O*-(2,4,6-trinitrophenyl)-(TNP)-substituted nucleotide derivatives constitute another class of inhibitors interacting with ACs in a competitive manner. In 2003 it was reported that MANT-GTP derivatives inhibited ACs directly and not like anticipated, G-proteins.<sup>18</sup> The search for further competitive inhibitors showed that all sorts of MANT-, ANT- (missing the methyl-group at the anthraniloyl-moiety) and TNP-nucleotides act as inhibitors, including MANT-ATP MANT-ITP $\gamma$ S, MANT-UTP, MANT-CTP, TNP-ATP, TNP-UTP and TNP-CTP.<sup>19,20, 21,22</sup>

As a matter of fact, the interaction of these derivatized nucleotides was surprising regarding the different nucleobases applied. The binding of bases other than adenosine was not expected in the first place. These data suggested that the catalytic site of ACs is flexible and base-specificity of ACs is much less stringent than presumably supposed. Modeling data and crystal structures confirmed this assumption.<sup>19,20</sup>

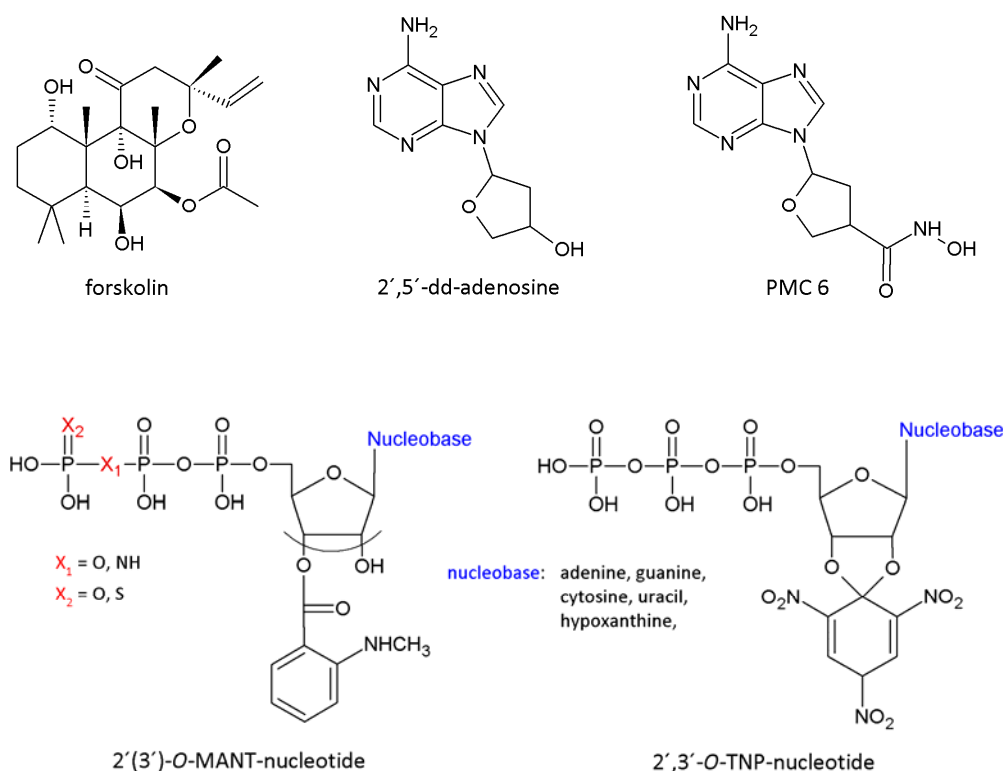


**Fig. 1.2.** Chemical structures of different AC effectors including diterpene forskolin, P-site inhibitors 2',5'-dd-adenosine and PMC 6, and competitive inhibitors based on nucleotides derivatized with fluorescent MANT- or TNP-moieties

Most astonishing was the potency of MANT- and TNP-nucleotides bearing uracil, cytosine or hypoxanthine moieties.  $K_i$  values for TNP-CTP and -UTP were in the same order of magnitude than for TNP-ATP on VC1:IIC2 domains, AC I, AC II, and AC V preparations. The same holds true for MANT-ITP, MANT CTP and MANT-UTP at AC I, AC II, AC V, AC VI and

mouse heart AC. Surprisingly, these three MANT-nucleotides showed higher potency on ACs than MANT-ATP.<sup>21,22,23</sup>

One might argue that these unexpected data may originate from the use of  $Mn^{2+}$  in the experiments as  $Mn^{2+}$  tends to enhance inhibitor potency and to reduce base specificity.<sup>19</sup> However, the exchange of  $Mn^{2+}$  by  $Mg^{2+}$  decreased inhibitor potency for all nucleobases alike.<sup>19,21</sup> This raises the question whether mammalian ACs may use other nucleotides than ATP as substrate.

## 1.2. Bacterial Adenylyl Cyclase Toxins

### 1.2.1. *Bacillus anthracis*, the Causative Agent of Anthrax

In 2001 anthrax disease was brought to broad public attention by the deliberate attack on several news media offices and two Senators in the US. Until November 28<sup>th</sup> 2001 twenty-three cases of anthrax infections due to bioterrorism had been identified in the USA.<sup>24</sup> A recent outbreak of cutaneous anthrax in Aachen, Germany in a heroin addict in December 2009 who died a week after being hospitalized caused public sensation. This incident is probably associated with similar cases of anthrax being diagnosed in fourteen heroin addicts in Scotland seven of which died within a few days.<sup>25</sup> Although people seem to believe that anthrax is a problem of third world countries, twenty-eight cases of anthrax in humans have been reported by the World Health Organization (WHO) in 2001 and an average of sixty-two cases per year in the decade before, in Spain.<sup>26</sup>



**Fig. 1.3.** Development of a black eschar induced by cutaneous anthrax infection. Pictures taken from the Centers for Disease Control and Prevention (<http://phil.cdc.gov>)

Anthrax is caused by *Bacillus anthracis*, a Gram-positive, spore-forming, rod-shaped bacterium. The disease is zoonotic and primarily affects herbivores but can occasionally be transferred from animals to humans by handling contaminated animal products or inhaling airborne spores. Dormant spores of *B. anthracis* are highly resistant to environmental conditions while the bacilli *per se* are poor survivors. The life cycle of *B. anthracis* almost exclusively takes place within the mammalian host. Spores ingested by herbivores germinate

within the body and produce the vegetative form. These bacilli multiply, killing the host. Bacilli sporulate in the presence of free oxygen when shed by the dying or dead animal.<sup>27,28</sup>

Disease occurs when spores enter the host in three possible ways. The mode of spore entry into the human body predetermines the etiopathology and the chance of survival. Spores invading the organism *via* skin abbrations leads to the least dangerous and cutaneous form. This form manifests itself by small pimples developing to painless black eschars accompanied by substantial edema (see Fig. 1.3.). Gastrointestinal and inhalational (pulmonary) anthrax forms evolve after ingestion or inhalation of spores. In these two forms, the infection proceeds insidiously with mild symptoms of gastroenteritis and flu. Therefore, diagnosis in an early stage is challenging and each form of anthrax may abruptly develop into a systemic form that becomes treatment-resistant and rapidly fatal with shock-like symptoms, sepsis and respiratory failure often accompanied by acute meningitis (see Fig. 1.4.).<sup>27,28</sup>

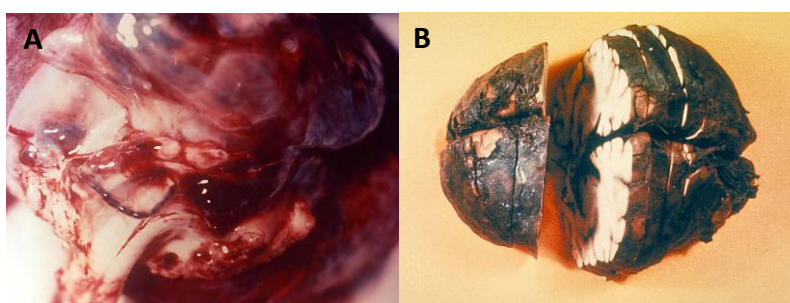


**Fig. 1.4.** **A** Gross pathologic prosterior view of a chimpanzee's lungs that had suffered inhalation anthrax. **B** Hemorrhagic meningitis due to inhalation anthrax. Pictures were taken from Centers of Disease Control and Prevention (<http://phil.cdc.gov>)

*B. anthracis* survival and lethality is attributed to the production of a capsule and the tripartite anthrax toxin. The genetic information for these virulence factors is encoded on two different plasmids – pXO1 and pXO2. pXO2 contains information for the biosynthesis of a polyglutamate capsule, protecting the vegetative cells from phagocytotic killing by macrophages which is important for evading the immune system. pXO1 encodes the components for anthrax toxin comprising edema factor (EF), an adenylyl cyclase toxin, lethal factor (LF), a  $Zn^{2+}$ -dependent metalloprotease inactivating mitogen activated protein kinase kinases (MAPKKs), and protective antigen (PA), binding to cell surface receptors and enabling cell entry of EF and LF *via* endocytosis (for further information see Chapter 1.2.3).<sup>29,30,31</sup>



### 1.2.2. *Bordetella pertussis*, the Etiological Pathogen of Whooping Cough

Whooping cough or pertussis is a typical childhood disease against which has been vaccinated in developed countries since the 1940s. However, the WHO has counted 136,331 cases of whooping cough in 2008. Yet, the number of unreported cases is high. In 2000, approximately 190,000 cases were reported but 39 million cases and 297,000 deaths due to pertussis estimated. Whooping cough has become one of the ten most common causes of death from infectious disease.<sup>32</sup>

Whooping cough is caused by the Gram-negative aerobic coccobacillus *Bordetella pertussis* that is found alone or in pairs. It belongs to the genus *Bordetella* and is pathogenic exclusively for humans. *B. pertussis* is a non-motile organism that is transferred from host to host by aerosolized droplets. The infection progresses by attachment of the coccobacillus to airway tissue (see Fig. 1.5.), avoidance of host defence mechanisms, cellular destruction and systemic effects. The disease normally undergoes three distinct stages called catarrhal, paroxysmal, and convalescent.<sup>33,34</sup>

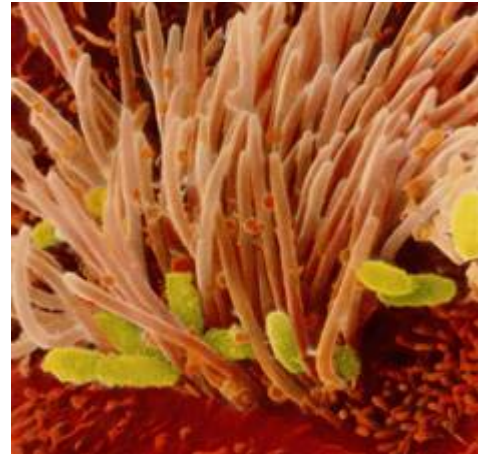


**Fig. 1.5.** Colonization of tracheal epithelial cells by *Bordetella pertussis* (yellow) taken from [www.nibsc.ac.uk/science/vaccines/pertussis.aspx](http://www.nibsc.ac.uk/science/vaccines/pertussis.aspx)

The catarrhal phase is indistinguishable from viral upper respiratory tract infections and characterized by non-specific coryzal illness with mild cough, generally lasting one to two weeks. Then, the cough becomes more severe and frequent with spasmodic conditions, inspiratory whoops and post-tussive vomiting, lasting up to six to eight weeks. This stage is referred to as paroxysmal. When the symptoms finally start improving and the coughs become milder, the phase is referred to as convalescent.<sup>34,35</sup>



**Fig. 1.6.** Child with ruptured blood vessels in eyes and bruising on face due to pertussis coughing taken from [www.cdc.gov/vaccines/vpd-vac/pertussis/photos/htm](http://www.cdc.gov/vaccines/vpd-vac/pertussis/photos/htm)

Pertussis may be associated with various complications from subcutaneous emphysema, pneumothorax, seizures and encephalopathy, dehydration and malnutrition in young children as well as hemorrhages from coughing (see Fig. 1.6.). Older patients may experience rib fractures, back pain, and hearing loss. The risks of complications, hospitalization and mortality are related to age. Infants have the highest risk of morbidity with 24% compared to older children with only 5% and adolescents with 16%. Adults have an even higher morbidity of 28%. However, complications in infants are

typically more severe, and hospitalization rates are highest among children less than one year old. Similarly, mortality rates are highest among infants younger than six months and lowest among adolescents.<sup>33,36,37</sup>

The pathogenicity of *Bordetella pertussis* is ascribed to a multitude of virulence factors comprising three major surface agglutinogens, fimbriae required for colonisation of the trachea, pertactin and filamentous haemagglutinin acting as adhesins for the organism, lipopolysaccharide with immunomodulating activity, tracheal colonisation factor, serum resistance factor enabling resistance to killing by human serum, tracheal cytotoxin, and dermonecrotic toxin causing necrotic lesions if injected subcutaneously. Remarkably, only three virulence factors secreted by the bacillus are able to enter target cells. A recently discovered protein, BteA, is injected into host cells by a type III secretion system. Its exact function is still unknown but it is required for cytotoxicity *in vitro* and persistence *in vivo*. Pertussis toxin ADP-ribosylates G<sub>i</sub>-proteins and thereby inhibits their coupling to receptors of intracellular signaling cascades. The third enzyme to enter host cells is an adenylyl cyclase/hemolysin toxin called CyaA. CyaA self-translocates into the cytosol and raises intracellular cAMP levels in cells of the immune system (for further detail see Chapter 1.2.3).<sup>38,39</sup>

### 1.2.3. Adenylyl Cyclase Toxins EF and CyaA: a Comparison

At first glance, anthrax and pertussis are two completely different diseases with differing clinical pictures, route of infection and survival rates. However, both pathogens possess AC toxins which are classified as Class II adenylyl cyclases; CyaA from *B. pertussis* and EF from *B. anthracis*.<sup>6</sup> Both systems are closely related, although sequence alignment only shows structure similarity of 23% predominantly in the catalytic core of the proteins.<sup>40</sup>

#### *Structure and function*

EF and CyaA are CaM-dependent AC toxins comprising no cysteine residues. Very low basal activity prior CaM-binding has been detected in both EF and CyaA. Although the activation mechanism was similar there was only little sequence homology in both enzymes.<sup>41,42</sup>

EF is a 92.5 kDa soluble protein with a 30 kDa N-terminal PA binding and a 60 kDa C-terminal AC domain approximately 380 amino acids in size. In contrast, CyaA consists of 1706 amino acids and has a molecular weight of 188 kDa. Soon it became clear that only the 400 N-terminal amino acids comprise AC activity and the remaining 1306 amino acids bear the so-called hemolysin moiety important for cell entry. However, there are conserved regions in the CaM-sensitive AC domain of both enzymes with 34% sequence homology (see Fig. 1.7.).<sup>42,43,44,45,46</sup>

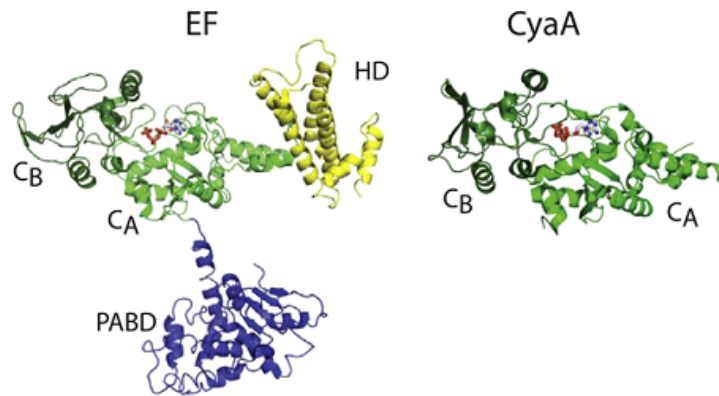


**Fig. 1.7.** Structural comparison of EF and the AC-domain of CyaA without CaM-bound. Catalytic core domains,  $C_A$  and  $C_B$ , helical domain (HD) and PA binding domain (PABD) are colored in light green, dark green, yellow and dark blue, respectively. CyaA lacks the helical and PA binding domain. The structures are depicted with ATP analogues colored according to their atoms. The illustration was taken from Tang and Guo<sup>47</sup>.

The AC domain of EF consists of a catalytic core ( $C_A$  and  $C_B$ ) and a helical domain that are linked by the so-called Switch C. In the non-CaM bound state Switch C and the  $C_A$  domain have close contact thereby locking EF in an open, inactive conformation. CaM possesses two globular domains connected by an  $\alpha$ -helix and binds four  $Ca^{2+}$  ions, inducing a conformational change that results in the exposure of a hydrophobic pocket. CaM inserts between  $C_A$  and the helical domain. Surprisingly, in complex with EF only the two C-terminal  $Ca^{2+}$ -binding sites of CaM are occupied. Lys 525 is seen as “hot-spot” for interaction of EF and CaM. As a matter of fact, an extensive interaction between CaM and Switch A and C occurs, triggering conformational changes in Switch C. Thus, a twelve amino acid loop called Switch B containing several residues crucial for catalysis is stabilized. The enzyme complex has engaged a closed and active conformation.<sup>45,46,48,49</sup>

Catalysis of AC reaction occurs *via* two divalent metal cations. These are presumably two  $Mg^{2+}$  under physiological conditions, but they can also be replaced by  $Mn^{2+}$  or even  $Zn^{2+}$ . The divalent metal ions are coordinated by Asp 491, Asp 493 and His 577. The negatively charged phosphate tail of ATP is stabilized by Lys 346, Arg 329, Lys 372 and Lys 353 or Ser 354. The adenine moiety interacts with the backbone of Asp 582, Asn 583 and the N6 nitrogen is within hydrogen-bonding distance of Thr 548. Phe 586 and Leu 348 lie above and below the plane of the ribose, respectively, and the O4' of the ribose is coordinated by a hydrogen-bond with Asn 583. His 351 is highly conserved and was initially thought to replace a  $Mg^{2+}$  and to catalyze the reaction by deprotonation of 3'OH. However, it has become clear that probably a hybrid mechanism of deprotonation by  $Mg^{2+}$  and His 351 is used for catalysis. A salt bridge between Glu 588 and Lys 353 locks ATP within the catalytic site. The

nucleotide cyclization reaction proceeds by nucleophilic attack on the  $\gamma$ -phosphate (see Fig. 1.8.).<sup>45,48,50,51,52,53</sup>

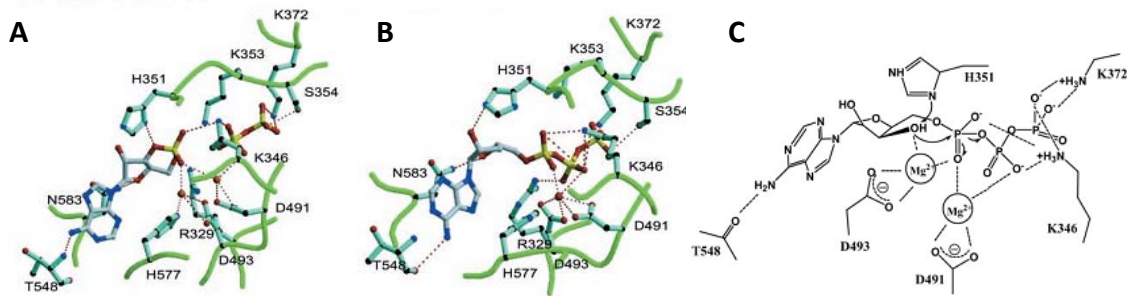


**Fig. 1.8.** **A** and **B** show the active sites of EF in EF-CaM-cAMP-PP<sub>i</sub> and EF-CaM-3'dATP complex, respectively. The backbone of EF is colored green, the molecules in the catalytic core are colored according to their atoms (carbon: gray, oxygen: red, nitrogen: blue, phosphorus: yellow). **C** shows the proposed mechanism for catalysis by EF. For clarity several key residues, such as Arg 329 (salt-bridge with phosphorus chain), Asn 583 (hydrogen bonding with O4' ribose) and His 577 (involved in metal ion binding), were omitted. Pictures are taken from Guo *et al.*<sup>51</sup>

The catalytic site and the involved amino acids in catalysis are highly conserved in CyaA and the domains are analogously called C<sub>A</sub> and C<sub>B</sub>. Two metal ions are coordinated by Asp 188, Asp 190 and His 298. The phosphorous backbone of ATP is held in position by Arg 37, Lys 58, Lys 65 and Lys 84. The ribose oxygen interacts with Asn 304. An additional catalytic base His 63 also found in EF at position 351 is thought to be crucial for catalysis. However, in CyaA there is a third Mg<sup>2+</sup> ion found that is coordinated between Asp 188, Asp 190 and Gln 297. This third metal ion is not found in structures of EF and is positioned in such a way that it is believed to only play a role for structural integrity.<sup>51,54,55</sup>

Despite a striking sequence similarity in the catalytic domain, the binding and activation of CyaA by CaM differs significantly from the mechanism found in EF. In contrast to EF, CyaA is also being fully activated by CaM mutants with defective C-terminal Ca<sup>2+</sup> binding sites or by the N- or C-terminal domain of CaM alone. Compared to EF CyaA has a 100-fold higher affinity to CaM and surprisingly binds CaM in a Ca<sup>2+</sup> independent way. CyaA completely lacks a structure similar to the helical domain in EF that is strongly involved in CaM interaction. The CaM-binding site in CyaA partially overlaps the N- and C-terminal subdomains of the AC moiety, and 72 amino acids comprise 90% of the binding energy released upon interaction with CaM. The key residue in CaM binding is Trp 242. Generally, the binding pocket of CyaA adopts a more open catalytic conformation than EF.<sup>40,46,55</sup>

The class II AC toxins share no structure similarities with mammalian ACs. Upon activation in the cytosol of host cells by CaM they exhibit a turnover number at least 100-times higher than mammalian ACs. Both toxins show  $k_{\text{cat}}$ -values of 1000-2000 s<sup>-1</sup>, thereby, elevating cAMP levels to a supraphysiologic level.<sup>44,51</sup>

### Cell entry mechanism

The cell entry mechanisms for both AC toxins are very different. EF cannot enter host cells on its own but needs PA a second virulence factor of *B. anthracis*. PA binds to cell surface receptors widely distributed over a broad range of tissues. The first receptor identified was tumor endothelial marker-8 (TEM8) containing a von Willebrand factor type A domain, also called integrin-like domain. A second receptor for PA is capillary morphogenesis protein 2 (CMG2) also widely expressed and possessing an integrin-like domain highly homologous to TEM8. Once bound to the receptor, the 83 kDa PA is cleaved by furin or furin-like endoproteases leaving a 63 kDa activated fragment. PA<sub>63</sub> oligomerizes into a heptamer and is able to bind three toxin molecules per heptamer. LF and EF compete for the binding sites of the PA oligomer. The complete complex is endocytosed and translocated to acidic compartments. PA<sub>63</sub> heptamers form cation selective pores when shifted to lower pH and translocates EF into the cytosol.<sup>27,28,47,56,57,58</sup>

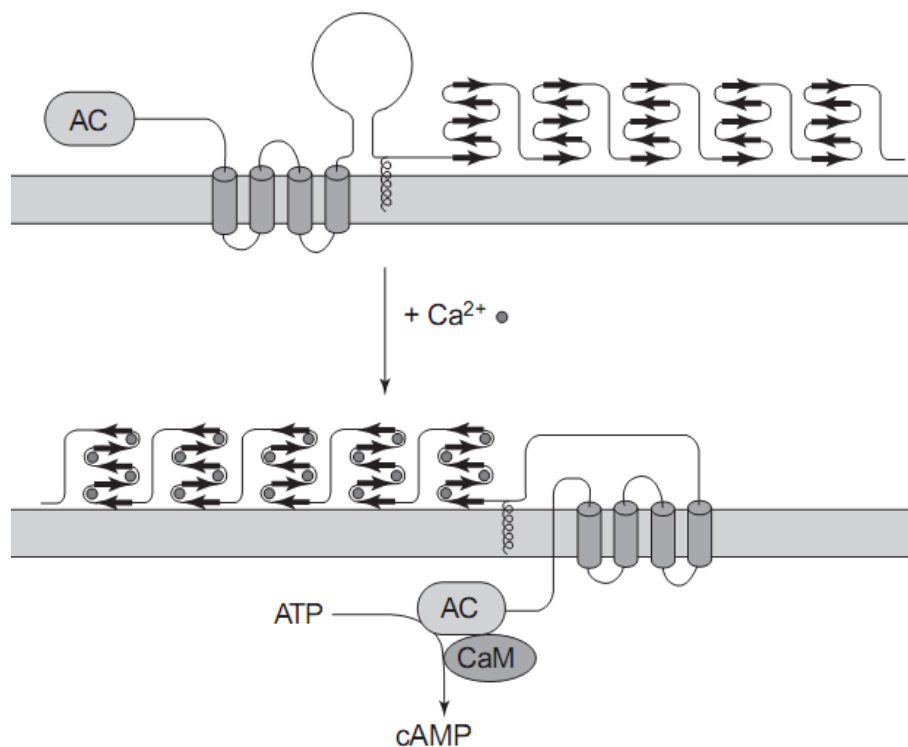


**Fig. 1.9.** Hypothetical internalization mechanism of CyaA taken from Ladant and Ullmann.<sup>44</sup> At low  $\text{Ca}^{2+}$  concentration hydrophobic domains (cylinders) are inserted into the plasma membrane. After binding of  $\text{Ca}^{2+}$  by the repeated motifs (thicker arrows) a conformational change occurs, translocating the AC domain into the cytosol.

Contrary to EF, CyaA is a bifunctional enzyme with AC- and hemolytic activity. CyaA is expressed as inactive precursor protein that has to be palmitoylated at Lys 983 to become

active. The AC domain resides in the first 400 amino acids, the residual 1306 amino acids are hemolytically active and are needed for translocation of the AC domain into the cytosol. The pore-forming region consists of four hydrophobic segments, a small section where palmitoylation occurs, a characteristic glycine- and aspartate-rich nonapeptide repeat representing the main  $\text{Ca}^{2+}$ -binding sites of the protein and a non-processed carboxy-terminal secretion signal.<sup>44,57,59</sup>

CyaA targets  $\alpha_M\beta_2$ -integrin receptors (CD11b/CD18, Mac-1 or CR-3) that are found on cells of the immune system, i.e. neutrophils, macrophages and dendritic cells, although CyaA is also able to penetrate cell membrane without the presence of the receptor mentioned above. The four hydrophobic spans of the C-terminal part of CyaA integrate into the cell membrane at low  $\text{Ca}^{2+}$  concentrations and form small cation-selective pores that are the reason for the low hemolytic activity of the enzyme. When the  $\text{Ca}^{2+}$  concentration rises,  $\text{Ca}^{2+}$  is bound by the glycine- and aspartate-rich nonapeptide repeats inducing a conformational change of the protein and subsequent direct translocation of the AC domain through the channel formed by the hydrophobic domains into the cell.<sup>44,57,60,61,62</sup>

This internalization mechanism is unique in bacterial enzymes and happens directly without endocytosis. Due to its specific repeat regions CyaA is classified as “repeat in toxin” (RTX). The prototype of this toxin family is the  $\alpha$ -hemolysin of *E. coli*.<sup>44,57,62</sup>

### *Contribution to pathogenesis*

Both AC toxins originate from different species and have quite different mechanisms of activation and cell entry. However, their enzymatic action is the same: generation of supraphysiological levels of cAMP in host cells. Therefore, the list of effects sound intriguingly similar. By cAMP accumulation, both bacteria achieve protection from phagocytic destruction<sup>57,61,63</sup> and compromise the function of dendritic cells<sup>57,61</sup>. CyaA inhibits killing by neutrophils and natural killer cells<sup>38,62,64</sup> and may even induce apoptosis in macrophages,<sup>44,57,60</sup> whereas EF impairs activation and proliferation of T-cells.<sup>57</sup> Both toxins are able to depress superoxide formation,<sup>57,62</sup> oxidative activity,<sup>38,62,65</sup> and chemotaxis.<sup>27,62,64</sup> Additionally, the cytokine secretion is being manipulated under the influence of AC toxins concerning TNF- $\alpha$ , IL-6 and IL-10.<sup>57,61</sup>

The deletion of EF impairs germination of *Bacillus anthracis* in mouse peritoneal macrophages and raises the LD<sub>50</sub> two orders of magnitude in a rodent model for anthrax. CyaA-deficient mutants of *Bordetella pertussis* are avirulent due to impaired colonization of the respiratory tract.<sup>56,61</sup>

A report on effects of edema toxin in mice suggests that the importance of AC toxins for pathology is still underestimated. When injecting highly purified EF and PA into Balb/cJ

mice, the AC toxin caused death at lower doses than previously seen with lethal factor. The pathology revealed intestinal intraluminal fluid accumulation, focal hemorrhaging of the ileum and adrenal glands and lesions in adrenal glands, lymphoid organs, bone, bone marrow, gastrointestinal mucosa, heart, and kidney. A simultaneous cytokine increase was monitored, specifically for granulocyte colony-stimulating factor, eotaxin, kretinocyte-derived cytokine, IL-6, IL-10, and IL-1 $\beta$ . Concurrent hypotension and brachycardia was detected. As a matter of fact, death occurred due to multiorgan failure quicker and at lower concentrations than expected.<sup>58</sup>

The AC toxins, therefore, contribute substantially to establishment and pathogenesis of the infections. However, in a recent experiment with EF no correlation between cAMP-levels and cell death could be observed in different cell types leading to two possible explanations. On the one hand, different cell types could be differently sensitive to elevated cAMP levels, on the other hand, a yet undiscovered activity of EF could contribute to cell death.<sup>66</sup>

#### 1.2.4. Fluorescent Nucleotide Derivatives and Their Interaction with AC Toxins

MANT-, ANT- and TNP-nucleotides (see Fig. 1.10.) are environmentally sensitive probes with an excitation maximum at  $\lambda_{\text{ex}} = 350 \text{ nm}$  that show increased fluorescence ( $\lambda_{\text{em}} = 450 \text{ nm}$ ) and blue shift of the emission maximum upon interaction with a hydrophobic environment.<sup>67,68</sup>

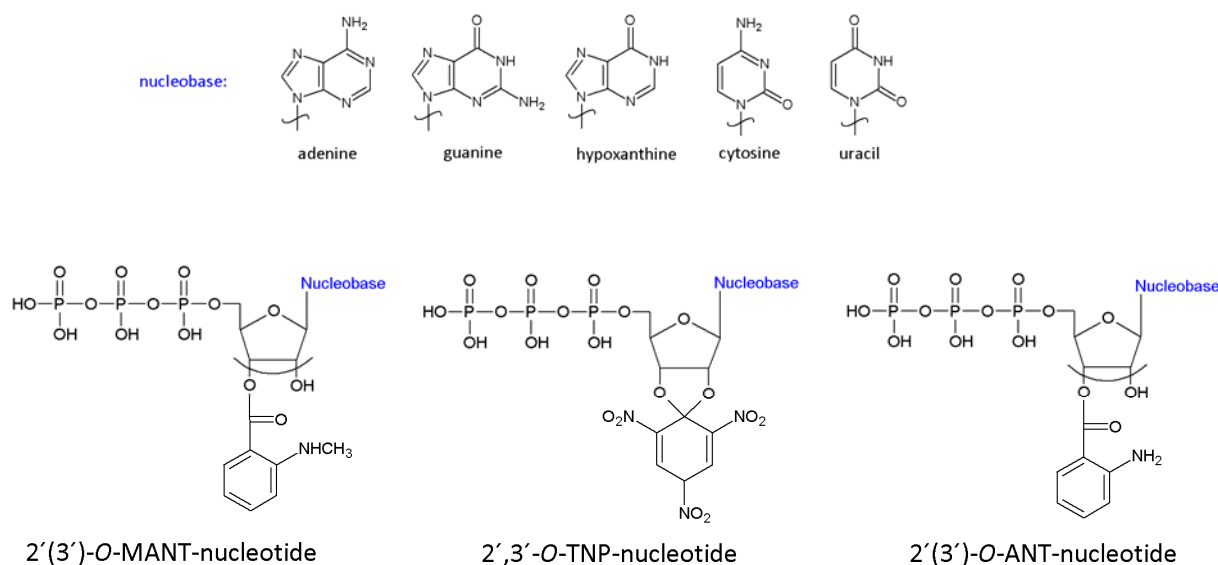


**Fig. 1.10.** Structures of MANT-, TNP- and ANT nucleotides.

The catalytic sites of CyaA and EF possess a hydrophobic phenylalanine residue interacting with the probe. CyaA has two tryptophan residues, and EF one tryptophan and a tyrosine residue in the vicinity of the catalytic site allowing fluorescence resonance energy

transfer (FRET). Therefore, these fluorescent nucleotides have been used to study interactions of probe and enzyme.<sup>69,70</sup>

MANT-substituted nucleotides potently inhibit mAC and AC toxins from *Bacillus anthracis* and *Bordetella pertussis*. These experiments in combination with crystallographic and molecular modeling approaches have revealed substantial conformational flexibility accomodating purine as well as pyrimidine analogues.<sup>19,20,23,69,70</sup>

EF and CyaA displayed unexpected affinity for the nucleotide CTP and its derivatives. The  $K_i$  value of CTP at EF in presence of  $Mn^{2+}$  and  $Mg^{2+}$  were lower in comparison to other non-modified nucleoside triphosphates. The  $K_i$  values of CTP and GTP were comparably low at CyaA. The modification of CTP with fluorescent residues led to surprising data: MANT-CTP showed higher affinity for EF than MANT-ATP in presence of  $Mn^{2+}$  and  $Mg^{2+}$ . Concerning CyaA, the order of potency under  $Mn^{2+}$  conditions was MANT-ITP > MANT-CTP > MANT-UTP > MANT-ATP > MANT-GTP. The inhibitory potencies of all tested nucleotides were differentially decreased when applying  $Mg^{2+}$  instead of  $Mn^{2+}$  (see Table 1.2.).<sup>69,70</sup>

**Table 1.2.** Inhibitory potencies of NTPs and MANT-nucleotides at EF and CyaA in the presence of  $Mn^{2+}$  and  $Mg^{2+}$ . Values were taken from Göttele *et al.*<sup>69</sup> and Taha *et al.*<sup>70</sup>

| Compound | $K_i$ [ $\mu$ M] at EF |                 | $K_i$ [ $\mu$ M] at CyaA |                 |
|----------|------------------------|-----------------|--------------------------|-----------------|
|          | $Mn^{2+}$              | $Mg^{2+}$       | $Mn^{2+}$                | $Mg^{2+}$       |
| GTP      | $9.2 \pm 0.79$         | $73.6 \pm 6.02$ | $27 \pm 6$               | $260 \pm 32$    |
| ITP      | $45.4 \pm 3.6$         | $233 \pm 15.8$  | $100 \pm 20$             | $1,100 \pm 220$ |
| UTP      | $63.9 \pm 9.21$        | $138 \pm 2.53$  | $120 \pm 14$             | $330 \pm 80$    |
| CTP      | $5.10 \pm 0.38$        | $45.2 \pm 9.18$ | $35 \pm 1$               | $270 \pm 43$    |
| MANT-ATP | $0.58 \pm 0.09$        | $1.36 \pm 0.57$ | $4.3 \pm 0.4$            | $51 \pm 1$      |
| MANT-GTP | $2.49 \pm 0.08$        | $4.70 \pm 0.32$ | $5.9 \pm 1.0$            | $16 \pm 2$      |
| MANT-ITP | $4.06 \pm 0.06$        | $10.6 \pm 3.29$ | $0.6 \pm 0.1$            | $16 \pm 4$      |
| MANT-UTP | $3.67 \pm 0.08$        | $32.2 \pm 0.82$ | $2.6 \pm 0.3$            | $42 \pm 9$      |
| MANT-CTP | $0.10 \pm 0.01$        | $1.26 \pm 0.09$ | $1.1 \pm 0.1$            | $36 \pm 4$      |



### 1.3. Cyclic nucleotides – Small Molecules in Signal Transduction

cAMP and cGMP have been identified as second messengers and play an important role in various biological regulatory mechanisms. However, this field has ever since been determined by scepticism, misunderstanding, and sometimes even ignorance until certain facts were accepted by the research community, e.g. when discovering that the first second messenger to be found was not acid-labile like all other nucleotide phosphates, that hormone-sensitive cAMP production required GTP, that a small reactive gas like NO should be activator of soluble guanylyl cyclase (sGC), and that cAMP and cGMP concentrations are regulated on a millisecond timescale.<sup>71</sup>

The importance of these cyclic nucleotide second messengers has been awarded with five Nobel prizes between 1971 and 2000. Second messengers are defined as low molecular-mass messenger substances transmitting extracellular signals to intracellular sites. Second messengers are released by specific enzyme reactions during the signal transduction process and act as effectors regulating activity of proteins within the signaling cascade. Second messengers are diffusible signal molecules that may be hydrophobic and membrane-located such as 1,2-diacyl glycerol or hydrophilic and cytosolic such as cAMP, cGMP, inositol phosphates and  $\text{Ca}^{2+}$ .<sup>72</sup>

cAMP produced by ACs regulates such diverse processes as gluconeogenesis, glycolysis, lipogenesis, muscle contraction, learning process, ion transport, differentiation, growth control and apoptosis *via* several mechanisms that may be specifically localized and compartmentalized in order to achieve specific and precise activity. Control of cAMP concentrations within the cell not only occurs *via* synthesis but also *via* degradation by phosphodiesterases (PDEs). Hitherto, three groups of proteins have been identified that are allosterically activated by cAMP namely cAMP-gated ion channels, PKA and guanine nucleotide exchange factors (GEF). cAMP-gated ion channels regulate  $\text{Ca}^{2+}$  as well as  $\text{Na}^+$  and  $\text{K}^+$  flows and, therefore, engage in depolarization or hyperpolarization of membranes. GEFs are known as regulators for small GTPases. cAMP activates for example Epac, a GEF of Rap1. Epac undergoes conformational change upon cAMP binding and has increased exchange activity. GEFs are involved in activation of protein kinase B-Raf and mitogen activated signaling (MAPK) pathways eventually leading to changes in transcription.<sup>72,73</sup>

PKA has two regulatory (R) and two catalytic (C) subunits, forming a mixed tetramer  $\text{R}_2\text{C}_2$  in the inactive state. cAMP binds cooperatively to the two cAMP-binding sites at subunit R and activates the complex. The R subunits dissociate from the C subunits, thereby, activating PKA. PKA phosphorylates several down-stream enzymes, changing their conformation. PKA may e.g. phosphorylate and activate a PDE, specifically degrading cAMP

acting as autoinhibitory feedback loop, additional protein kinases involved e.g. in glucogen metabolism, and the CREB. CREB is a transcription factor for genes with *cis*-regulatory, cAMP sensitive DNA elements (cAMP responsive elements (CREs)). By activating CREB PKA induces transcriptional changes in target genes leading to an alteration in protein inventory.<sup>72,74</sup>

cGMP signaling is mediated by soluble and particulate guanylyl cyclases (sGC and pGC). sGC is a heterodimeric, soluble protein regulated by NO, whereas pGC has transmembrane spans and integrated receptor functionality. pGCs are also called natriuretic peptide receptors (NPRs) for their ligand was discovered to be atrial natriuretic peptide (ANP) leading to vasodilation of blood vessels. Furthermore, pGCs and photosensitive cGMP-specific PDEs are involved in phototransduction. However, there are still orphan pGCs reported where no stimulator is known, yet. The produced cGMP activates cation channels at intracellular sites, a cAMP-specific PDE, and cGMP-dependent protein kinase (PKG) targeting e.g.  $\text{Ca}^{2+}$ -channels and myosin specific protein phosphatase.<sup>72,75</sup>

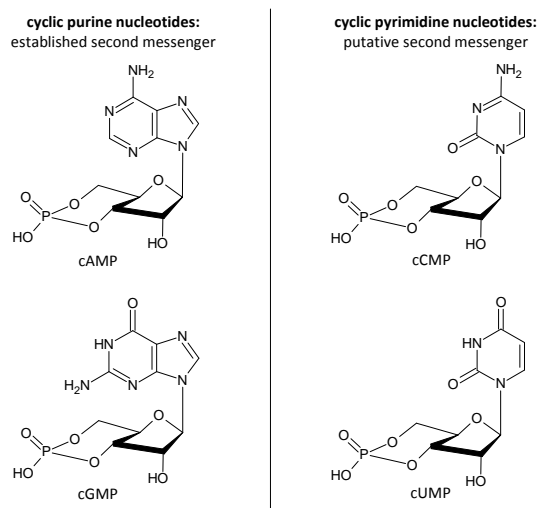


**Fig. 1.11.** Molecular structures of known second messenger cAMP and cGMP and putative pyrimidine cyclic nucleotide messenger molecules.

The past years have brought the realization that many newly discovered pathways that regulate cellular processes are themselves regulated by cNMP-dependent processes. Beavo and Brunton have once commented on the history of cyclic nucleotide research: “For researchers in the field who thought that all of the important reasons to study cyclic nucleotides had largely passed 10 years ago, it is exciting, but also sobering, to study these new systems. It is exciting because of the high interest in these areas of research. It is sobering because we now realize that we did not get all of it right the first time.”<sup>71</sup>

Apart from the cyclic purine bases cAMP and cGMP the existence of cCMP (for structures of cNMPs see Fig. 1.11.) had been claimed in the 1970s. A cCMP-specific PDE and measurable amounts of cCMP by radioimmunoassay in rat liver and kidney were claimed, as well.<sup>3,76</sup> The subject heading of the publication “Cytidine 3',5'-monophosphate (cCMP) is not an endogenous nucleotide in normal or regenerating rat liver” illustrates of how controversial the issue is.<sup>4</sup> It was argued, that in chromatography, the fractions thought to be cCMP had to be CMP or CDP and that antibodies applied were cross-reactive and did not solely detect cCMP. Although Newton *et al.* tried to provide evidence for the presence of

cCMP in tissue homogenates by fast-atom bombardment mass spectrometry (FAB-MS), doubts remained.<sup>5</sup>

Newton and his research group announced the identification of cCMP, cUMP, cIMP and cTMP in tissue extracts by FAB-MS, in 1993, and the detection of cytidylyl cyclase activity and acetylated and aspartylated cCMP side-products in rat liver, brain and heart homogenates, supernatants, precipitates, and washed precipitates, in 1997.<sup>77,78</sup> What is curious, however, is the fact that all fractions of the tissue homogenates showed cytidylyl cyclase activity, but no  $V_{\max}$  values were given leaving the suspicion that something may have gone wrong with the assay. Furthermore, the signals for cCMP, cUMP, cIMP and cTMP in tissue extracts could also be interpreted as “noise” or “background signal” from a critical point of view.

Nevertheless, physiological effects when treating neutrophils and macrophages with the cell-permeable cCMP analog  $N^4,2'$ -*O*-dibutyryl cCMP (Bt<sub>2</sub>cCMP) including inhibition of superoxide formation, increase of intracellular  $\text{Ca}^{2+}$  concentration and modulated eicosanoid synthesis have been reported.<sup>79,80</sup> More recently, the unexpected binding preference for cCMP of the radial spoke protein-2 (RSP2) in flagella of *Chlamydomonas reinhardtii* with yet undefined function has been discovered. RSP2 is known to contain a GAF domain, which may be a target for cCMP binding.<sup>81</sup> Additionally, the phosphorylation of proteins including Rab23 present in murine brain in response to cCMP involved in cell organization, proliferation, cell cycle regulation, cell development, and transcription was shown.<sup>82,83</sup>

Due to cCMP history, cCMP has become the “bad seed” in cyclic nucleotide research. Due to the controversial discussion and the suspicion that some of the results obtained with cCMP may be artefacts cCMP research has become a subject considered off-limits.

## 1.4. Detection and Quantitation Methods for Nucleotides

### 1.4.1. Luminescent Lanthanide Complexes for the Determination of Nucleotides

Lanthanides are, strictly seen, the 14 elements that follow lanthanum in the periodic table. Lanthanides are hard, electropositive metals. The preference for binding donor atoms is, therefore, in the order  $\text{O} > \text{N} > \text{S}$ . Ligand coordination occurs predominantly *via* ionic interactions, leading to a strong preference for donor groups with negatively charged oxygen (hard bases). Water molecules also can act as strong ligands for lanthanides. In aqueous solution these can usually only be replaced by other hard donor groups. Lanthanide complexes exhibit coordination numbers from six to twelve, with eight and nine being most common.<sup>84,85,86,87</sup>

The possession of an unfilled 4f electronic shell imparts some unique properties to these elements. The lanthanides are easily oxidized and prefer the oxidation state +III. The electronic shielding of the f-orbitals is quite weak. Therefore, they are contracted and insulated from the environment. The interaction with ligand orbitals is very weak and the  $f \rightarrow f$  transitions result in very sharp peaks with quite long-lived luminescence lifetimes. The luminescence spectra of  $\text{Eu}^{3+}$  complexes, which exhibit a  $4f^6$  electronic configuration, are dominated by emission bands corresponding to the  $^5\text{D}_0 \rightarrow ^7\text{F}_j$  transitions. The strongest intensities are observed for  $^5\text{D}_0 \rightarrow ^7\text{F}_1$  and  $^5\text{D}_0 \rightarrow ^7\text{F}_2$  transitions (see Fig. 1.12.). Particularly the latter one with its very strong and sharp emission line around 615 nm is the basis for the application of europium complexes as luminescent probes and labels. The same is the case for the  $^5\text{D}_4 \rightarrow ^7\text{F}_5$  transition of  $\text{Tb}^{3+}$  compounds ( $4f^8$  electronic configuration) centered at 543 nm. The hypersensitivity of this transition is due to its electric dipole character, and the radiative transition probability is very sensitive to the nature of the ligand environment. Thus, the emission intensity responds to chemical (or biochemical) analytes that interfere with these transitions.

The most interesting lanthanide ions are  $\text{Eu}^{3+}$  and  $\text{Tb}^{3+}$  due to their emission in the visible range of light accompanied by long luminescence decay-times and show in contrast to other lanthanide ions strong ion luminescence. Nevertheless, there are also probes developed containing Yb or Nd emitting in the near infrared.<sup>88,89</sup> However, direct excitation of a lanthanide ion is not easily achieved because of low absorption coefficients and nonradiative deactivation processes mediated by solvent molecules, especially by water. Therefore, a sensitizing chromophore is applied, which is often called the “antenna”.<sup>84,85,86,87</sup>

Sensitization of lanthanide luminescence occurs when energy is transferred from a triplet excited state of a chelating (intramolecular transfer) or a non-chelating (intermolecular transfer) organic compound. The excitation takes place between singlet states ( $S_0 \rightarrow S_1$ ) of the “antenna”. These chromophores have a small energy gap between the lowest singlet excited state ( $S_1$ ) and the triplet state ( $T_1$ ). After intersystem crossing to this triplet excited state of the organic compound, energy is transferred from the triplet state of the antenna to the lanthanide ion. The mechanism of energy transfer is depicted in Fig. 1.12.

The hypersensitivity of certain emission bands turns lanthanide ligand complexes (LLCs) into promising candidates as probes for analytes such as anions, pH, oxygen, nucleic acids, DNA, proteins, cofactors and coenzymes. The number of probes that have been reported in literature is rather large. Therefore, this chapter is confined to complexes with certain characteristics. Foremost, they have to be responsive in aqueous solution at a pH range from 6 to 9. Furthermore, this overview does not cover lanthanide systems in which

the analyte itself actuates as sensitizer for the lanthanide ion. This principle can be used for the determination of antibiotics in aqueous solution.<sup>90,91,92</sup>

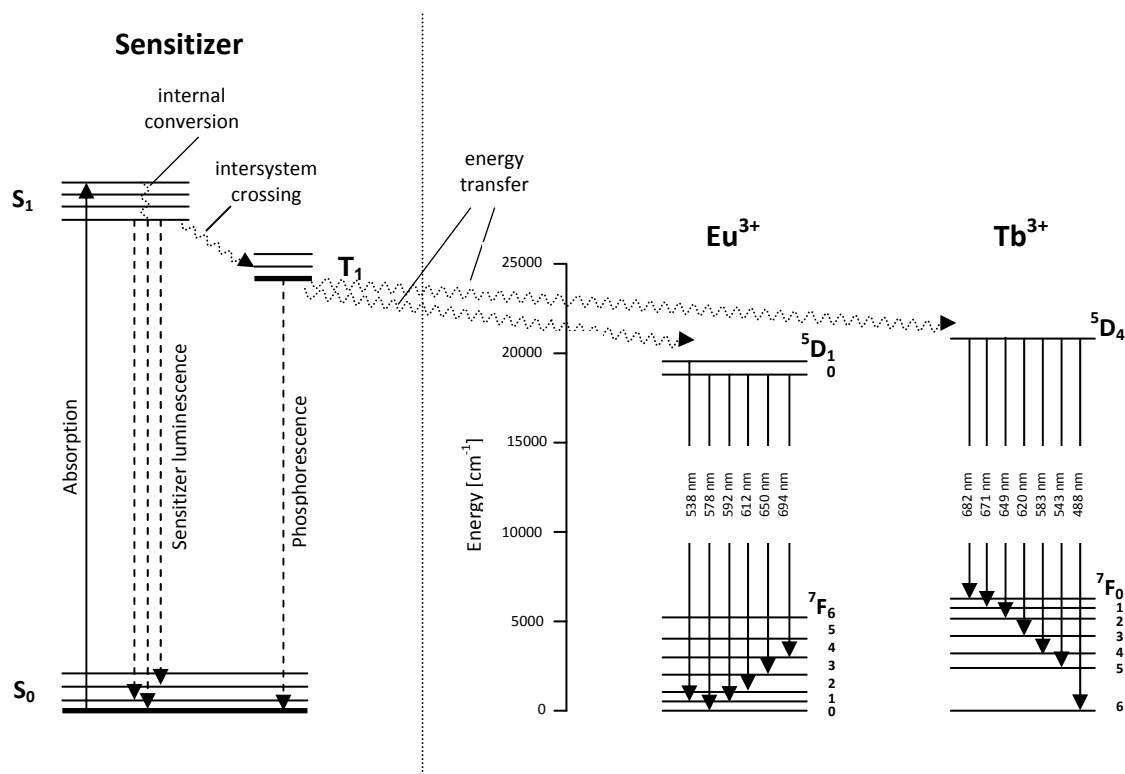


**Fig. 1.12.** Electronic energy schemes and photophysical processes for the sensitization of  $\text{Eu}^{3+}$  and  $\text{Tb}^{3+}$  ions from the triplet state of an organic compound. The absorption process takes place between the singlet ground state and the singlet excited state of the ligand.

Generally, lanthanide complexes can be divided into two subgroups. The first comprises antennae that satisfy a high degree of coordination and rigidity. These ligands bear macrocyclic or polydentate moieties that form chelate complexes with the lanthanide ion. Such ligands are often based on cyclen, cryptand, crown ether, or diethylenetriaminepentaacetic acid structures.<sup>93,94</sup>

The second group of lanthanide complexes includes ligands such as tetracyclines that interact less strongly with the respective lanthanide ions. In these cases, the analyte acts as additional ligand for the lanthanide center. The response occurs due to the exchange of more or less quenching ligands. The overall structure of these complexes is often not known and best sensitivities are sometimes obtained by combining an odd ratio of lanthanide ion to ligand, usually with an excess of metal ions. In a general perspective, the probes of the first type are based on an intramolecular energy transfer between sensitizer and lanthanide ion. Modulation of luminescence emission occurs *via* ligand-centered processes. Probes of the second type depend on an intermolecular energy transfer. Their luminescence is actuated by metal-centered interactions.<sup>84,85,86,87</sup>

The complexes applied in this work belong to the family of non-chelating ligand complexes (for structures see Fig. 1.13.).  $\text{Eu}^{3+}$  tetracycline (EuTc) was first reported by *Hirschy et al.* as 1:1 complex with high energy transfer efficiency from tetracycline to  $\text{Eu}^{3+}$ .<sup>95</sup> Later, it was discovered that the luminescence intensity of this complex is strongly increased in presence of hydrogen peroxide.<sup>96</sup> This is the first reported  $\text{Eu}^{3+}$  probe that can be excited at wavelengths  $>400$  nm.

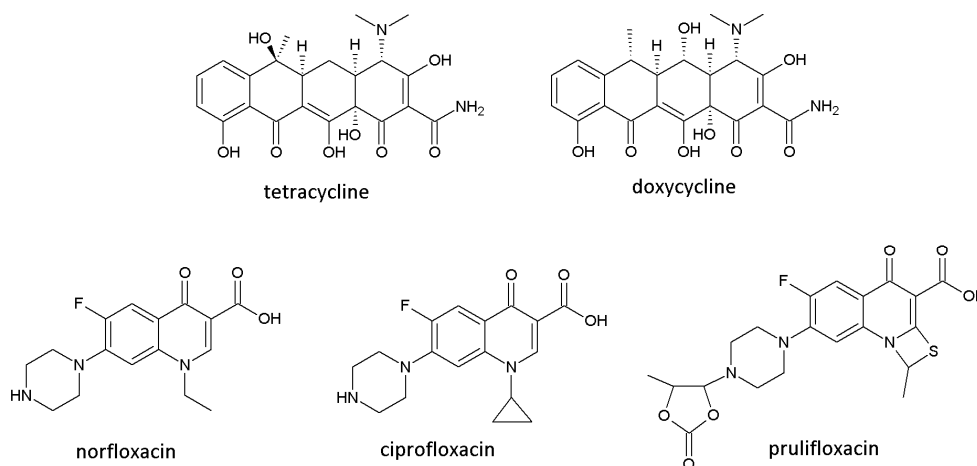


**Fig. 1.13.** Antibiotics of the tetracycline and fluoroquinolone family serving as antenna chromophores for lanthanide luminescence. Complexes with these substances are used for detection of nucleotides.

EuTc in a 3:1 stoichiometry responds to phosphate by a strong fluorescence enhancement,<sup>97</sup> whereas its luminescence in a 1:1 stoichiometry is quenched by phosphate<sup>98</sup> as well as by nucleoside 5'-phosphates such as ATP, ADP, or GTP<sup>99</sup>. Both effects can be used to apply EuTc as probe for the determination of the activities of alkaline phosphatase<sup>97</sup> and creatine kinase.<sup>99</sup> The  $\text{Eu}^{3+}$  oxytetracycline and doxycycline complexes are both sensitive to ATP in that their luminescence emission is increased.<sup>100,101</sup>

Apart from the  $\text{Eu}^{3+}$  complexes specified above, several  $\text{Tb}^{3+}$  complexes stand out because of their resistance towards interferences of ubiquitous metal ions like  $\text{Mg}^{2+}$ ,  $\text{Ca}^{2+}$ , or  $\text{Mn}^{2+}$ , and of proteins such as BSA. Terbium(III) norfloxacin is one prominent example. With a stoichiometry of 4.5:1 of  $\text{Tb}^{3+}$  to norfloxacin its luminescence responds to several biologically relevant analytes. *Miao et al.* reported that ATP enhances the luminescence of  $\text{Tb}^{3+}$  norfloxacin.<sup>102</sup> The same is observed in case of NADP,<sup>103</sup> DNA,<sup>104</sup> heparin,<sup>105</sup> GTP and GDP.<sup>106</sup> On the other hand, the emission is quenched by phosphate,<sup>103</sup> and lecithin.<sup>107</sup>

Norfloxacin belongs to a group of antibiotics referred to as fluoroquinolones. Other members of the fluoroquinolone group have also been applied to sensitize lanthanide luminescence. A further interesting example of a fluoroquinolone as sensitizer for terbium

based probes is ciprofloxacin.  $\text{Tb}^{3+}$  and ciprofloxacin were applied in a 10:1 stoichiometry to determine ATP,<sup>108</sup> heparin,<sup>109</sup> coenzyme A,<sup>110</sup> and lecithin.<sup>111</sup>

$\text{Tb}^{3+}$  prulifloxacin can be applied for the determination of ATP in pharmaceutical samples.<sup>112</sup> It is worthwhile to remind that all these complexes can act as reversible indicators for the specified analytes, as the luminescence response is based on the exchange of water ligands.

Fluorescence detection is a versatile, fast, inexpensive and straight-forward method of monitoring enzyme kinetics. It enables real-time monitoring and high throughput screening of inhibitors. However, the response of fluorescent probes is often not selective enough and fluorescence changes upon interaction with interfering substances.

#### 1.4.2. Determination and Quantitation Methods for Cyclase Reactions

Since the discovery of cAMP and cGMP as second messengers in the middle of the 20<sup>th</sup> century, the detection and quantitation of these small molecules have played an important role in nucleotide research. cAMP and cGMP are present at only very small amounts within tissues and concentrations are changing on millisecond timescales.<sup>71</sup>

Most methods for the determination of cNMPs have been developed in the 1970s but are still in use today. These techniques may be grouped into assays based on radioactivity, immunochemistry, luminescence, high pressure liquid chromatography (HPLC) or capillary electrophoresis (CE), or applicable in living cells. However, most assays satisfy more than one criterion.

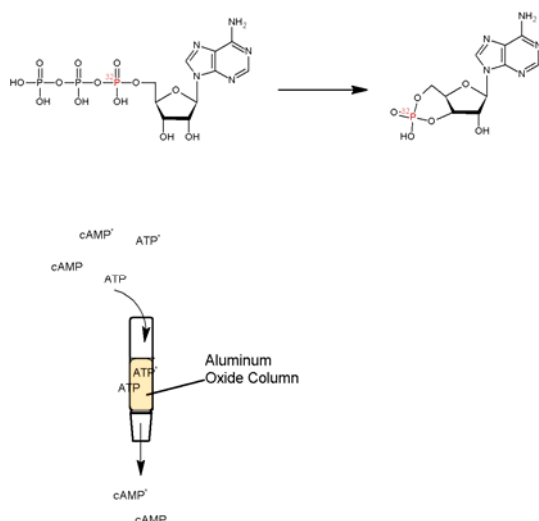


**Fig. 1.14.** The principle of radioactive determination of AC activity by separation of [ $^{32}\text{P}$ ]cAMP from its substrate [ $\alpha\text{-}^{32}\text{P}$ ]ATP via column chromatography

One prominent example for a radioactive cAMP assay is applying [ $\alpha\text{-}^{32}\text{P}$ ]-labeled ATP which is converted into [ $^{32}\text{P}$ ]cAMP. The formed [ $^{32}\text{P}$ ]cAMP has to be separated from [ $\alpha\text{-}^{32}\text{P}$ ]ATP in order to determine AC activity. The sensitivity of this assay strongly depends on low blank values and the amount of radioactivity used. The separation of the labeled cyclic nucleotide from the substrate ATP is achieved by column chromatography (see Fig. 1.14.). Various chromatographic methods have been reported, including separations on neutral alumina, Dowex anion-exchange resins combined with  $\text{ZnSO}_4$  and  $\text{Ba}(\text{OH})_2$  precipitation, and hydrous

zirconium oxide. In some cases [ $^3\text{H}$ ]cAMP was added as recovery marker. This approach is also suitable for the determination of [ $^{32}\text{P}$ ]cGMP formed in GC reactions.<sup>113,114,115,116</sup>

A further radioactive quantitation method has been in use for the determination of GC activity. [ $^{14}\text{C}$ ]GTP is converted into [ $^{14}\text{C}$ ]cGMP which is isolated by thin-layer chromatography (TLC). Part of the [ $^{14}\text{C}$ ]cGMP was then treated with PDEs and an alkaline phosphatase (ALP) in order to validate the identity of the spot on TLC plates.<sup>117</sup>

Furthermore, [ $^3\text{H}$ ]adenine is used to detect amounts of cAMP generated in living cells. The radioactively labeled base is added to cell culture medium and is transported or diffuses into the cytosol within four hours. The  $^3\text{H}$ -containing medium is replaced and stimuli for AC activity and PDE inhibitors are added. However, a disadvantage of this approach is the inevitable lysis of cells leaving no information on spatial or temporal distribution. [ $^{14}\text{C}$ ]cAMP is added to lysates as recovery marker and cell debris is eliminated by centrifugation. cAMP in the supernatant is isolated by chromatography similar to that described for [ $\alpha\text{-}^{32}\text{P}$ ]ATP (see Fig. 1.15.). [ $^3\text{H}$ ]cAMP and [ $^{14}\text{C}$ ]cAMP are determined simultaneously by a scintillation counter.<sup>118,119</sup>

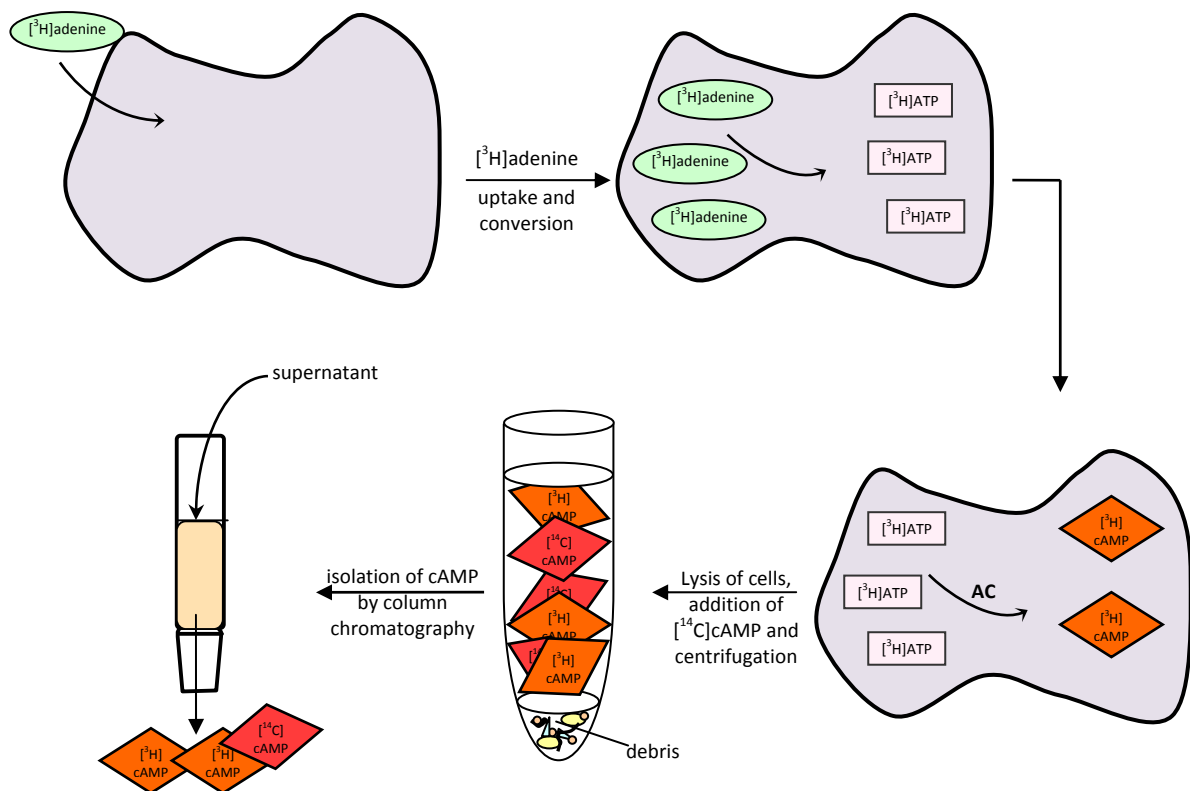


**Fig. 1.15.** [ $^3\text{H}$ ] labeled adenine is taken up into the cell and converted into [ $^3\text{H}$ ]ATP. [ $^3\text{H}$ ]ATP is converted into [ $^3\text{H}$ ]cAMP by ACs. cAMP is isolated by column chromatography after removal of cell debris by centrifugation.



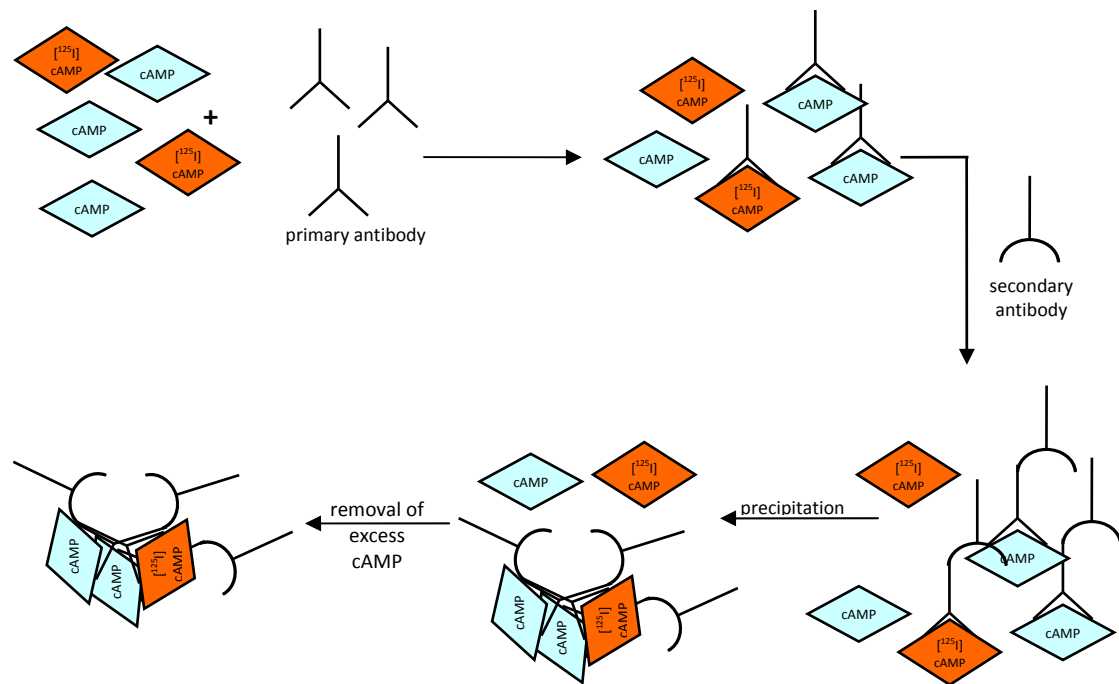


**Fig. 1.16.** Mode of operation of a RIA with immunoprecipitation.  $^{125}\text{I}$ -labeled and sample cAMP compete for primary antibodies. Antibody-bound and free cAMP are separated by immunoprecipitation with a secondary antibody.

Radioimmunoassays (RIAs) utilize antibodies directed against cNMPs in combination with competition of radioactively labeled cNMPs with free cNMPs from samples. Primary antibodies are obtained by conjugation of succinyl-cAMP to human serum albumin (HSA) and its injection into rabbits. After several booster injections the rabbits are bled out and antibodies are preserved. A high-specific activity derivative of cAMP is generated by iodinating succinyl-cAMP tyrosine methyl ester at the phenolic hydroxy group with  $^{125}\text{I}$  ( $^{125}\text{I}$ -ScAMP-TME). In general, cAMP from samples is succinylated and competes with  $^{125}\text{I}$ -ScAMP-TME for the binding sites of the cAMP-specific antibodies. Succinylation of cNMPs increases the affinity to the specific IgG. Separation of free and antibody-bound  $^{125}\text{I}$ -ScAMP-TME may be achieved either by chemical means, by immunoprecipitation with a secondary antibody (anti-rabbit IgG), or by solid phase extraction with secondary antibodies bound to a surface (see Fig. 1.16.). Several improvements have rendered dilution after succinylation of samples redundant and provided a linear range of 50-1,000 fmol. The specificity of the antibodies strongly depends on the antisera themselves. The cross-reactivity and selectivity towards cGMP and ATP for a cAMP-specific antibody may vary over two to three orders of magnitude. RIA-kits are also commercially available.<sup>120,121,122,123</sup>

Enzyme-linked immunosorbent assays (ELISAs) are based on the same principle but use different detection methods, as ELISAs work without radioactivity. The generation of primary antibodies is identical to the method described for RIAs. In general, there are

different ways to conduct an ELISA. First, cAMP may be labeled with an enzyme enabling detection. This labeled cAMP competes with succinylated standard or sample cAMP for antibody binding sites. Antibody-bound and free cAMP-derivatives are separated by secondary antibodies immobilized to a solid phase. Second, a cAMP-HSA hapten may be used to coat a surface. Residual binding sites are blocked and sample is added. Primary antibody is added and binds proportionately to immobilized and free cAMP. After washing a secondary antibody labeled with enzyme is added (see Fig.1.17.). A third method immobilizes primary anti-cAMP antibodies to a surface. cAMP is added and binds to the immobilized IgGs. A further primary antibody binds to cAMP in relation to the amount in the sample and a second antibody labeled with an enzyme is added subsequently. This format is called sandwich ELISA. Enzymes used for ELISA techniques are  $\beta$ -D-galactosidase ( $\beta$ -gal) transferring e.g. the non-fluorescent 4-methylumbelliferyl- $\beta$ -D-galactoside into the fluorescent 4-methyl-umbelliferone, ALP turning a non-colored substrate such as *p*-nitrophenylphosphate into the yellow *p*-nitrophenole, and horseradish peroxidase (HPO) catalyzing a chromogenic reaction upon oxidation of 3,3',5,5'-tetramethylbenzidine with  $H_2O_2$ . The use of monoclonal antibodies has reduced cross-reactivity further and decreased the limit of detection (LOD) to 1.56 fmol/well.<sup>124,125,126,127</sup>

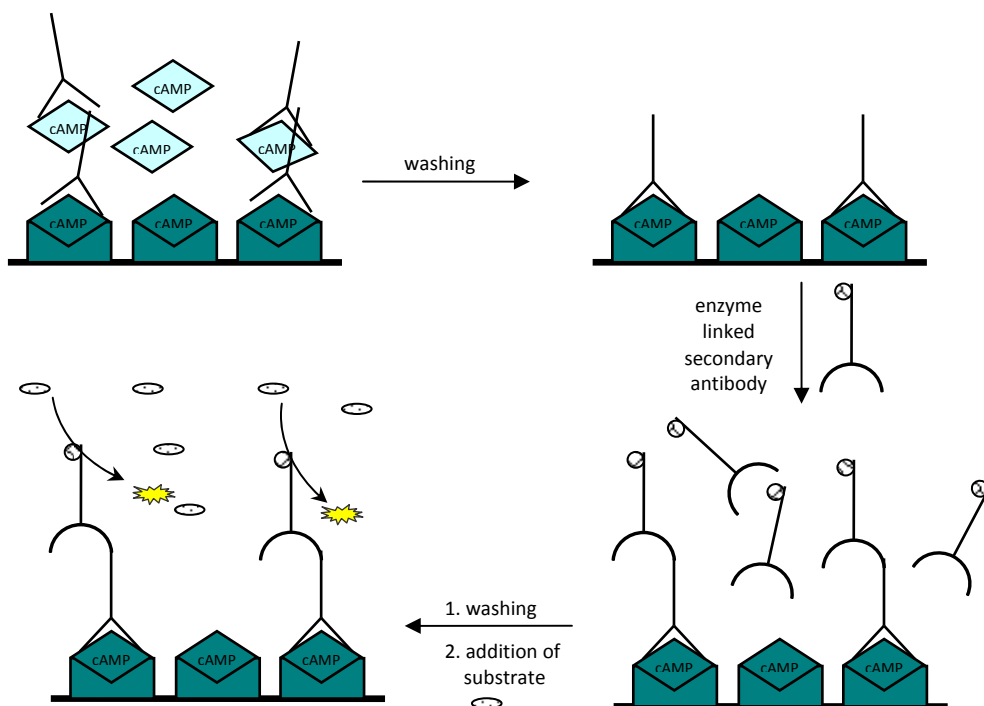


**Fig. 1.17.** The mechanism of an ELISA is shown. Immobilized and free cAMP compete for primary antibodies. After washing an enzyme-linked secondary antibody is added. The enzyme accomplishes a chromogenic or fluorogenic reaction.

Immunochemistry has also been directly combined with fluorescence techniques. cAMP may be quantified either by polarization or by FRET (see Fig. 1.18.). cAMP is

conjugated to a fluorescent label (FL-cAMP) and competes with cAMP from the sample for antibody binding. Excitation with polarized light leads to depolarized emission owing to the rotation of the molecule. The rotational freedom decreases upon binding to large molecules such as antibodies. Therefore, a higher degree of polarization is obtained when FL-cAMP is antibody-bound. Furthermore, the antibody may be labeled with another fluorescent dye which allows FRET between both labels when antibody and FL-cAMP are in close proximity.<sup>128,129</sup>

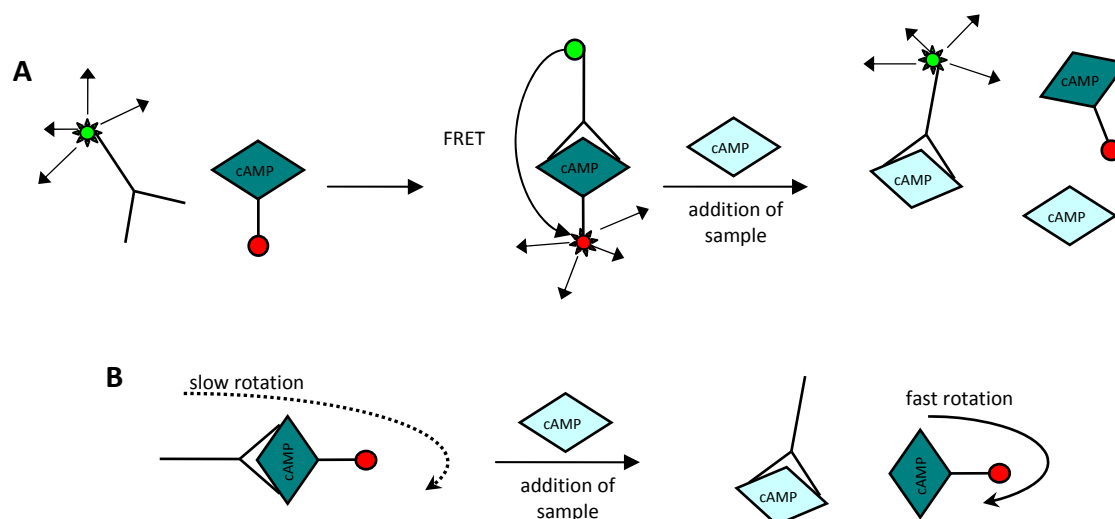


**Fig 1.18. A** Quantitation of cAMP *via* FRET techniques. When donor-labeled antibody and acceptor-labeled cAMP get in close proximity, FRET occurs. When unlabeled sample cAMP is added, the labeled cAMP is displaced from the antibody and FRET is reduced. **B** Fluorescence polarization is based upon rotational freedom of labeled cAMP. When labeled cAMP is bound to an antibody, the rotation is slowed down and depolarization decreases.

The detection of cyclase reactions may also be attained by fluorescence methods. Bodipy-GTP $\gamma$ S is used as substrate for mutant ACs. The fluorescence of the Bodipy moiety is quenched by the guanine base. Upon conversion of Bodipy-GTP $\gamma$ S to Bodipy-PP $_i$  and cGMP the quenching guanine residue is removed from the molecule and the fluorescence quantum yield increases strongly. This method can be performed in microtiter-plates without separation of analytes which renders it useful for real-time monitoring and high-throughput screening. Nevertheless, a mutant AC is required or the application of the non-physiological Mn<sup>2+</sup> ion.<sup>130</sup>

Furthermore, there are methods described using HPLC or CE to separate cNMPs from other nucleotides and the subsequent detection *via* UV-absorption, MS, or fluorescence emission upon derivatization of cNMPs. HPLC separation of cNMPs is usually achieved on reversed phase columns. Mobile phase systems base on phosphate buffers at mildly acidic pH (3.0 to 4.3) and methanol, or on formic acid in water and in acetonitrile. Total analysis times are approximately ten minutes. The lower limits of quantitation were reported to be

10 pmol for cGMP by UV detection, 10 fmol after fluorescence derivatization with (3,4-dimethoxyphenyl)glyoxal and 0.25 ng/mL for quantitation with electron spray ionisation tandem mass spectrometry (ESI-MS/MS). Additionally, one method determining AC activity uses the fluorescent Bodipy-ATP derivative which is separated by CE from generated Bodipy-cAMP. The smallest concentration of produced Bodipy-cAMP detectable was 125 nM.<sup>131,132,133,134,135</sup>

Protein binding assays exploit the high affinity of certain proteins for cAMP. One well-known example is PKA. cAMP from samples and [<sup>3</sup>H]cAMP are added to a preparation of PKA. After equilibration the solution is harvested on cellulose filters, washed several times and the filter is placed into scintillation vials (see Fig. 1.19.). A linear range of 0.15-8 pmol was reached. The use of a semiautomatic cell harvester and 96-well microtiterplates led to a throughput of 500 samples in six hours. Before the separation on cellulose filters, albumin-saturated charcoal or ammonium sulfate precipitation was used.<sup>136,137</sup>

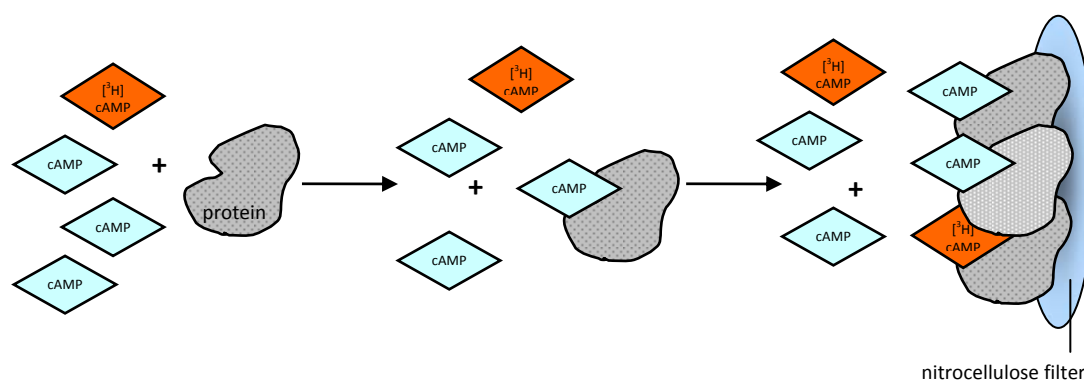


**Fig. 1.19.** A protein binding assay is presented here. Radioactively labeled cAMP and cAMP from samples compete for binding sites on high-affinity proteins that are separated from free [<sup>3</sup>H]cAMP by adsorption onto nitrocellulose filters

Another assay used  $\beta$ -gal from *E. coli* genetically engineered into two fragments. One is the enzyme acceptor (EA), the other one is an enzyme donor (ED) bound to cAMP. Individually, both fragments are inactive but upon mixing they spontaneously reassemble to form an active tetrameric protein by complementation. An anti-cAMP antibody is added to the mixture of both enzyme fragments and complexes all cAMP-ED, completely inhibiting complementation. cAMP from samples competes with cAMP-ED for the antibody binding sites. The more cAMP is present in the sample the more cAMP-ED is free for complementation. Read-out results from chromogenic, fluorogenic or chemiluminescent  $\beta$ -gal substrates.<sup>129,138</sup>

Reporter gene assays are used when apart from cAMP concentrations in cells the impact of changing cAMP concentrations on expression levels of genes is of interest. These cAMP-sensitive genes are regulated by CREB. Enzymes delivering information on their

presence *via* chromogenic or fluorogenic reactions or by being fluorescent themselves are introduced into the genome of cells. Such enzymes are  $\beta$ -lac, green fluorescent protein (GFP), or luciferase from firefly that catalyse the oxidation of luciferin into oxyluciferin resulting in chemiluminescence.<sup>128,129</sup>

The methods presented so far are suited to cell or tissue homogenates, membrane or enzyme preparations and even whole cells but do not display temporal or spatial resolution of cAMP concentrations within living cells. FRET of fluorescently labeled PKA subunits was thought to be an appropriate system. The R and C subunits were conjugated to fluorescein and rhodamine, respectively, and microinjected into cells. When the subunits form an inactive complex FRET occurs. Upon activation by cAMP the R and C subunits dissociate and FRET is prohibited. However, the process of cAMP binding and release from PKA is too slow and temporary. Moreover, spatial resolution is lost. Therefore, R and C subunits connected to cyan and yellow fluorescent protein (CFP and YFP) were transfected into cells. After expression of PKA the kinase is targeted to regions within the cell *via* A-kinase anchoring proteins (AKAPs). This system offers at least spatial distribution of cAMP compartments. Another and quicker approach is the use of genetically altered cyclic nucleotide gated ion channels (CNG-channels). They bind cAMP with even higher affinity and react quicker to changes in cAMP concentrations. The  $\text{Ca}^{2+}$  influx after activation of these CNG-channels can be quantified by Ca-sensitive dyes like fura-2, membrane-potential sensitive dyes or patch clamp experiments.<sup>139,140</sup>

All of the methods presented in this chapter exhibit several advantages and drawbacks alike. Radioactive approaches are for example extremely robust and sensitive. However, it implies the handling of radioactive material, including expensive waste disposal and risks to the health of the lab personnel due to radiation. Chromatographic or electrophoretic steps – as well in HPLC and CE as in radioactivity methods – are laborious and time-consuming. Hardly any approach described enables real-time monitoring of the cyclase activity due to the required isolation of generated cNMPs. In comparison to immunoassays, protein binding assays are less expensive as the production of monoclonal antibody is time-consuming, implies several booster injections of lab animals, and the purification of the antibodies. Cross-sensitivity of antibodies cannot be completely excluded, either. Fluorescence methods are prone to artifacts that may interfere with the fluorescence intensity such as quenching or autofluorescence of other biomolecules in reaction mixtures or non-specific interactions. The need for robust and sensitive cyclase assays enabling spatial and temporal resolution *in vivo* with no artefacts is still urgent although the LODs have been driven to the femtomolar region lately.

## 1.5. References

- <sup>1</sup> Sunahara RK, Taussig R (2002) Isoforms of mammalian adenylyl cyclase: multiplicities of signaling, *Mol Interv* **2**, 168-184
- <sup>2</sup> Defer N, Best-Belpomme M, Hanoune J (2000) Tissue specificity and physiological relevance of various isoforms of adenylyl cyclase, *Am J Physiol Renal Physiol* **279**, F400-F416
- <sup>3</sup> Cheng Y-C, Bloch A (1978) Demonstration, in leukemia L-1210 cells, of a phosphodiesterase acting on 3':5'-cyclic CMP but not on 3':5'-cyclic AMP or 3':5'-cyclic GMP, *J Biol Chem* **253**, 2522-2524
- <sup>4</sup> Wikberg JE, Wingren GB, Anderson GB (1981) Cytidine 3',5' monophosphate (cCMP) is not an endogenous nucleotide in normal or regenerating rat liver, *Acta Pharmacol Toxicol Copenh* **49**, 452-454
- <sup>5</sup> Newton RP, Hakeem NA, Salvage BJ, Wassenaar G, Kingston EE (1988) Cytidylate cyclase activity: identification of cytidine 3',5'-cyclic monophosphate and four novel cytidine cyclic phosphates as biosynthetic products from cytidine triphosphate, *Rapid Commun Mass Spectrom* **2**, 118-126
- <sup>6</sup> Kermenetsky M, Middelhaufe S, Bank EM, Levin LR, Buck, Steegborn C (2006) Molecular details of cAMP generation in mammalian cells: a tale of two systems, *J Mol Biol* **362**, 623-639
- <sup>7</sup> Sadana R, Dessauer CW (2008) Physiological roles for G protein-regulated adenylyl cyclase isoforms: insights from knockout and overexpression studies, *Neurosignals* **17**, 5-22
- <sup>8</sup> Sunahara RK, Dessauer CW, Gilman AG (1996) Complexity and diversity of mammalian adenylyl cyclases, *Annu Rev Pharmacol Toxicol* **36**, 461-480
- <sup>9</sup> Cooper DMF (2003) Regulation and organization of adenylyl cyclases and cAMP, *Biochem J* **375**, 517-529
- <sup>10</sup> Weinstein LS, Chen M, Xie T, Liu J (2006) Genetic diseases associated with heterotrimeric G proteins, *Trends Pharmacol Sci* **27**, 260-266
- <sup>11</sup> Hanoune J, Defer N (2001) Regulation and role of adenylyl cyclase isoforms, *Annu Rev Pharmacol Toxicol* **41**, 145-174
- <sup>12</sup> Tang W-J, Hurley JH (1998) Catalytic mechanism and regulation of mammalian adenylyl cyclases, *Mol Pharmacol* **54**, 231-240
- <sup>13</sup> Wang Z, Li V, Chan GC, Phan T, Nudelman AS, Xia Z, Storm DR (2009) Adult type 3 adenylyl cyclase-deficient mice are obese, *PLoS One* **4**, e6979
- <sup>14</sup> Reiaich JS, Li PP, Warsh JJ, Kish SJ, Young LT (1999) Reduced adenylyl cyclase immunolabeling and activity in postmortem temporal cortex of depressed suicide victims, *J Affect Disord* **56**, 141-151

- 
- <sup>15</sup> Abdel-Majid RM, Tremblay F, Baldrige WH (2002) Localization of adenylyl cyclase proteins in the rodent retina, *Brain Res Mol Brain Res* **101**, 62-70
- <sup>16</sup> Yan S-Z, Huang Z-H, Andrews RK, Tang W-J (1998) Conversion of forskolin-insensitive to forskolin-sensitive (mouse-type IX) adenylyl cyclase, *Mol Pharmacol* **53**, 182-187
- <sup>17</sup> Iwatsubo K, Minamisawa S, Tsunematsu T, Nakagome M, Toya Y, Tomlinsons JE, Umemura S, Scarborough RM, Levy DE, Ishikawa Y (2004) Direct inhibition of type 5 adenylyl cyclase prevents myocardial apoptosis without functional deterioration, *J Biol Chem* **279**, 40938-40945
- <sup>18</sup> Gille A, Seifert R (2003) 2'(3')-O-(N-Methylantraniloyl)-substituted GTP analogs: a novel class of potent competitive adenylyl cyclase inhibitors, *J Biol Chem* **278**, 12672-12679
- <sup>19</sup> Gille A, Lushington GH, Mou T-C, Doughty MC, Johnson RA, Seifert R (2004) Differential inhibition of adenylyl cyclase isoforms and soluble guanylyl cyclase by purine and pyrimidine nucleotides, *J Biol Chem* **279**, 19955-19969
- <sup>20</sup> Mou T-C, Gille A, Fancy DA, Seifert R, Sprang SR (2005) Structural basis for the inhibition of mammalian membrane adenylyl cyclase by 2'(3')-O-(N-methylantraniloyl)-guanosine 5'-triphosphate
- <sup>21</sup> Göttle M, Geduhn J, König B, Gille A, Höcherl K, Seifert R (2009) Characterization of mouse heart adenylyl cyclase, *J Pharmacol Exp Ther* **329**, 1156-1165
- <sup>22</sup> Suryanarayana S, Göttle M, Hübner M, Gille A, Mou T-C, Sprang SR, Richter M, Seifert R (2009) Differential inhibition of various adenylyl cyclase isoforms and soluble guanylyl cyclase by 2',3'-O-(2,4,6-trinitrophenyl)-substituted nucleoside 5'-triphosphates, *J Pharmacol Exp Ther* **330**, 687-695
- <sup>23</sup> Mou T-C, Gille A, Surayanarayana S, Richter M, Seifert R, Sprang SR (2006) Broad specificity of mammalian adenylyl cyclase for interaction with 2',3'-substituted purine- and pyrimidine nucleotide inhibitors, *Mol Pharmacol* **70**, 878-886
- <sup>24</sup> Center of Disease Control and Prevention (2001) Update: investigation of bioterrorism-related inhalational anthrax – Connecticut 2001, *MMWR Morb Mort Wkly Rep* **50**, 1049-1051
- <sup>25</sup> Robert Koch-Institut (2010) Kutaner Milzbrand nach intravenösem Heroinabusus, *Epidem Bull* **2**, 13-18
- <sup>26</sup> <http://vetmed.lsu.edu/whocc/AnthraxStats2001-DataFiles/Europe1/Spain.htm>
- <sup>27</sup> Mock M, Fouet A (2001) Anthrax, *Annu Rev Microbiol* **55**, 647-671
- <sup>28</sup> Mourez M (2004) Anthrax toxins, *Rev Physiol Biochem Pharmacol* **152**, 135-164
- <sup>29</sup> Kolstø A-B, Tourasse NJ, Økstad OA (2009) What sets *Bacillus anthracis* apart from other *bacillus* species, *Annu Rev Microbiol* **63**, 451-476

- <sup>30</sup> Friedlander AM, Little SF (2009) Advances in the development of next-generation anthrax vaccines, *Vaccine* **27**, D28-D32
- <sup>31</sup> Moldonado-Arocho FJ, Averette-Mirrashidi MA, Bradley KA (2009) Anthrax toxin, *Microbial Toxins – Current Research and Future Trends (Edited by T Proft)* Norfolk UK, Caister Academic Press, 41-79
- <sup>32</sup> [http://www.who.int/immunization\\_monitoring/diseases/pertussis/en](http://www.who.int/immunization_monitoring/diseases/pertussis/en)
- <sup>33</sup> Raguckas SE, VandenBussche HL, Jacobs C, Klepser ME (2007) Pertussis resurgence: diagnosis, treatment, prevention, and beyond, *Pharmacotherapy* **27**, 41-52
- <sup>34</sup> Wood N, McIntyre P (2008) Pertussis: review of epidemiology, diagnosis, management and prevention, *Paediatr Respir Rev* **9**, 201-212
- <sup>35</sup> Gregory DS (2006) Pertussis: a disease affecting all ages, *Am Fam Phys* **74**, 420-426
- <sup>36</sup> Singh M, Lingappan K (2006) Whooping cough, *Chest* **130**, 1547-1553
- <sup>37</sup> McIntyre P, Wood N (2009) Pertussis in early infancy: disease burden and preventive strategies, *Curr Opin Infect Dis* **22**, 215-223
- <sup>38</sup> Kerr JR, Matthews RC (2000) *Bordetella pertussis* infection: pathogenesis, diagnosis, management, and the role of protective immunity, *Eur J Clin Microbiol Infect Dis* **19**, 77-88
- <sup>39</sup> Shrivastava R, Miller JF (2009) Virulence factor secretion and translocation by *Bordetella* species, *Curr Opin Microbiol* **12**, 88-93
- <sup>40</sup> Galley J, Vincent M, de la Sierra IML, Munier-Lehmann H, Renouard M, Sakamoto H, Bârză O, Gilles AM (2004) Insight into the activation mechanism of *Bordetella pertussis* adenylate cyclase by calmodulin using fluorescence spectroscopy, *Eur. J Biochem* **271**, 821-833
- <sup>41</sup> Sarfati RS, Kansal VK, Munier H, Glaser P, Gilles A-M, Labruyère E, Mock M, Danchin A, Bârză O (1990) Binding of 3'-anthraniloyl-2'-deoxy-ATP to calmodulin activated adenylate cyclase from *Bordetella pertussis* and *Bacillus anthracis*, *J Biol Chem* **265**, 18902-18906
- <sup>42</sup> Escuyer V, Duflot E, Sezer O, Danchin A, Mock M (1988) Structural homology between virulence-associated bacterial adenylate cyclases, *Gene* **71**, 293-298
- <sup>43</sup> Ladant D, Michelson S, Sarfati R, Gilles A-M, Predeleanu R, Bârză O (1989) Characterization of the calmodulin-binding and of the catalytic domain of *Bordetella pertussis* adenylate cyclase, *J Biol Chem* **264**, 4015-4020
- <sup>44</sup> Ladant D, Ullmann A (1999) *Bordetella pertussis* adenylate cyclase: a toxin with multiple talents, *Trends Microbiol* **7**, 172-176
- <sup>45</sup> Drum CL, Yan S-Z, Sarac R, Mabuchi Y, Beckingham K, Bohm A, Grabarek Z, Tang W-J (2000) An extended conformation of calmodulin induces interactions between the structural domains of adenylate cyclase from *Bacillus anthracis* to promote catalysis, *J Biol Chem* **275**, 36334-36340



- 
- <sup>46</sup> Shen Y, Lee Y-S, Soelaiman S, Bergson P, Lu D, Chen A, Beckingham K, Grabarek Z, Mrksich M, Tang W-J (2002) Physiological calcium concentrations regulate calmodulin binding and catalysis of adenylyl cyclase exotoxins, *EMBO J* **21**, 6721-6732
- <sup>47</sup> Tang W-J, Guo Q (2009) The adenylyl cyclase activity of anthrax edema factor, *Mol Aspects Med* **30**, 423-430
- <sup>48</sup> Drum CL, Yan S-Z, Bard J, Shen Y-Q, Lu D, Soelaiman S, Grabarek Z, Bohm A, Tang W-J (2002) Structural basis for the activation of anthrax adenylyl cyclase exotoxin by calmodulin, *Nature* **414**, 396-402
- <sup>49</sup> Ulmer TS, Soelaiman S, Li S, Klee CB, Tang W-J, Bax A (2003) Calcium dependence of the interaction between calmodulin and anthrax edema factor, *J Biol Chem* **278**, 29261-29266
- <sup>50</sup> Shen Y, Guo Q, Zhukovskays NL, Drum CL, Bohm A, Tang W-J (2004) Structure of anthrax edema factor-calmodulin-adenosine 5'-( $\alpha,\beta$ -methylene)-triphosphate complex reveals an alternative mode of ATP binding to the catalytic site, *Biochem Biophys Res Commun* **317**, 309-314
- <sup>51</sup> Guo Q, Shen Y, Zhukovskaya NL, Florián J, Tang W-J (2004) Structural and kinetic analyses of the interaction of anthrax adenylyl cyclase toxin with reaction products cAMP and pyrophosphate, *J Biol Chem* **279**, 29427-29435
- <sup>52</sup> Shen Y, Zhukovskays NL, Guo Q, Florián J, Tang W-J (2005) Calcium-independent calmodulin binding and two-metal-ion catalytic mechanism of anthrax edema factor, *EMBO J* **24**, 929-941
- <sup>53</sup> Gupta M, Alam S, Bhatnagar R (2006) Kinetic characterization and ligand binding studies of His 351 mutants of *Bacillus anthracis* adenylate cyclase, *Arch Biochem Biophys* **446**, 28-34
- <sup>54</sup> Munier H, Bouhss A, Krin E, Danchin A, Gilles A-M, Glaser P, Bârză O (1992) The role of histidine 63 in the catalytic mechanism of *Bordetella pertussis* adenylate cyclase, *J Biol Chem* **267**, 9816-9820
- <sup>55</sup> Guo Q, Shen Y, Lee Y-S, Gibbs CS, Mrksich M, Tang W-J (2005) Structural basis for the interaction of *Bordetella pertussis* adenylyl cyclase toxin with calmodulin, *EMBO J* **24**, 3190-3201
- <sup>56</sup> Soelaiman S, Wei BQ, Bergson P, Lee Y-S, Shen Y, Mrksich M, Shoichet BK, Tang W-J (2003) Structure-based inhibitor discovery against adenylyl cyclase toxins from pathogenic bacteria that cause anthrax and whooping cough, *J Biol Chem* **278**, 25990-25997
- <sup>57</sup> Ahuja N, Kumar P, Bhatnagar R (2004) The adenylate cyclase toxins, *Crit Rev Microbiol* **30**, 187-196
- <sup>58</sup> Firoved AM, Miller GF, Moayeri M, Kakkar R, Shen Y, Wiggins JF, McNally EM, Tang W-J, Leppla SH (2005) *Bacillus anthracis* edema toxin causes extensive tissue lesions and rapid lethality in mice, *Am J Pathol* **167**, 1309-1320

- 
- <sup>59</sup> Glaser P, Ladant D, Sezer O, Pichot F, Ullmann A, Danchin A (1988) The calmodulin-sensitive adenylate cyclase of *Bordetella pertussis*: cloning and expression in *Escherichia coli*, *Mol Microbiol* **2**, 19-30
- <sup>60</sup> Carbonetti NH, Artamonova GV, Andreasen C, Bushar N (2005) Pertussis toxin and adenylate cyclase toxin provide a one-two punch for establishment of *Bordetella pertussis* infection of the respiratory tract, *Infect Immun* **73**, 2698-2703
- <sup>61</sup> Boyd AP, Ross PJ, Conroy H, Mahon N, Lavelle EC, Mills KHG (2005) *Bordetella pertussis* adenylate cyclase toxin modulates innate and adaptive immune responses: distinct roles for acylation and enzymatic activity in immunomodulation and cell death, *J Immun* **175**, 730-738
- <sup>62</sup> Basler M, Masin J, Osicka R, Sebo O (2006) Pore-forming and enzymatic activities of *Bordetella pertussis* adenylate cyclase toxin synergize in promoting lysis of monocytes, *Infect Immun* **74**, 2207-2214
- <sup>63</sup> Leppla SH (1982) Anthrax toxin edema factor: a bacterial adenylate cyclase that increases cyclic AMP concentrations in eukaryotic cells, *Proc Natl Acad Sci USA* **79**, 3162-3166
- <sup>64</sup> Kamanova J, Kofronova O, Masin J, Genth H, Vojtova J, Linhartova I, Benada O, Just I, Sebo P (2008) Adenylate cyclase toxin subverts phagocyte function by RhoA inhibition and unproductive ruffling, *J Immunol* **181**, 5587-5597
- <sup>65</sup> Crawford MA, Aylott CV, Bourdeau RW, Bokoch GM (2006) *Bacillus anthracis* toxins inhibit human neutrophil NADPH oxidase activity, *J Immunol* **176**, 7557-7565
- <sup>66</sup> Voth DE, Hamm EE, Nguyen LG, Tucker AE, Salles II, Oritz-Leduc W, Ballard JD (2005) *Bacillus anthracis* oedema toxin as a cause of tissue necrosis and cell type-specific cytotoxicity, *Cell Microbiol* **7**, 1139-1149
- <sup>67</sup> Hiratsuka T (1983) New ribose-modified fluorescent analogs of adenine and guanine nucleotides available as substrates for various enzymes, *Biochim Biophys Acta* **742**, 496-508
- <sup>68</sup> Hiratsuka T (2003) Fluorescent and colored trinitrophenylated analogs of ATP and GTP, *Eur J Biochem* **270**, 3479-3485
- <sup>69</sup> Göttle M, Dove S, Steindel P, Shen Y, Tang W-J, Geduhn J, König B, Seifert R (2007) Molecular analysis of the interaction of *Bordetella pertussis* adenylate cyclase with fluorescent nucleotides, *Mol Pharmacol* **72**, 526-535
- <sup>70</sup> Taha HM, Schmidt J, Göttle M, Suryanarayana S, Shen Y, Tang W-J, Gille A, Geduhn J, König B, Dove S, Seifert R (2009) Molecular analysis of the interaction of anthrax adenylate cyclase toxin, edema factor, with 2'(3')-O-(N-(methyl)anthraniloxy)-substituted purine and pyrimidine nucleotides, *Mol Pharmacol* **75**, 693-703

- 
- <sup>71</sup> Beavo JA, Brunton LL (2002) Cyclic nucleotide research – still expanding after half a century, *Nature Rev Mol Cell Biol* **3**, 710-718
- <sup>72</sup> Krauss G (2003) Biochemistry of signal transduction and regulation, 3<sup>rd</sup> *Completely Revised Edition*, Wiley-VCH Weinheim, 231-236
- <sup>73</sup> Antoni FA (2000) Molecular diversity of cyclic AMP signalling, *Front Neuroendocrin* **21**, 103-132
- <sup>74</sup> Daniel PB, Walker WH, Habener JF (1998) Cyclic AMP signaling and gene regulation, *Annu Rev Nutr* **18**, 353-383
- <sup>75</sup> Kots AY, Martin E, Sharina IG, Murad F (2009) A short history of cGMP, guanylyl cyclases, and cGMP-dependent protein kinases, *HHHW Schmidt, F Hofman, J-P Stasch: cGMP: Generators, Effectors and Therapeutic Implications Handbook of Experimental Pharmacology* **191**, Springer-Verlag Berlin-Heidelberg, 1-14
- <sup>76</sup> Cailla HL, Roux D, Delaage M, Goridis C (1978) Radioimmunological identification and measurement of cytidine 3',5'-monophosphate in rat tissue, *Biochem Biophys Res Commun* **85**, 1503-1509
- <sup>77</sup> Newton RP (1993) Contributions of fast-atom bombardment mass spectrometry to studies of cyclic nucleotide biochemistry, *Rapid Commun Mass Spectrom* **7**, 528-537
- <sup>78</sup> Newton RP, Groot N, van Geyschem J, Diffley PE, Walton TJ, Bayliss MA, Harris FM, Games DE, Brenton AG (1997) Estimation of cytidylyl cyclase activity and monitoring of side-product formation by fast-atom bombardment mass spectrometry, *Rapid Commun Mass Spectrom* **11** 189-194
- <sup>79</sup> Ervens J, Seifert R (1991) Differential modulation by *N*<sup>4</sup>,2'-*O*-dibutyryl cytidine 3':5'-cyclic monophosphate of neutrophil activation, *Biochem Biophys Res Commun* **174**, 258-267
- <sup>80</sup> Elliot GR, Lauwen APM, Bonta IL (1991) Dibutyryl cytidine 3':5'-cyclic monophosphate; an inhibitor of A23187-stimulated macrophage leukotriene B<sub>4</sub> synthesis, *Agents Actions* **32**, 90-91
- <sup>81</sup> Yao H, Sem DS (2005) Cofactor fingerprinting with STD NMR to characterize proteins of unknown function: identification of a rare cCMP cofactor preference, *FEBS Lett* **579**, 661-666
- <sup>82</sup> Bond AE, Dudley E, Tuytten R, Lemièrre F, Smith CJ, Esmans EL, Newton RP (2007) Mass spectrometric identification of Rab23 phosphorylation as a response to challenge by cytidine 3',5'-cyclic monophosphate in mouse brain, *Rapid Commun Mass Spectrom* **21**, 2685-2692
- <sup>83</sup> Ding S, Bond AE, Lemièrre F, Tuytten R, Esmans EL, Brenton AG, Dudley E, Newton RP (2008) Online immobilized metal affinity chromatography/mass spectrometric analysis of

- changes elicited by cCMP in the murine brain phosphoproteome, *Rapid Commun Mass Spectrom* **22**, 4129-4138
- <sup>84</sup> Dos Santos CMG, Harte AJ, Quinn SJ, Gunnlaugson T (2008) Recent developments in the field of supramolecular lanthanide luminescent sensors and self-assemblies, *Coord Chem Rev* **252**, 2512-2527
- <sup>85</sup> Georges J (1993) Lanthanide sensitized luminescence and applications to the determination of organic analytes, *Analyst* **118**, 1481-1486
- <sup>86</sup> Gunnlaugsson T, Stomeo F (2007) Recent advances in the formation of luminescent lanthanide architectures and self-assemblies from structurally defined ligands, *Org Biomol Chem* **5**, 1999-2009
- <sup>87</sup> Richardson FS (1982) Terbium(III) and europium(III) ions as luminescent probes and stains for biomolecular systems, *Chem Rev* **82**, 541-552
- <sup>88</sup> Glover PB, Ashton PR, Childs LJ, Rodger A, Kercher M, Williams RM, De Cola L, Pikramenou Z (2003) Hairpin-shaped heterometallic luminescent lanthanide complexes for DNA intercalative recognition, *J Am Chem Soc* **125**, 9918-9919
- <sup>89</sup> Beeby A, Dickins RS, FitzGerald S, Govenlock LJ, Parker D, Williams JAG, Maupin CL, Riehl JP, Siligardi G (2000) Porphyrin sensitization of circularly polarized near-IR lanthanide luminescence: enhanced emission with nucleic acid binding, *Chem Commun*, 1183-1184
- <sup>90</sup> Rodriguez-Diaz RC, Fernandez-Romero JM, Aguilar-Cabellos MP, Gmoez-Hens A (2006) Determination of fluoroquinolones in milk samples by postcolumn derivatization liquid chromatography with luminescence detection, *J Agric Food Chem* **54**, 9670-9676
- <sup>91</sup> Hernandez-Arteseros JA, Compano R, Prat MD (1998) Determination of ciprofloxacin and enrofloxacin in edible animal tissues by terbium-sensitized luminescence, *Analyst* **123**, 2729-2732
- <sup>92</sup> Arnaud N, Georges J (2001) Sensitive detection of tetracyclines using europium-sensitized fluorescence with EDTA as co-ligand and cetyltrimethylammonium chloride as surfactant, *Analyst* **126**, 694-697
- <sup>93</sup> Li C, Law G-L, Wong W-T (2004) Luminescent Tb<sup>3+</sup> complex with pendant crown ether showing dual-component recognition of H<sup>+</sup> and K<sup>+</sup> at multiple pH windows, *Org Lett* **6**, 4841-4844
- <sup>94</sup> Tremblay MS, Sames D (2006) Synthesis of luminescent heterometallic bis-lanthanide complexes *via* selective, sequential metalation, *Chem Commun*, 4116-4118
- <sup>95</sup> Hirschy LM, Van Geel TF, Winefordner JD, Kelly RN, Schulman SG (1984) Characteristics of the binding of europium(III) to tetracycline, *Anal Chim Acta* **166**, 207-219

- 
- <sup>96</sup> Rakicioglu Y, Perrin JH, Schulman SG (1999) Increased luminescence of the tetracycline-europium(III) system following oxidation by hydrogen peroxide, *J Pharm Biomed Anal* **20**, 397-399
- <sup>97</sup> Schrenkhammer P, Rosnizeck IC, Dürkop A, Wolfbeis OS, Schäferling M (2008) Time-resolved fluorescence-based assay for the determination of alkaline phosphatase activity and application to the screening of its inhibitors, *J Biomol Screen* **13**, 9-16
- <sup>98</sup> Duerkop A, Turel M, Lobnik A, Wolfbeis OS (2006) Microtiter plate assay for phosphate using a europium-tetracycline complex as a sensitive luminescent probe, *Anal Chim Acta* **555**, 292-298
- <sup>99</sup> Schäferling M, Wolfbeis OS (2007) Europium tetracycline as a luminescent probe for nucleoside phosphates and its application to the determination of kinase activity, *Chem Eur J* **13**, 4342-4349
- <sup>100</sup> Hou F, Miao Y, Jiang C (2005) Determination of adenosine disodium triphosphate (ATP) using oxytetracycline-Eu<sup>3+</sup> as a fluorescence probe by spectrofluorimetry, *Spectrochim Acta A* **61**, 2891-2895
- <sup>101</sup> Hou F, Wang X, Jiang C (2005) Determination of ATP as a fluorescence probe with europium(III)-doxycycline, *Anal Sci* **21**, 231-234
- <sup>102</sup> Miao Y, Liu J, Hou F; Jiang C (2004) Determination of adenosine disodium triphosphate (ATP) using norfloxacin-Tb<sup>3+</sup> as a fluorescence probe by spectrofluorimetry, *J Lumin* **116**, 67-72
- <sup>103</sup> Wang Y, Liu J, Jiang C (2005) Spectrofluorimetric determination of trace amounts of coenzyme II using norfloxacin-terbium complex as a fluorescent probe, *Anal Sci* **21**, 709-711
- <sup>104</sup> Tong C, Hu Z, Liu W (2005) Sensitive determination of DNA based on the interaction between norfloxacin-Tb<sup>3+</sup> complex and DNA, *J Agric Food Chem* **53**, 6207-6212
- <sup>105</sup> Wang H, Wang Y, Jiang C (2005) Fluorimetric study of the interaction between heparin and norfloxacin-terbium complex and its application, *Anal Lett* **38**, 167-178
- <sup>106</sup> Spangler C, Spangler CM, Spoerner M, Schäferling M (2009) Kinetic determination of the GTPase activity of Ras proteins by means of a luminescent terbium complex, *Anal Bioanal Chem* **394**, 989-996
- <sup>107</sup> Bian W, Jiang C (2006) Highly sensitive spectrofluorimetric determination of trace amounts of lecithin using a norfloxacin-terbium probe, *Clin Chim Acta* **368**, 144-148
- <sup>108</sup> Huo F, Liu J, Jiang C (2005) Fluorescence study of the interaction between adenosine disodium triphosphate (ATP) and ciprofloxacin-Tb<sup>3+</sup> and its analytical application, *Anal Lett* **38**, 281-289

- <sup>109</sup> Miao Y, Hou F, Jiang C (2005) Determination of heparin using ciprofloxacin-Tb<sup>3+</sup> as a fluorescence probe, *Anal Sci* **21**, 1207-1211
- <sup>110</sup> Li J, Ge X, Jiang C (2007) Spectrofluorimetric determination of trace amounts of coenzyme A using a terbium ion-ciprofloxacin complex probe in the presence of periodic acid, *Anal Bioanal Chem* **387**, 2083-2089
- <sup>111</sup> Bian W, Jiang C (2006) Highly sensitive spectrofluorimetric determination of trace amounts of lecithin, *Anal Bioanal Chem* **385**, 861-865
- <sup>112</sup> Yu F, Li L, Chen F (2008) Determination of adenosine disodium triphosphate using prulifloxacin-terbium(III) as a fluorescence probe by spectrofluorimetry, *Anal Chim Acta* **610**, 257-262
- <sup>113</sup> Salomon Y, Londos C, Rodbell M (1974) A highly sensitive adenylate cyclase assay, *Anal Biochem* **58**, 541-548
- <sup>114</sup> White AA, Zenser TV (1971) Separation of cyclic 3',5'-nucleoside monophosphates from other nucleotides on aluminum oxide columns: application to the assay of adenylyl cyclase and guanylyl cyclase, *Anal Biochem* **41**, 372-396
- <sup>115</sup> Ramachandran J (1971) A new simple method for separation of adenosine 3',5'-cyclic monophosphates from other nucleotides and its use in the assay of adenylyl cyclase, *Anal Biochem* **43**, 227-239
- <sup>116</sup> Bockaert J, Hunzicker-Dunn M, Birnbaumer L (1976) Hormone-stimulated desensitization of hormone-dependent adenylyl cyclase: dual action of luteinizing hormone on pig graafian follicle membranes, *J Biol Chem* **251**, 2653-2663
- <sup>117</sup> Schultz G, Bohme E, Hardman JG (1969) Guanylyl cyclase. Determination of enzyme activity, *Life Sci* **8**, 1323-1332
- <sup>118</sup> Soderstrom K, Choi H, Berman FW, Aldrich JV, Murray TF (1997) N-Alkylated derivatives of [D-pro<sup>10</sup>]dynorphin A-(1-11) are high affinity partial agonists at the cloned rat  $\kappa$ -opioid receptor, *Eur J Pharmacol* **338**, 191-197
- <sup>119</sup> Bennett MA, Murray TF, Aldrich JV (2005) Structure-activity relationships of arodyn, a novel acetylated kappa opioid receptor antagonist, *J Peptide Res* **65**, 322-332
- <sup>120</sup> Steiner AL, Kipnis DM, Utiger R, Parker C (1969) Radioimmunoassay for the measurement of adenosine 3',5'-cyclic phosphate, *Biochem* **64**, 367-373
- <sup>121</sup> Hubich AI, Zheldakova TA, Chernikova TV, Koroleva EV, Lakhvich FA, Sholukh MV (2006) Synthetic heteroprostanoids of A- and E-types as novel non-comprehensive inhibitors of adenylyl cyclase in rat hepatocytes, *Biochem Biophys Res Commun* **341**, 357-362
- <sup>122</sup> Honma M, Satoh T, Takezawa J, Ui M (1977) An ultrasensitive method for the simultaneous determination of cyclic AMP and cyclic GMP in small-volume samples from blood and tissue, *Biochem Med* **18**, 257-273

- <sup>123</sup> Steiner AL, Parker CW, Kipnis DM (1972) Radioimmunoassay for cyclic nucleotides, *J Biol Chem* **25**, 1106-1113
- <sup>124</sup> Yamamoto I, Tsuji J, Takai T, Fujimoto M (1982) Double antibody enzyme immunoassay for the quantitation of adenosine 3',5-cyclic monophosphate (cyclic AMP) and guanosine 3',5'-cyclic monophosphate (cyclic GMP) in tissue and plasma, *J Immunoassay Immunochem* **3**, 173-196
- <sup>125</sup> Tsugawa M, Iida S, Fujii H, Moriwaki K, Tarui S (1990) An enzyme-linked immunosorbent assay (ELISA) for adenosine 3',5'-cyclic monophosphate (cAMP) in human plasma and urine using monoclonal antibody, *J Immunoassay Immunochem* **11**, 49-61
- <sup>126</sup> Kingan TG (1989) A competitive enzyme-linked immunosorbent assay: applications in the assay of peptides, steroids and cyclic nucleotides, *Anal Biochem* **183**, 283-289
- <sup>127</sup> Willipinski-Stapelfeldt B, Lübberstedt J, Stelter S, Vogt K, Mukhopadhyay AK, Müller D (2004) Comparative analysis between cyclic GMP and cyclic AMP signalling in human sperm, *Mol Hum Reprod* **10**, 543-552
- <sup>128</sup> Williams C (2004) cAMP detection methods in HTS: selecting the best from the rest, *Nature Rev Drug Disc* **3**, 125-135
- <sup>129</sup> Gabriel D, Vernier M, Pfeifer MJ, Dasen B, Tenaillon L, Bouhelal R (2003) High throughput screening technologies for direct cyclic AMP measurement, *Assay Drug Dev Tech* **1**, 291-303
- <sup>130</sup> Vadakkadathmeethal K, Cunliffe JM, Swift J, Kennedy RT, Neubig RR, Sunahara RK (2007) Fluorescence-based adenylyl cyclase assay adaptable to high throughput screening, *Comb Chem High Throughput Screen* **10**, 289-298
- <sup>131</sup> Cunliffe JM, Sunahara RK, Kennedy RT (2006) Detection of adenylyl cyclase activity using a fluorescent ATP substrate and capillary electrophoresis, *Anal Chem* **78**, 1731-1738
- <sup>132</sup> Pietta PG, Mauri PL, Gardana C, Benazzi L (1997) Assay of soluble guanylate cyclase activity by isocratic high-performance liquid chromatography, *J Chromatogr B* **690**, 343-347
- <sup>133</sup> Schmidt H (2009) From past to present: an overview, *HHHW Schmidt, F Hofman, J-P Stasch: cGMP: Generators, Effectors and Therapeutic Implications Handbook of Experimental Pharmacology* **191**, Springer-Verlag Berlin-Heidelberg, 195-228
- <sup>134</sup> Reysz LJ, Carroll AG, Jarrett HW (1987) An automated assay for adenylate cyclase using reversed-phase high-performance liquid chromatography, *Anal Biochem* **166**, 107-112
- <sup>135</sup> Lorenzetti R, Lilla S, Donato JL, de Nucci G (2007) Simultaneous quantification of GMP, AMP, cyclic GMP and cyclic AMP by liquid chromatography coupled to tandem mass spectrometry, *J Chromatogr B* **859**, 37-41

- 
- <sup>136</sup> Nordstedt C, Fredholm BB (1990) A modification of a protein-binding method for rapid quantification of cAMP in cell-culture supernatants and body fluid, *Anal Biochem* **189**, 231-234
- <sup>137</sup> Gilman AG (1970) A protein binding assay for adenosine 3',5'-cyclic monophosphate, *Proc Natl Acad Sci USA* **67**, 305-312
- <sup>138</sup> Golla R, Seethala R (2002) A homogenous enzyme fragment complementation cyclic AMP screen for GPCR agonists, *J Biomol Screen* **7**, 515-525
- <sup>139</sup> Rich TC, Karpen JW (2002) Review article: cyclic AMP sensors in living cells: what signals can they actually measure?, *Ann Biomed Eng* **30**, 1088-1099
- <sup>140</sup> Tang Y, Li X, He J, Lu J, Diwu Z (2006) Real-time and high throughput monitoring of cAMP in live cells using a fluorescent membrane potential-sensitive dye, *Assay Drug Dev Tech* **4**, 461-471



## 2. Aim of Work

Whooping cough is caused by *Bordetella pertussis* and considered as severe “childhood disease” with high morbidity rates and a high number of complications including hospitalization and death in infants. However, adults are also affected, although it is often not recognized by the attending physician. Anthrax is caused by *Bacillus anthracis* and is specified by a very high mortality rate and extremely severe progress of disease. However, the morbidity rate for anthrax compared to pertussis is much lower due to a different way of disease transmission comprising physical contact with contaminated animal products or infected hosts or the inhalation of spores embedded in the soil.

Both diseases share common characteristics: The diseases have a “point-of-no-return” where antibiotic treatment does not lead to an improvement of the health state of patients; both pathogens produce several virulence factors responsible for establishment of disease including AC toxins; both AC toxins, EF and CyaA, impair host immune responses and facilitate survival of the bacteria. As a matter of fact, the “point-of-no-return” is attributed to the action of toxins further compromising the already weakened body although bacteria have been eradicated.

Therefore, the development of new inhibitors acting selectively against AC toxins would increase survival rates and moderate the course of disease. Hence, the development of an easy, fast and inexpensive assay for screening of AC inhibitors is presented in this work.

Furthermore, the AC toxins EF and CyaA are still not entirely characterized and the biological mode of action is still not fully understood. The interaction of EF and CyaA with GTP-, CTP-, UTP- and ITP-derivatives showed a lower base-specificity than previously expected. Therefore, the substrate-specificity of EF and CyaA was explored and described in this thesis. Additionally, the generation of these “rare” cyclic nucleotides *in vivo* by cell-permeable holotoxins is analyzed by a highly specific and extremely sensitive HPLC-MS/MS method. The impact of cNMP formation in murine macrophages on gene expression was surveyed by microarray and RT-PCR techniques. This work presents as yet unknown nucleotidyl cyclase activity *in vivo* and evidence for the existence of further cyclic nucleotide second messengers apart from the well-known adenine- and guanine cyclic monophosphates.

### 3. A Fluorimetric Assay for Real-time Monitoring of Adenylyl Cyclase Activity Based on Terbium Norfloxacin

#### 3.1. Abstract

ACs catalyze the production of the second messenger cyclic AMP from ATP. Until now, there is no fluorescent AC assay known which is applicable to high throughput screening and kinetic determinations which can directly monitor the turnover of the unmodified substrate ATP. In this study, a fluorescence-based assay is described using the  $\text{Ca}^{2+}$ - and calmodulin-dependent AC EF from *Bacillus anthracis* and  $\text{Tb}^{3+}$ -norfloxacin as probe for the enzyme activity. This assay can be utilized to study enzyme regulators, allows real-time monitoring of AC activity and does not substitute ATP by fluorescent derivatives. These derivatives have to be judged critically due to their interference on the activity of enzymes and their specificity towards inhibitors. Furthermore, the new assay makes the application of radioactively labeled substrates such as  $[\alpha\text{-}^{32}\text{P}]\text{ATP}$  or fluorescently labeled antibodies like anti-cyclic AMP redundant. We determined the Michaelis-Menten-constant  $K_M$ , the  $V_0^{\text{max}}$ -value of ATP turnover as well as  $\text{IC}_{50}$  values for three inhibitors of EF by this newly developed fluorescent method.

#### 3.2. Introduction

ACs represent a very important class of enzymes in mammalian cells regulated by G-proteins. ACs catalyze the conversion of ATP to cAMP and  $\text{PP}_i$ , the latter being formed as a by-product. Until now, ten mammalian ACs have been identified, nine of which (AC1-9) are membrane-bound.<sup>1,2,3,4</sup> Furthermore, invasive micro-organisms like *Bacillus anthracis* or *Bordetella pertussis* causing anthrax and whooping cough, respectively, have exploited the dependency of higher mammals on the second messenger cAMP and produce AC toxins. Bacterial AC toxins are activated by CaM in the eucaryotic host cell and show a very high catalytic activity.<sup>5,6,7,8</sup>

The activation of membrane-bound ACs in mammalian cells is mediated by G-proteins, which in turn are regulated by G-protein coupled receptors. Binding of hormones, neurotransmitters and sensory signals to cell surface receptors initiates the G-protein signaling cascade. ACs constitute members in a chain of events regulating cellular attributes like membrane potential, the rate of cell division and differentiation, glycogen metabolism

as well as brain and smooth muscle function. The role of ACs is dependent on the cell type and the type of AC itself.<sup>9,10</sup>

Therefore, interference with the G-protein signaling cascade by bacterial AC toxins leads to severe and fatal infections. Hence, AC inhibitors for bacterial toxins constitute potential drug candidates for the treatment thereof. *B. anthracis*, for example, induces anthrax by secreting three bacterial toxins. One of these toxins is a highly active and CaM-stimulated AC. These toxins remain active in the body, although the cause of infection which is the bacterium may have been successfully treated. The same situation applies for several other bacteria like *Bordetella pertussis*, *Pseudomonas aeruginosa* and *Yersinia pestis*.<sup>5</sup>

Several cAMP detection methods in high throughput screening are commercially available. Among these are ALPHAScreen®, FP, HTRF®, HitHunter® EFC and DELFIA® kits.<sup>11</sup> The principle of detection is comparable: after stimulation and lysis of cells, labeled cAMP competes with cellularly synthesized cAMP for limited cAMP antibody binding sites. Furthermore, radiometric assays such as scintillation proximity assays by GE Healthcare and Flashplate technology by Perkin Elmer enable the direct detection of <sup>125</sup>I-labeled cAMP. Reporter gene assays exploit changes in the expression level of a particular gene *via* receptor-mediated changes in cAMP levels. The transcription of these genes is regulated by the transcription factor cAMP response-element binding protein. Several reporter genes have been utilized in these assays including  $\beta$ -galactosidase, green fluorescent protein, luciferase and  $\beta$ -lactamase.<sup>11,12</sup>

A cAMP-dependent protein kinase is used to monitor cAMP levels in living cells. This kinase forms a holoenzyme complex R<sub>2</sub>C<sub>2</sub> with two catalytic (C) and regulatory (R) subunits each labeled with a different fluorescent dye capable of fluorescence resonance energy transfer, e.g. fluorescein and rhodamine. The C subunits dissociate when cAMP binds to the R subunits, thereby eliminating energy transfer.<sup>13</sup>

Recently, a fluorescent AC assay was developed which is also adaptable to high throughput screening. The approach takes advantage of a conjugate of GTP with the commercially available fluorophore Bodipy. The fluorescence of this self-quenched fluorogenic substrate is enhanced dramatically after cleavage by ACs. However, this assay suffers from the need of a mutant AC with decreased purine selectivity or of the non-physiological ion Mn<sup>2+</sup> instead of Mg<sup>2+</sup> when using a wild-type AC.<sup>14</sup> In a previous approach a Bodipy-ATP derivative was used. In this case, the fluorescence detection has to be combined with capillary electrophoresis in order to separate the substrate Bodipy FL ATP from the product Bodipy cAMP, that both show the same fluorescence properties.<sup>15</sup>

Several lanthanide complexes are known to respond to the presence of nucleotides and inorganic phosphates and have already been applied in determining enzyme activity. For

example, the  $\text{Eu}^{3+}$ -tetracycline (1:1) complex has been utilized to determine the activity of creatine kinase as a model for non-membrane-bound kinases.<sup>16</sup>  $\text{Eu}^{3+}$ -tetracycline (3:1) has been used to monitor alkaline phosphatase.<sup>17</sup> The formation of AMP *via* hydrolysis of cAMP by a phosphodiesterase was detected in an assay using a  $\text{Cd}^{2+}$ -complex. This complex did not respond to cAMP but showed a strong increase of its fluorescence by AMP.<sup>18</sup>

The application of terbium norfloxacin (TbNflx) for probing ATP and the influence thereof on the spectrum of the complex have been described previously.<sup>19</sup> The ratio of Tb:norfloxacin was reported to be 4.5:1. Lanthanide ions emit a weak fluorescence in aqueous solution. The luminescence quantum yield increases upon interaction with an organic ligand. Upon excitation of the ligand norfloxacin a non-radiative energy transfer between the triplet level of the ligand and the resonance state of the ion occurs followed by radiative emission. The emission is observed as sharp multiplet bands due to several electronic transitions. The emission wavelength used in this study is the  $^5\text{D}_4 \rightarrow ^7\text{F}_5$  transition centered at 543 nm.<sup>20</sup>

The objective of this work was to develop a robust fluorescent AC assay which does not rely on radioactively labeled nucleotides. The TbNflx complex was reported to respond to ATP by a five-fold increase of its fluorescence.<sup>19</sup> No additional enzymes such as luciferase in bioluminescent ATP assays or fluorescently labeled antibodies such as anti-cAMP are necessary. This assay is inexpensive, straightforward, and fast and shows versatile applicability including high throughput screening for numerous regulators simultaneously. This novel approach based on a probe for ATP conversion enables real-time monitoring of enzymatic kinetics instead of endpoint measurements as in the case of immuno- or radioassays.

### 3.3. Materials and Methods

#### 3.3.1. Edema Factor (EF)

EF from *B. anthracis* was chosen as a model AC for use in the TbNflx assay because of the relative simplicity of enzyme recovery, its robustness and good water solubility, but mainly because of its high catalytic activity. EF belongs to the three bacterial toxins of *B. anthracis* and produces cAMP in the host cell after formation of an active complex composed of the enzymes EF and CaM and  $\text{Ca}^{2+}$  ions.<sup>5,6,7,8</sup> CaM acts as a cofactor of EF activity. EF like all ACs catalyzes the following reaction according to equation (a):



### 3.3.2. Protein Purification

*E. coli* cells were transfected with plasmid pProExH6-EF and EF was extracted from *E. coli* similar to the method described by Shen *et al.*<sup>6</sup> CaM was purified from calf brain according to Gopalakrishna *et al.*<sup>21</sup> The activity of the extracted enzymes was tested by assays with [ $\alpha$ -<sup>32</sup>P]ATP.<sup>22</sup> [ $\alpha$ -<sup>32</sup>P]ATP (3,000 Ci/mmol) was purchased from Perkin Elmer Life Sciences.

### 3.3.3. Microwell-Plate Based Fluorescence Assays

Fluorescence intensities (time-resolved) were acquired by using a BMG FLUOstar OPTIMA microplate reader (Jena, Germany). Excitation/emission filters were set to 337 and 545 nm, respectively. All dilution series and calibration plots were obtained in 96-microwell plates with eight replicates, enzyme assays with three replicates applying time-gated measurements at a lag time of 60  $\mu$ s after the excitation pulse and a signal-integration time of 60  $\mu$ s. All experiments were performed at 25 °C. The 96-well microplates were obtained from Greiner Bio-One GmbH (Frickenhausen, Germany).

### 3.3.4. Reagents

All chemicals were obtained in analytical purity. Calcium dichloride (water-free) was obtained from Carl-Roth GmbH (Karlsruhe, Germany). Magnesium dichloride hexahydrate, tetrasodium pyrophosphate decahydrate (PP<sub>i</sub>) and tris(hydroxymethyl)aminomethane (TRIS) were purchased from Merck KgaA (Darmstadt, Germany). Bovine serum albumin (BSA) ( $\geq$  96%, essentially fatty acid free), terbium(III) trichloride hexahydrate, norfloxacin, adenosine-5'-triphosphate disodium salt (grade II, minimum 99%) and adenosine-3',5'-cyclic monophosphate sodium salt (minimum 99%, HPLC) were obtained from Sigma-Aldrich Chemie GmbH (Steinheim, Germany).

Buffered solutions contained 10 mM TRIS-HCl at pH 7.4. TRIS/BSA solution contained in addition to 10 mM TRIS 0.1 wt% of BSA. Except for TbNflx all salt and nucleotide solutions were filled up with TRIS/BSA.

TbNflx solutions contained 0.5 mM TbCl<sub>3</sub>·6H<sub>2</sub>O and 0.111 mM norfloxacin. The ratio of Tb:norfloxacin was 4.5:1 as reported in literature.<sup>19</sup> 0.22 mM norfloxacin solution was prepared by dissolving norfloxacin in a small amount of 0.1 mM hydrochloric acid and dilution with TRIS-buffered solution to the appropriate volume. Equal amounts of a 1 mM Tb<sup>3+</sup> solution and a 0.22 mM norfloxacin solution were combined. The amount of TbNflx in solution is represented by the concentration of Tb<sup>3+</sup> always containing the respective amount of norfloxacin.

Solution of PMEApp was donated by Gilead Sciences (Forster City, CA, USA). A 5 mM solution of MANT-CTP was provided by Dr. Jens Geduhn and Prof. Burkhard König and was synthesized as reported by Göttle *et al.*<sup>23</sup> Calmidazolium chloride was purchased from Sigma Aldrich Chemie GmbH (Steinheim, Germany). A 10 mM stock solution of calmidazolium was prepared in DMSO.

### 3.3.5. Enzyme-Activity Assays Using TbNflx as Indicator

The assays were recorded in 96-well microplates with each well containing a final volume of 100  $\mu$ L with final concentrations of 5 mM  $Mg^{2+}$ , 10  $\mu$ M  $Ca^{2+}$  and 0.1 wt% BSA. In this work the analytical  $Ca^{2+}$  concentration was used instead of the calculated free  $Ca^{2+}$  concentration as most of the times used in research with EF due to the fact that we did not use a chelator to keep the level of free  $Ca^{2+}$  ions constant in order to exclude artifacts and interferences on the TbNflx complex. The TbNflx concentration was 60  $\mu$ M when using 500  $\mu$ M ATP. The TbNflx and ATP concentrations were reduced to 10  $\mu$ M and 100  $\mu$ M, respectively, in order to increase the sensitivity of the assay. Application of an incubation time was not necessary. All solutions were equilibrated at 25 °C before starting the measurements.

The CaM concentrations were varied from 1 nM to 200 nM in assays where EF was activated by its cofactor CaM with [EF] of 50 nM. The ATP and  $Tb^{3+}$  concentrations were 500  $\mu$ M and 60  $\mu$ M, respectively. The EF concentration was changed from 5 nM to 100 nM with a constant CaM concentration of 200 nM for measurements of enzyme activity. The ATP and  $Tb^{3+}$  concentrations were 100  $\mu$ M and 10  $\mu$ M, respectively.

Screening for inhibitors of EF activity was accomplished with 5 nM EF, 50 nM CaM and an initial ATP concentration of 100  $\mu$ M. The concentration of  $Tb^{3+}$  was 10  $\mu$ M.

Determination of  $K_M$  and  $V_0^{max}$  was performed with 5 nM EF, 50 nM CaM and 10  $\mu$ M  $Tb^{3+}$ . The initial maximal enzyme velocity  $V_0^{max}$  was determined by a series of different ATP concentrations from 10  $\mu$ M to 750  $\mu$ M.

AC assays with [ $\alpha$ -<sup>32</sup>P]ATP as substrate were conducted according to Gille *et al.*<sup>24</sup> and Alvarez *et al.*<sup>25</sup> under the conditions as described for screening EF inhibitors and the determination of  $K_M$  and  $V_0^{max}$ . The total volume was 50  $\mu$ L in case of radioassays. Each tube contained 0.3  $\mu$ Ci [ $\alpha$ -<sup>32</sup>P]ATP.

All calculations and fits were conducted with Microcal Origin 6.0.

### 3.4. Results

#### 3.4.1. Calibration Plots for the AC System and Enzyme Toxicity of TbNflx

The response of TbNflx to the analytes of the AC reaction (ATP, cAMP, PP<sub>i</sub>) was examined resulting in a five-fold increase upon addition of ATP (1:1 ATP:Tb<sup>3+</sup>), a five-fold decrease upon addition of PP<sub>i</sub> (1:2 PP<sub>i</sub>:Tb<sup>3+</sup>) and no significant change in fluorescence emission in presence of cAMP (see Fig. 3.1.A).



**Scheme 3.1.** Enzymatic conversion of ATP to PP<sub>i</sub> and cAMP by AC leads to a significant decrease of lanthanide luminescence of TbNflx

The luminescence lifetimes of the TbNflx complex hint to the mechanism of interaction between the analytes and TbNflx. TbNflx alone displays a luminescence lifetime  $\tau$  of approximately 180  $\mu$ s.  $\tau$  is only negligibly altered by cAMP, whereas it is increased in presence of ATP and PP<sub>i</sub> to 663  $\mu$ s and 723  $\mu$ s, respectively. In case of ATP which increases the fluorescence intensity five-times an increase in  $\tau$  is expected. In case of PP<sub>i</sub>, which quenches the fluorescence one would anticipate the lifetime to decrease with increasing amounts of PP<sub>i</sub>. In fact, a ternary complex of Tb<sup>3+</sup>, norfloxacin and PP<sub>i</sub> is formed. PP<sub>i</sub> impairs the energy transfer from the ligand norfloxacin to the Tb<sup>3+</sup> ion. The fluorescence quantum efficiency is decreased and the luminescence is quenched despite a rising in lifetime.

Calibration plots were recorded for different mole fractions of ATP, cAMP and PP<sub>i</sub> upon TbNflx mimicking the conversion of ATP by ACs. The samples contained all essential additives for the AC assay. The overall TbNflx fluorescence decrease in AC reaction is dependent on the ratio of ATP:PP<sub>i</sub> and does not respond to the total amount of ATP in the sample. On account of this, the normalized fluorescence intensity was plotted against the mole fraction  $\chi(\text{ATP}) = [\text{ATP}]/([\text{ATP}] + [\text{PP}_i])$  representing the fraction of the initial ATP concentration still present in the enzymatic assay with  $[\text{PP}_i] = [\text{cAMP}]$ . A decrease in ATP concentration is followed by a decrease in fluorescence emission as expected (see Fig. 3.1.B). The slope of the calibration plot is determined from equation (b) to be 0.848.

$$I/I_0 = 0.848 \chi + 0.133 \quad (b)$$

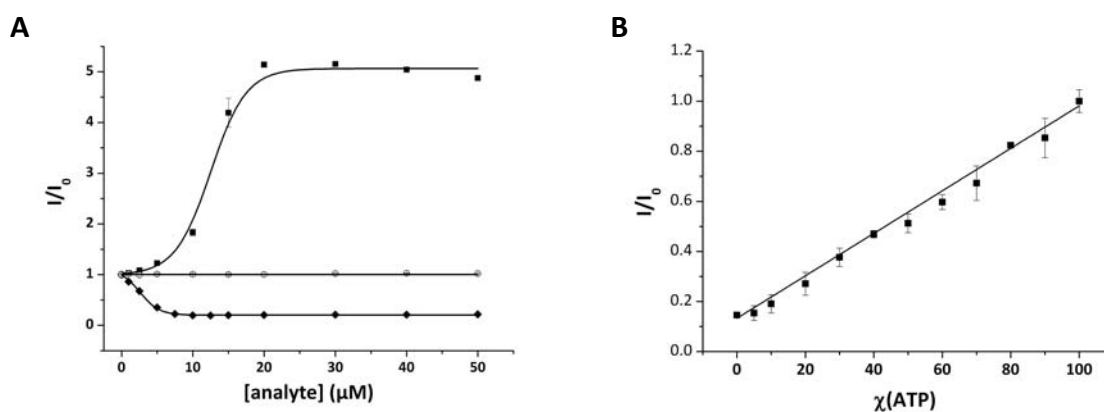


**Fig. 3.1.** **A** Normalized fluorescence intensity  $I/I_0$  of the TbNflx complex (20  $\mu\text{M}$   $\text{Tb}^{3+}$ ) in the presence of various concentrations of ATP (■), cAMP (○), and  $PP_i$  (◆). **B** Effect of varying mole fractions  $\chi(ATP)$  with  $\chi(ATP) = [\text{ATP}]/([\text{ATP}] + [\text{cAMP}])$  on the normalized fluorescence intensity of TbNflx (10  $\mu\text{M}$   $\text{Tb}^{3+}$  with  $[\text{ATP}] + [\text{cAMP}] = 100 \mu\text{M}$

The TbNflx complex was tested for toxicity on the enzymes EF and CaM by means of an  $[\alpha\text{-}^{32}\text{P}]\text{ATP}$  assay. The  $\text{Tb}^{3+}$  concentration did not influence the activity of the enzyme until an excess of  $7 \times 10^6:1$  was reached. The activity was reduced to 60% when an excess of  $10^7$  of  $\text{Tb}^{3+}$  to enzyme was adjusted (data not shown).

### 3.4.2. Specificity of TbNflx Response

The fluorescence response of the TbNflx complex must meet some requirements in order to be capable of detecting enzymatic activity. The response time of TbNflx to ATP is in a time scale smaller than two seconds. Therefore, no preincubation time is necessary for the application of TbNflx.

The fluorescence change of TbNflx was monitored for a solution containing the catalytically active EF-CaM complex,  $\text{Ca}^{2+}$ ,  $\text{Mg}^{2+}$ , and BSA but no ATP in order to exclude any unspecific response of the TbNflx to the enzyme. Only a negligible fluorescence change over time was observed as anticipated (data not shown).

Further negative controls were conducted. Assays lacking essential  $\text{Mg}^{2+}$  ions or CaM as well as a kinetic with EF denatured at 95 °C were performed. In contrast to measurements containing all ingredients as described in the experimental section no significant fluorescence change could be detected.

Moreover, the TbNflx assay was found to be insensitive to DMSO in concentrations of up to 5 vol%. Neither the fluorescence of the complex nor the activity of the enzyme EF showed any change (data not shown). This is important for high throughput screening as many test compounds are dissolved in DMSO due to their poor water solubility.



### 3.4.3. Monitoring of Enzyme Activity

After addition of EF to a substrate solution containing the cofactor CaM, the fluorescence intensity decreased due to the enzymatic conversion of ATP to cAMP and PP<sub>i</sub>. The rate of turnover was dependent on the concentration of EF (see Fig. 3.2.) or of CaM (see Fig. 3.3.) present in solution.

The turnover of ATP was increased with increasing concentrations of EF. All assays contained 200 nM CaM as activator. The initial ratio of ATP and Tb<sup>3+</sup> present in solution were critical for the sensitivity of enzyme activity determination. With 500 μM ATP and 60 μM Tb<sup>3+</sup> a higher concentration of EF (approx. 50 to 100 nM EF, (data not shown)) was necessary to obtain a reasonable kinetic measurement as with 100 μM ATP and 10 μM Tb<sup>3+</sup> (see Fig. 3.2.).

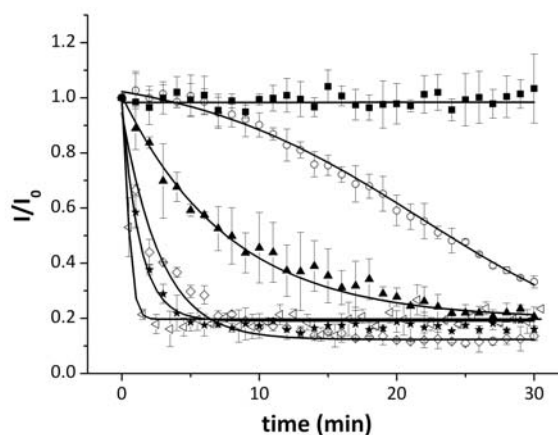


**Fig. 3.2.** Kinetics of varying concentrations of EF in nM (5 (○), 10 (▲), 25 (◇), 50 (★) and 100 (◁)) and a negative control with heat-denatured EF (■). Measurements were conducted with [CaM] = 200 nM, [ATP] = 100 μM and [Tb<sup>3+</sup>] = 10 μM. Curves were fitted sigmoidally.

CaM acts as activator for EF and is a cofactor of EF. In an enzyme activation assay the EF concentration was kept constant and the CaM concentration was varied from 1 nM to 200 nM, where enzyme activity reached saturation (see Fig. 3.3.). The state of activation of EF was dependent on the concentration of the cofactor CaM. The CaM concentration was essential for the ATP turnover as shown by a control measurement lacking CaM.

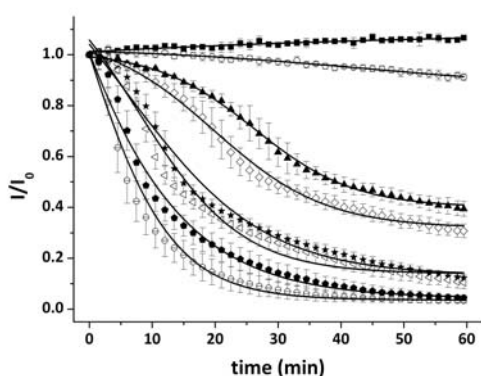


**Fig. 3.3.** The concentrations of CaM (nM) were 1 (○), 5 (▲), 10 (◇), 25 (★), 50 (◁), 100 (●) and 200 (⊙), respectively, including one negative control lacking CaM (■). [EF] = 50 nM, [ATP] = 500 μM and [Tb<sup>3+</sup>] = 60 μM. The curves were fitted sigmoidally.

essential for the ATP turnover as shown by a control measurement lacking CaM.

Both plots (Figs. 3.2., 3.3.) show the normalized fluorescence intensity  $I/I_0$ .  $I_0$  represents the fluorescence intensity immediately after addition of the enzyme at  $t = 0$  when the measurement was started. A reference time trace of a blank sample was superfluous when the temperature is thoroughly controlled and kept constant at 25 °C as no shift in fluorescence intensity occurred over time under these conditions.

### 3.4.4. Screening of EF Inhibitors

PMEApp (9-[2-(phosphonomethoxy)ethyl]adenine diphosphate), MANT-nucleotides (2'(3')-O-(N-methylanthraniloyl)-substituted nucleotide triphosphate analogues) and calmidazolium are known inhibitors of bacterial AC activity. PMEApp which is sold as Adefovir<sup>26</sup> and MANT-CTP<sup>23</sup> as example for MANT-nucleotides are competitive inhibitors of bacterial AC toxins, whereas calmidazolium prevents binding of CaM to other proteins including EF<sup>27</sup> and therefore inhibits initiation of AC activity.

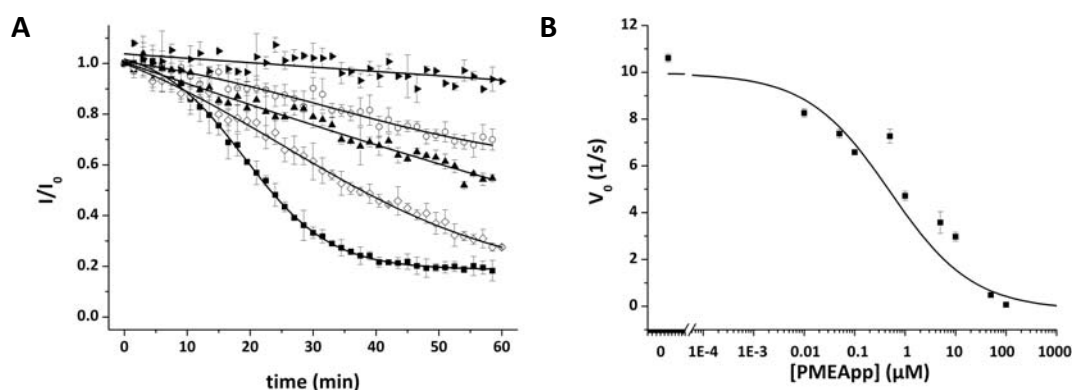


**Fig. 3.4.** **A** Selected kinetics recorded with different concentrations of PMEApp in  $\mu\text{M}$  (50 ( $\blacktriangleright$ ), 10 ( $\circ$ ), 5 ( $\blacktriangle$ ), 1 ( $\diamond$ ) and no PMEApp added ( $\blacksquare$ ) containing  $[\text{EF}] = 5 \text{ nM}$ ,  $[\text{CaM}] = 50 \text{ nM}$ ,  $[\text{ATP}] = 100 \mu\text{M}$  and  $[\text{Tb}^{3+}] = 10 \mu\text{M}$ . **B**  $V_0$  of the kinetic responses plotted logarithmically against the inhibitor concentration.  $\text{IC}_{50}$  was calculated to be 498 nM. Sigmoidal fits were performed.

MANT-nucleotides and derivatives thereof have been reported to be inhibitors of AC activity, including the bacterial toxins EF of *B. anthracis* and the soluble AC of *Bordetella pertussis* (CyaA). EF and CyaA share sequence homologies and are both  $\text{Ca}^{2+}$ - and CaM-dependent ACs.<sup>24</sup> MANT-CTP inhibited CyaA with a  $K_i$  of 36  $\mu\text{M}$ .<sup>23</sup>

The influence of the inhibitors on TbNflx was examined before screening assays were carried out. MANT-CTP is a fluorescent nucleotide that is excited at 337 nm and shows an emission between 400-500 nm. However, despite these properties, MANT-CTP did not interfere with the detection of TbNflx. All selected inhibitors (MANT-CTP, PMEApp and calmidazolium) did not induce a fluorescence change of TbNflx-ATP emission over time.

Screening for inhibitors was performed with solutions containing 5 nM of EF, 50 nM of CaM, 100  $\mu\text{M}$  of ATP and 10  $\mu\text{M}$  of  $\text{Tb}^{3+}$ . For these particular conditions the slope from the calibration plot shown in Fig. 3.1.B was used to determine the initial speed  $V_0$  of EF according to equation (c). Equation (c) was deduced from the equation for molar catalytic activity  $Z_m = \Delta(\text{ATP})/(\Delta t \cdot n(\text{EF}))$ .

$$v_0 \left( \frac{1}{s} \right) = - \frac{\text{slope of kinetic} \left( \frac{1}{\text{min}} \right)}{\text{slope of calibration} (1)} \cdot \frac{[\text{ATP}] (\mu\text{mol}^{-1})}{[\text{EF}] (\mu\text{mol}^{-1})} \cdot \frac{1(\text{min})}{60(s)} \quad (c)$$

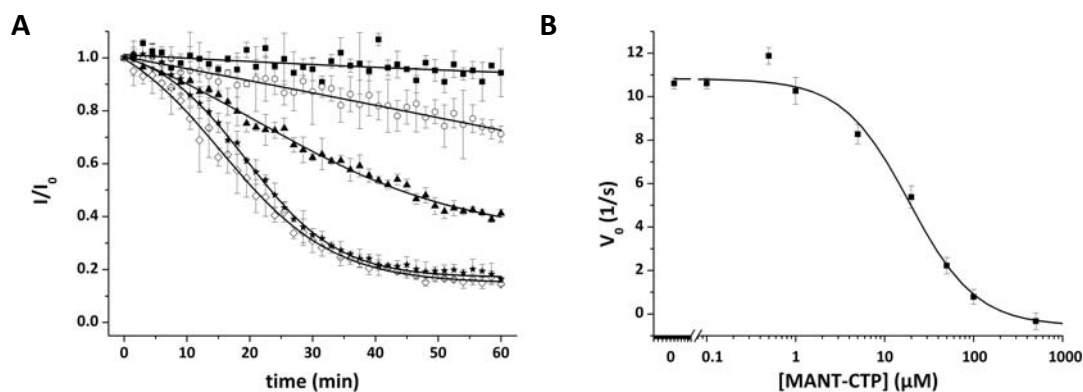


**Fig. 3.5. A** Selected kinetics recorded with different concentrations of MANT-CTP (500 (■), 50 (○), 20 (▲), 0.5 (◇)  $\mu\text{M}$  and no MANT-CTP added (★)) containing  $[\text{EF}] = 5 \text{ nM}$ ,  $[\text{CaM}] = 50 \text{ nM}$ ,  $[\text{ATP}] = 100 \mu\text{M}$  and  $[\text{Tb}^{3+}] = 10 \mu\text{M}$ . **B**  $V_0$  of the kinetic responses plotted logarithmically against the inhibitor concentration.  $\text{IC}_{50}$  was determined to be  $19 \mu\text{M}$ . The curves were fitted sigmoidally.

PMEApp and MANT-CTP are competitive inhibitors for EF. The concentration of PMEApp was varied between  $10 \text{ nM}$  and  $100 \mu\text{M}$ . MANT-CTP was added at concentrations between  $100 \text{ nM}$  and  $750 \mu\text{M}$ . Selected kinetics were plotted in Fig. 3.4.A and Fig. 3.5.A.  $V_0$  of each kinetic was determined according to equation (c) and plotted logarithmically against the inhibitor concentration (Figs. 3.4.B, 3.5.B). The  $\text{IC}_{50}$  values determined at half-maximal activity from our assay were  $498 \pm 55 \text{ nM}$  and  $19 \pm 2 \mu\text{M}$  for PMEApp and MANT-CTP, respectively. The  $K_i$  value reported for PMEApp with  $17 \text{ pM}$  EF and  $1 \mu\text{M}$  CaM at  $30^\circ\text{C}$  was  $27 \text{ nM}$ <sup>26</sup> and differs by a factor of  $\sim 18$  to the results found by the TbNflx assay. The  $\text{IC}_{50}$  value found for MANT-CTP inhibition of EF is  $19 \mu\text{M}$  and in the same order of magnitude as described for CyaA toxin. The  $K_i$  value of MANT-CTP for CyaA was reported to be  $36 \mu\text{M}$ .<sup>23</sup> Possible explanations for differences in  $\text{IC}_{50}$ - and  $K_i$ -values found in the TbNflx assay and reported in literature are discussed below.

Calmidazolium differs from the inhibitors PMEApp and MANT-CTP. Calmidazolium does not competitively inhibit EF but binds allosterically to the cofactor CaM and prevents binding thereof to the AC. Thus, the activity of EF is impaired. Selected kinetics are shown in Fig. 3.6.A. The corresponding  $V_0$  values are plotted logarithmically against the calmidazolium concentrations (Fig. 3.6.B). The steep concentration dependence on calmidazolium indicates cooperative binding of calmidazolium to CaM. This is explained by calmidazolium exerting a positive cooperativity on CaM with a Hill-coefficient  $n_H$  of 2.<sup>27,28</sup> The  $\text{IC}_{50}$  was determined to

be  $136 \pm 2$  nM. The  $IC_{50}$  for calmidazolium on 100 nM CaM was reported to be approximately 70 nM.<sup>29</sup>

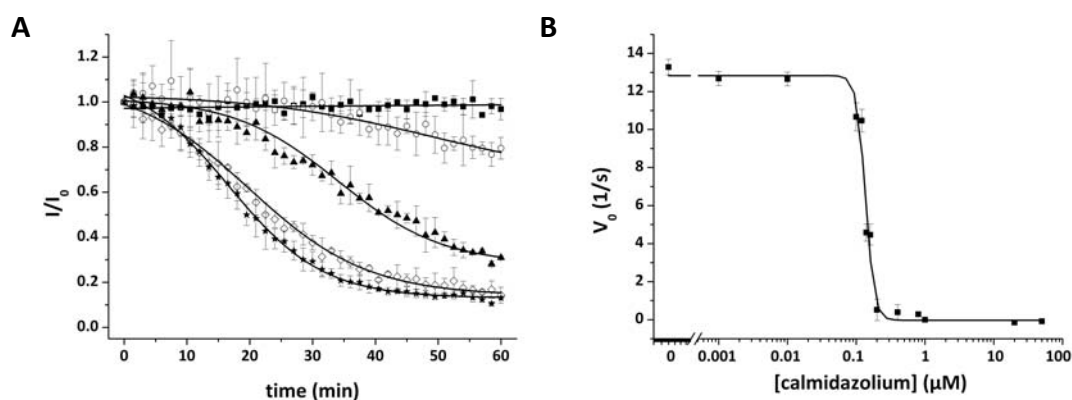


**Fig. 3.6.** **A** Selected kinetics recorded with different concentrations of calmidazolium (20 μM (■), 200 (○), 160 (▲), 120 (◇) nM and no calmidazolium added (★)) containing [EF] = 5 nM, [CaM] = 50 nM, [ATP] = 100 μM and  $[Tb^{3+}] = 10$  μM. **B**  $V_0$  of the kinetic responses plotted logarithmically against the inhibitor concentration.  $IC_{50}$  was determined to be 136 nM. All curves were fitted sigmoidally.

### 3.4.5. Determination of $V_0^{max}$ and $K_M$

Using the TbNflx assay, the Michaelis-Menten-constant  $K_M$  and the maximal initial velocity  $V_0^{max}$  were determined by addition of different ATP concentrations ranging from 10 μM to 750 μM (Fig. 3.7.).  $V_0$  increases with increasing ATP concentration until it reaches saturation. This saturation value corresponds to  $V_0^{max}$ .  $K_M$  is read off at half-maximal activity.  $V_0^{max}$  and  $K_M$  were determined to be  $71 \pm 3$  s<sup>-1</sup> and  $231 \pm 18$  μmol L<sup>-1</sup>, respectively. The  $K_M$ -values for Mg<sup>2+</sup>-nucleotide turnover are reported to be  $220 \pm 60$  μM. The  $V_{max}$ -value given is  $2,200 \pm 200$  s<sup>-1</sup> at 30 °C and differed to the value found in our determinations.<sup>24</sup>

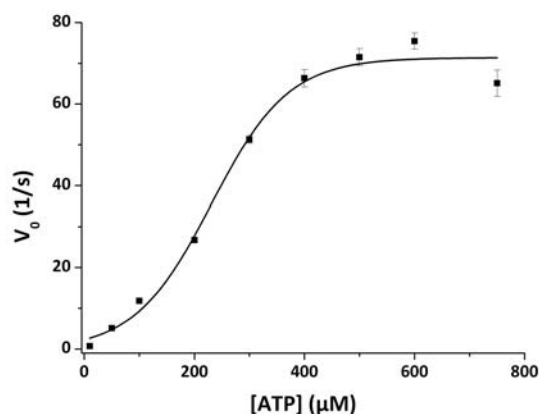


**Fig. 3.7.** Determination of  $V_0^{max}$  and  $K_M$  from kinetics with different initial concentrations of ATP ranging from 10 μM to 750 μM. The enzyme concentrations were constant at [EF] = 5 nM, [CaM] = 50 nM,  $[Tb^{3+}] = 10$  μM. The sigmoidal fit of the data gives a  $V_0^{max}$  of 71 s<sup>-1</sup> and a  $K_M$  of 231 μM. The kinetics were fitted sigmoidally.

### 3.4.6. Validation of Fluorescence Assay by a Radiometric Assay Using [ $\alpha$ - $^{32}$ P]ATP

The values for  $IC_{50}$  and  $V_0^{\max}$  differed in part from the values reported in literature. Radioassays were conducted under the experimental conditions which were chosen for the fluorescence assay in order to validate the values determined therein. The [ $\alpha$ - $^{32}$ P]ATP-assays were performed with and without TbNflx to exclude influences of the complex on the potency of inhibitors.

For calmidazolium the radioassays yielded  $IC_{50}$ -values of  $164 \pm 98$  nM with TbNflx and  $336 \pm 33$  nM without TbNflx. In case of the inhibitor MANT-CTP the [ $\alpha$ - $^{32}$ P]ATP-assay yielded  $IC_{50}$ -values of  $25 \pm 7$   $\mu$ M with and  $22 \pm 1$   $\mu$ M without TbNflx in solution. The  $K_M$  and  $V_0^{\max}$  were determined without TbNflx to be  $252 \pm 24$   $\mu$ M and  $111 \pm 5$  s $^{-1}$ , respectively. Thus, the values found in the radioassays support the fluorescence assay by similar results. Furthermore, the comparison of findings with and without TbNflx in the radioassay indicate that TbNflx has only little influence on the potency of inhibitors.

### 3.4.7. Calculation and Illustration of ATP Turnover

So far, enzyme activity was expressed as the fluorescence intensity ratio  $I/I_0$ . This is the most straightforward way to monitor enzyme activity. Nevertheless, the activity of EF may also be presented as the residual ATP concentration or the concentration of produced cAMP over time.

For calculation of the residual ATP and produced cAMP concentration equation (b) from the calibration plot is used and solved for  $\chi$ . The residual ATP concentration results from multiplication of  $\chi$  with the starting concentration  $c_0$  as demonstrated in equation (d). The produced amount of cAMP is then deduced by subtraction of the residual ATP concentration from the initial concentration  $c_0$  as shown in (e).

$$[ATP]_t = c_0 \cdot \chi_t = c_0 \cdot \left( \frac{\frac{I_t}{I_0} - 0.133}{0.848} \right) \quad (d)$$

$$[cAMP]_t = c_0 - [ATP]_t = c_0 - c_0 \cdot \chi_t = c_0 \cdot \left( 1 - \left( \frac{\frac{I_t}{I_0} - 0.133}{0.848} \right) \right) \quad (e)$$

As an example the inhibition of EF by calmidazolium (Fig. 3.6.A) is transferred by equations (d) (Fig. 3.8.A) and (e) (Fig. 3.8.B). The initial ATP concentration  $c_0$  was 100  $\mu$ M ATP. Figure 3.8.A shows the turnover of the substrate ATP and therefore the decrease in ATP

over time. During the cleavage of ATP, cAMP is produced in equal amounts. This is demonstrated by Figure 3.8.B.

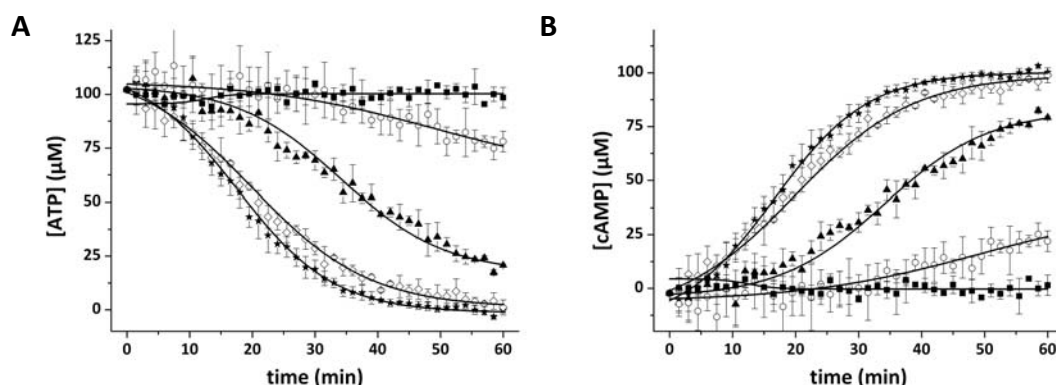


**Fig. 3.8.** **A** Selected kinetics recorded with different concentrations of calmidazolium (20 μM (■), 200 (○), 160 (▲), 120 (◇) nM and no calmidazolium added (★)) containing [EF] = 5 nM, [CaM] = 50 nM, [ATP] = 100 μM and [Tb<sup>3+</sup>] = 10 μM were used to calculate the residual ATP concentration from the normalized fluorescence signal  $I/I_0$ . **B** The normalized fluorescence signal  $I/I_0$  was transferred by equation (e) to result in the produced cAMP concentration.

### 3.4.8. Z-Factor

For high throughput screening purposes the Z-factor was introduced by Zhang *et al.*<sup>30</sup> The Z-factor provides a dimensionless and simple statistical characteristic for evaluation and comparison of the quality of high throughput screening assays. The Z-factor was calculated according to Zhang *et al.* and gave the value 0.84 for the TbNflx fluorescence assay. The correlation between Z-factor and quality of an assay is shown in Table 3.1.

**Table 3.1.** Correlation between Z-factor and assay quality according to Zhang *et al.*<sup>30</sup>

| $Z = 1 - \frac{3 \cdot \text{standard deviation of sample} + 3 \cdot \text{standard deviation of control}}{ \text{mean of sample} - \text{mean of control} }$ |                      |   |
|---|----------------------|---|
| Z-factor value  | Quality of Assay     | Comments  |
| 1   | An ideal assay       | No variation  |
| $0.5 \leq Z < 1$<br><i>(TbNflx assay: 0.84)</i>   | An excellent assay   | Separation band is large  |
| $0 < Z < 0.5$   | A double assay       | Small separation band   |
| 0   | “yes/no” type assay  | No separation band, sample and control signal variation bands overlap |
| < 0   | Screening impossible | Sample and control signal overlap                                     |

According to Zhang *et al.*<sup>30</sup> an excellent assay for high throughput screening affords Z values between 0.5 and 1. The TbNflx fluorescence assay provides a Z-factor of 0.84 and therefore, is well suited for application in a high throughput screening setup.

### 3.5. Discussion

[ $\alpha$ -<sup>32</sup>P]ATP assays are widely used for the determination of AC activity and exhibit several advantages and drawbacks, alike. The radioassay displays an extremely high sensitivity with very low blank values.<sup>22,23,24</sup> It turned out to be reliable and robust. It shows few artifacts and can be standardized. On the other hand the disadvantages of radioassays are quite obvious as it implies the handling of radioactive material including expensive waste disposal and risks to the health of the lab personnel due to radiation. A [ $\alpha$ -<sup>32</sup>P]ATP assay takes at least six hours from starting a kinetic measurement to the readout of the radioactivity by a  $\beta$ -counter including several steps like centrifugation, chromatography and washing. Furthermore, no high temporal resolution can be achieved as the radioassay is only an endpoint measurement. This assay cannot be used in high throughput screening.

An AC assay combining fluorescence techniques and capillary electrophoresis was reported by Cunliffe *et al.*<sup>15</sup> in 2006. This assay utilizes the Bodipy-FL-ATP analogue labeled at the 2'- or 3'-O-ribosyl position with a fluorescent Bodipy moiety. Cunliffe *et al.* demonstrated that Bodipy-FL-ATP can be used as substrate for AC. The enzymatic product Bodipy 2'-cAMP has the same fluorescence properties as the substrate Bodipy-FL-ATP. Therefore, product and substrate have to be separated by capillary electrophoresis. As suggested, this assay may be applicable to high throughput screening for AC regulators due to the development of capillary array electrophoresis. However, an assay with direct fluorescence readout of enzyme activity is advantageous because it is less laborious and time-consuming.

The AC assay reported by Vadakkadathmeethal *et al.*<sup>14</sup> was developed by the same group based on the electrophoretic assay<sup>15</sup> and employs the fluorescent GTP-derivative Bodipy-FL-GTP $\gamma$ S. Instead of radioisotopes this assay uses fluorescent dyes with different luminescence properties for product and substrate. It can be used in high throughput screening and the fluorophore can be excited in the visible wavelength range, which helps to reduce background fluorescence. Disadvantages of this assay are the need for either a mutant AC with decreased purine selectivity or the use of the non-physiologically Mn<sup>2+</sup> ion in case of a wild-type AC. Mn<sup>2+</sup> tends to alter the nucleotide specificity and to increase the potency of guanine nucleotide based inhibitors of AC activity.<sup>24</sup> This assay also suffers from higher K<sub>i</sub> values as reported earlier in literature but gives qualitatively similar results. An

incubation time of altogether 45 minutes is necessary prior to measurement. The applicability of this assay for kinetic measurements is not specified.

The TbNflx assay presented here does not require antibodies for cAMP, radioactive substrates, mutant enzymes or separation techniques. It is the first fluorescence assay of this kind that can be used for real-time determination of enzyme kinetics. A small drawback of this method is that the excitation of the fluorescent complex in the near UV evokes background fluorescence. An influence of the TbNflx on the potency of regulators of AC activity cannot be excluded in any case. Nevertheless, it seems to be negligible as the results from radioassays conducted in presence of TbNflx affirm the results of the TbNflx assay. We found  $IC_{50}$  values differing from the results reported earlier in literature. The divergence in  $V_0^{max}$ - and  $IC_{50}$ -values between the  $[\alpha\text{-}^{32}\text{P}]\text{ATP}$  in literature and the TbNflx assay may be explained by a temperature difference of 5 °C between the TbNflx-assay and the radioassay. Furthermore, the turnover rate may be reduced because in the TbNflx assay the analytical instead of the calculated free  $\text{Ca}^{2+}$  concentration is used. In the  $[\alpha\text{-}^{32}\text{P}]\text{ATP}$  assay the concentration of free  $\text{Ca}^{2+}$  ions is usually kept constant by using a chelator. We refrained from the addition of a chelator to exclude artifacts and interferences on the TbNflx complex. Compared to the  $[\alpha\text{-}^{32}\text{P}]\text{ATP}$  assay we used a higher EF concentration of 5 nM instead of approximately 10 pM and a smaller CaM concentration of 50 nM instead of 1  $\mu\text{M}$ .<sup>23,26</sup> In addition, the assay conditions of the fluorescent assay do not lead to a steady state as employed in Michaelis-Menten kinetics, as we reduced the ATP concentration to 100  $\mu\text{M}$  to increase sensitivity. We performed  $[\alpha\text{-}^{32}\text{P}]\text{ATP}$  assays under equal conditions as in case of the TbNflx assay to support our results. We found that the  $IC_{50}$ ,  $K_M$  and  $V_0^{max}$  values determined by means of the fluorescent assay were correct under the specified conditions. Besides, an influence of potent inhibitors or activators on the TbNflx fluorescence cannot be excluded in all cases.

The advantage of this method is that TbNflx responds immediately to changes in ATP and  $\text{PP}_i$  concentrations caused by the AC reaction. Thus, enzyme activity is transcribed directly into a decreasing fluorescence signal. This approach provides a sensitive tool for observing the turnover of ATP and therefore features real-time enzyme kinetics. The TbNflx assay works with the physiologically relevant ion  $\text{Mg}^{2+}$  instead of  $\text{Mn}^{2+}$  and does not require any mutant ACs. We suppose that the TbNflx assay can be applied in high throughput screening in order to identify potential enzyme inhibitors. The exact values of inhibition constants of identified inhibitors can be determined additionally by the classic  $[\alpha\text{-}^{32}\text{P}]\text{ATP}$  assay.

It can be assumed that this assay will work in the case of other purified bacterial AC toxins as well. Experiments with Sf9 insect cell membrane preparations overexpressing



mammalian AC isoforms 1, 2 and 5<sup>25</sup> failed due to interferences of the Tb-complex with the membrane itself (data not shown). Further studies with a human soluble AC construct (hsAC-CHD) will be accomplished. Enzyme conjugates with glutathione-S-transferase (GST) domains are not applicable because of unspecific interactions of the GST domain with the TbNflx complex (data not shown).

In addition to time-resolved detection of fluorescence intensity as presented in this work, the analytes ATP and PP<sub>i</sub> also induce a change in fluorescence lifetime of TbNflx. The fluorescence lifetime is an intrinsic referenced parameter at defined analyte concentrations and independent on fluctuations of the intensity of the excitation light source and on variations of probe concentrations. Therefore, the lifetime changes can alternatively be exploited to record enzyme kinetics.<sup>31</sup>

In conclusion, the TbNflx assay is inexpensive, straightforward, and fast and does not require any work-up or separation steps. A TbNflx based EF assay takes 30 to 60 minutes depending on the enzyme concentration and can be conducted in microwell plates. Therefore, it can be used for the screening of enzyme inhibitors. The uniqueness of this fluorescent method is that it opens the possibility to screen libraries of a number of different drug candidates for their impact on AC activity accompanied by the synchronous acquisition of kinetic data.

### 3.6. References

- <sup>1</sup> Sunahara RK, Taussig R (2002) Isoforms of mammalian adenylyl cyclase: multiplicities of signaling, *Mol Interv* **2**, 168-184
- <sup>2</sup> Defer N, Best-Belpomme M, Hanoune J (2000) Tissue specificity and physiological relevance of various isoforms of adenylyl cyclase, *Am J Physiol Renal Physiol* **279**, F400-F416
- <sup>3</sup> Weinstein LS, Chen M, Xie T, Liu J (2006) Genetic diseases associated with heterotrimeric G proteins, *Trends Pharmacol Sci* **27**, 260-266
- <sup>4</sup> Cooper DMF (2003) Regulation and organization of adenylyl cyclases and cAMP, *Biochem J* **375**, 517-529
- <sup>5</sup> Ahuja N, Kumar P, Bhatnagar R (2004) The adenylate cyclase toxins, *Crit Rev Microbiol* **30**, 187-196
- <sup>6</sup> Shen Y, Lee Y-S, Soelaiman S, Bergson P, Lu D, Chen A, Beckingham K, Grabarek Z, Mrksich M, Tang W-J (2002) Physiological calcium concentrations regulate calmodulin binding and catalysis of adenylyl cyclase exotoxins, *EMBO J* **21**, 6721-6732
- <sup>7</sup> Mock M, Fouet A (2001) Anthrax, *Annu Rev Microbiol* **55**, 647-671
- <sup>8</sup> Mourez M (2004) Anthrax toxins, *Rev Physiol Biochem Pharmacol* **152**, 135-164

- 
- <sup>9</sup> Sunahara RK, Dessauer CW, Gilman AG (1996) Complexity and diversity of mammalian adenylyl cyclases, *Annu Rev Pharmacol Toxicol* **36**, 461-480
- <sup>10</sup> Hanoune J, Defer N (2001) Regulation and role of adenylyl cyclase isoforms, *Annu Rev Pharmacol Toxicol* **41**, 145-174
- <sup>11</sup> Williams C (2004) cAMP detection methods in HTS: selecting the best from the rest, *Nat Rev Drug Discov* **3**, 125-135
- <sup>12</sup> Gabriel D, Vernier M, Pfeifer MJ, Dasen B, Tenaillon L, Bouhelal R (2003) High throughput screening technologies for direct cAMP measurement, *Assay Drug Dev Techn* **1**, 291-303
- <sup>13</sup> Adams SR, Harootunian AT, Buechler YJ, Taylor SS, Tsien RY (1991) Fluorescence ratio imaging of cyclic AMP in single cells, *Nature* **349**, 694-697
- <sup>14</sup> Vadakkadathmeethal K, Cunliffe JM, Swift J, Kennedy RT, Neubig RR, Sunahara RK (2007) Fluorescence-based adenylyl cyclase assay adaptable to high throughput screening, *Comb Chem High Throughput Screen* **10**, 289-298
- <sup>15</sup> Cunliffe JM, Sunahara RK, Kennedy RT (2006) Detection of adenylyl cyclase activity using a fluorescent ATP substrate and capillary electrophoresis, *Anal Chem* **78**, 1731-1738
- <sup>16</sup> Schäferling M, Wolfbeis OS (2007) Europium tetracycline as a luminescent probe for nucleoside phosphates and its application to the determination of kinase activity, *Chem Eur J* **13**, 4342-4349
- <sup>17</sup> Schrenkhammer P, Rosnizeck IC, Duerkop A, Wolfbeis OS, Schäferling M (2008) Time-resolved fluorescence-based assay for the determination of alkaline phosphatase activity and application to the screening of its inhibitors, *J Biomol Screening* **13**, 9-16
- <sup>18</sup> Mizukami S, Nagano T, Urano Y, Odani A, Kikuchi K (2002) A fluorescent anion sensor that works in neutral aqueous solution for bioanalytical application, *J Am Chem Soc* **124**, 3920-3925
- <sup>19</sup> Miao Y, Liu J, Hou F, Jiang C (2005) Determination of adenosine disodium triphosphate (ATP) using norfloxacin-Tb<sup>3+</sup> as a fluorescence probe by spectrofluorimetry, *J Lumin* **116**, 67-72
- <sup>20</sup> Georges J (1993) Lanthanide-sensitized luminescence and applications to the determination of organic analytes. A review, *Analyst* **118**, 1481-1486
- <sup>21</sup> Gopalakrishna R, Anderson WB (1982) Calcium(2+)-induced hydrophobic site on calmodulin: application for purification of calmodulin by phenyl-sepharose affinity chromatography, *Biochem Biophys Res Commun* **29**, 830-836
- <sup>22</sup> Gille A, Seifert R (2003) 2'(3')-O-(N-methylanthraniloyl)-substituted GTP analogs: a novel class of potent competitive adenylyl cyclase inhibitors, *J Biol Chem* **278**, 12672-12679

- 
- <sup>23</sup> Göttle M, Dove S, Steindel P, Shen Y, Tang W-J, Geduhn J, König B, Seifert R (2007) Molecular analysis of the interaction of *Bordetella pertussis* adenylyl cyclase with fluorescent nucleotides, *Mol Pharmacol* **75**, 526-535
- <sup>24</sup> Gille A, Lushington GH, Mou TC, Doughty MB, Johnson RA, Seifert R (2004) Differential inhibition of adenylyl cyclase isoforms and soluble guanylyl cyclase by purine and pyrimidine nucleotides, *J Biol Chem* **279**, 19955-19969
- <sup>25</sup> Alvarez R, Daniels DV (1990) A single column method for the assay of adenylate cyclase, *Anal Biochem* **187**, 98-103
- <sup>26</sup> Shen Y, Zhukovskays NL, Zimmer MI, Soelaiman S, Bergson P, Wang C-R, Gibbs CS, Tang W-J (2004) Selective inhibition of anthrax edema factor by adefovir, a drug for chronic hepatitis B virus infection, *Proc Natl Acad Sci USA* **101**, 3242-3247
- <sup>27</sup> Mills JS, Bailey BL, Johnson JD (1985) Cooperativity among calmodulin drug binding sites, *Biochem* **24**, 4897-4902
- <sup>28</sup> Anderson KW, Coll RJ, Murphy AJ (1984) Inhibition of skeletal muscle sarcoplasmic reticulum CaATPase activity by calmidazolium, *J Biol Chem* **259**, 11487-11490
- <sup>29</sup> Johnson JD, Wittenauer LA (1983) A fluorescent calmodulin that reports the binding of hydrophobic inhibitory ligands, *Biochem J* **211**, 472-479
- <sup>30</sup> Zhang J-H, Chung TDY, Oldenburg KR (1999) A simple statistical parameter for use in evaluation and validation of high throughput screening assays, *J Biomol Screen* **4**, 67-73
- <sup>31</sup> Spangler CM, Spangler C, Schäferling M (2008) Luminescent lanthanide complexes as probes for the determination of enzyme activities, *Ann NY Acad Sci* **1130**, 138-148

## 4. Cytidylyl Cyclase Activity of Bacterial and Mammalian “Adenylyl” Cyclases

### 4.1. Abstract

cAMP and cGMP are second messengers mediating cellular actions of extracellular factors such as hormones and neurotransmitters by the control of numerous functions from ion channel opening to regulation of gene expression. The exotoxins CyaA from *Bordetella pertussis* and edema factor (EF) from *Bacillus anthracis* compromise host immune defense by massive cAMP production, thereby facilitating survival of the bacteria. The interaction of the catalytically active domains of CyaA and EF with MANT-nucleotides revealed lower base-specificity than previously expected. The natural occurrence of a third cyclic nucleotide, cCMP, was discussed controversially. However, both CyaA and EF turn over other nucleotides than ATP and show low cytidylyl cyclase activity both *in vitro* and *in vivo*. The accumulation of cCMP in intact J774 murine macrophages and human leukemia HL-60 cells when treated with CyaA holoenzyme was demonstrated by specific and sensitive mass spectrometric methods. The data presented in this work also show that endogenous cCMP occurs in mammalian cells and that mammalian membranous and soluble ACs catalyze cCMP production at very low rates. Moreover, the presence of cUMP in cells and toxin-induced cUMP accumulation are demonstrated. This work points to novel roles of cCMP (and cUMP) as second messengers.

### 4.2. Introduction

The roles of cAMP and cGMP as intracellular second messengers are well established. In mammals, cAMP is synthesized from ATP by nine membrane-bound (mACs) and one soluble (sAC) AC isoform. Stimulatory or inhibitory regulation of mACs is mediated by G-proteins, CaM, protein kinases A and C, and  $\text{Ca}^{2+}$ , depending on the specific AC isoform.<sup>1,2</sup> G-proteins are membrane-associated heterotrimeric proteins composed of an  $\alpha$ -subunit and a  $\beta\gamma$ -subunit and are, in turn, regulated by G-protein-coupled receptors (GPCRs) *via* hormones and neurotransmitters.<sup>3,4</sup> cGMP is produced from GTP by a nitric oxide-stimulated soluble (sGC) and membrane-bound or particulate guanylyl cyclases (pGC).<sup>5,6</sup>

cAMP and cGMP regulate numerous cellular functions by binding to specific protein kinases, ion channels, PDEs, guanine nucleotide-exchange factors and transcription factors.<sup>5,6,7,8</sup> Furthermore, the concentration of cAMP and cGMP within the cell is not only

controlled by synthesis but also by degradation *via* eleven PDE families that differ from each other with respect to activation and substrate specificity.<sup>9</sup>

Apart from cAMP and cGMP, the existence of a third cyclic nucleotide, cCMP, in mammalian cells has been controversially discussed since the 1970s. A specific cCMP-forming cytidylyl cyclase (CC)<sup>10,11</sup> was postulated, a cCMP-degrading PDE<sup>12,13</sup> proposed, and cCMP supposedly identified in various organs<sup>14,15,16</sup> in the 1980s, but their existence was never definitely proven. More recently, several putative target proteins for cCMP-dependent phosphorylation have been identified in brain homogenates.<sup>17,18</sup> Furthermore, the membrane-permeable cCMP analogue, Bt<sub>2</sub>cCMP, was previously reported to inhibit superoxide formation in human neutrophils.<sup>19</sup>

However, early reports on stimulatory effects of cCMP on cell proliferation have not been substantiated and the putative CC and cCMP-PDE remained elusive. Overall, the cCMP field has been massively plagued by methodological problems, controversial and unconfirmed results and lack of biochemical tools.<sup>20,21</sup> As a matter of fact, the cyclic nucleotide research community has been extremely reluctant at investing resources and time into the cCMP field.

*Bordetella pertussis* and *Bacillus anthracis*, the causative agents of whooping cough and anthrax infection, respectively, produce and release the AC exotoxins CyaA and EF, respectively.<sup>22,23</sup> Both toxins are functionally closely related, although sequence alignment only shows structure similarity of 23% predominantly in the catalytic core of the proteins.<sup>24</sup> Both AC toxins are activated upon entry into host cells by the regulatory host-specific protein CaM.

CyaA and EF display unexpectedly high affinity for the nucleotide CTP and its derivatives. CTP showed very low  $K_i$  values at EF and CyaA in presence of  $Mn^{2+}$  and  $Mg^{2+}$ . The modification of CTP with fluorescent moieties led to surprising results: MANT-CTP possesses higher affinity for EF and CyaA than MANT-ATP.<sup>25,26</sup> Therefore, substrate-specificity of both toxins was explored using the catalytically active domain of CyaA (CyaA-N) and full-length EF. Here, it is demonstrated that both AC toxins additionally display a number of nucleotidyl cyclase (NC) activities *in vitro*. Furthermore, the generation of these “rare” cyclic nucleotides *in vivo* by cell-permeable holotoxins and their presence as endogenous cNMPs in J774 and HL-60 cells by a highly specific and extremely sensitive HPLC-MS/MS method is presented.

The unexpected presence of cCMP and cUMP as endogenous nucleotides in intact cells prompted us to explore the substrate-specificity of mammalian mACs and sAC. These enzymes exhibit very low CC activity as well. Additionally, several PDE isoforms representing important families have been tested for cCMP activity and no hydrolyzing cCMP activity was

found. This allows substantial cCMP accumulation despite very low CC activities of mammalian ACs.<sup>27</sup>

Intriguingly, the *in vivo*-effects of EF cannot readily be explained by increases in cAMP levels, suggesting that a yet unknown enzymatic activity of EF may contribute to its action.<sup>28</sup> Altogether, the endogenous occurrence of cCMP and cUMP in living cells and the accumulation of these nucleotides upon treatment of cells with toxins point to the importance of these cyclic nucleotides in cell signaling.

### 4.3. Materials and Methods

#### 4.3.1. Chemicals

Solvents used for extraction and in HPLC analysis were water, methanol and acetonitrile (HPLC-gradient grade, J. T. Baker, Deventer, The Netherlands). Ammonium acetate and bovine serum albumin (BSA) were purchased from Sigma-Aldrich Chemie (Steinheim, Germany), sodium hydroxide and tris(hydroxymethyl)-aminomethane (TRIS), magnesium chloride hexahydrate, and calcium chloride dihydrate were obtained from Merck (Darmstadt, Germany) and acetic acid was from Riedel-de Haen (Hannover-Seelze, Germany). Protective antigen (PA) was from Quadratech (Surrey, UK).

Inosine 5'-triphosphate trisodium salt (98%) (ITP), uridine 5'-triphosphate sodium salt (97%) (UTP), adenosine 5'-triphosphate disodium salt (99%) (ATP), and guanosine 5'-triphosphate sodium salt hydrate (> 95%) (GTP) and 3-isobutyl-1-methylxanthine (99%) (IBMX) were from Sigma-Aldrich Chemie (Steinheim, Germany). Cytidine 5'-triphosphate sodium salt (>95%) (CTP), xanthosine 5'-triphosphate triethylammonium salt (> 95%) (XTP), and 2'-deoxythymidine 5'-triphosphate sodium salt (> 95%) (TTP) were from Jena Bioscience (Jena, Germany). The cyclic nucleotides adenosine-3',5'-cyclic monophosphate sodium salt (> 99%) (cAMP), cytidine-3',5'-cyclic monophosphate sodium salt (> 98%) (cCMP), guanosine-3',5'-cyclic monophosphate sodium salt (> 98%) (cGMP), inosine-3',5'-cyclic monophosphate sodium salt (> 98%) (cIMP), cyclic thymidine-3',5'-cyclic monophosphate sodium salt (> 98%) (cTMP), uridine-3',5'-cyclic monophosphate sodium salt (> 98%) (cUMP), and xanthosine-3',5'-cyclic monophosphate sodium salt (> 98%) (cXMP) and the analogues *N*<sup>6</sup>,2'-*O*-dibutyryladenosine-3',5'-cyclic monophosphate (> 97%) (Bt<sub>2</sub>cAMP), and *N*<sup>4</sup>,2'-*O*-dibutyrylcytidine-3',5'-cyclic monophosphate (> 97%) (Bt<sub>2</sub>cCMP) were obtained from Biolog Life Science Institute (Bremen, Germany)

#### 4.3.2. Enzyme and Membrane Preparations

*E. coli* cells were transfected with plasmid pProExH6-EF and pExCyaA-N. Full-length EF and the catalytic domain of CyaA-N (amino acids 1 to 373) were purified from *E. coli* similar to the methods described by Shen *et al.*<sup>29</sup>. CaM was purified from calf brain according to Gopalakrishna *et al.*<sup>30</sup>. The activity of the extracted enzymes was tested by assays with [ $\alpha$ -<sup>32</sup>P]ATP.<sup>31</sup> [ $\alpha$ -<sup>32</sup>P]ATP (3,000 Ci/mmol) was purchased from Perkin Elmer Life Sciences (Boston, MA, USA). Sf9 cell culture, expression of recombinant AC isoforms I, II, and V and the preparation of Sf9 membranes were performed as described.<sup>32</sup> Human soluble AC (hsAC) was donated by T.-C. Mou (Center for Biomolecular Structure and Dynamics, University of Montana, Missoula, MT, USA) and was purified as described.<sup>33</sup>

*Bordetella pertussis* CyaA holo-toxin (CyaA-wt) and the enzymatically inactive variant CyaA-E5 (CyaA-mut) (lacking cAMP-synthesising activity as a result from a Leu-Gln dipeptide insertion between Asp 188 and Ile 189 in the catalytic core of the enzyme) were donated by Daniel Ladant (Department of Structural Biology and Chemistry, Institut Pasteur, Paris, France). Briefly, enzymes were expressed in *E. coli* and purified to near homogeneity by a previously established procedure<sup>34</sup> modified as described<sup>35</sup> in order to eliminate most of the contaminating endotoxin. The specific activity of CyaA, measured as described in Ladant *et al.*<sup>36</sup> was higher than 500 mmol cAMP/min mg, whereas CyaA-mut had no detectable enzymatic activity.

#### 4.3.3. Nucleotidyl Cyclase Assays

For Michaelis-Menten kinetics of EF and CyaA-N with the substrate ATP 100 pM enzyme was used, whereas 100 nM of AC toxins was applied when determining  $k_{cat}$  and  $K_M$  of other NTPs. The MgNTP concentrations were varied between 5  $\mu$ M and 1 mM. The CaM concentration was adjusted to a stoichiometry of 1:10 for AC toxin to CaM. The assay tubes contained final concentrations of 5 mM  $Mg^{2+}$ , 10  $\mu$ M  $Ca^{2+}$ , 10 mM TRIS·HCl pH 7.5, and 0.1 wt% BSA. The temperature for the assay was set to 37 °C and reaction times were varied according to nucleotide used (MgGTP: 30 min; MgTTP: 60 min; MgCTP, MgUTP: 10 min; MgATP: 5 min; MgXTP, MgITP: 90 min). The total volume was 50  $\mu$ L per tube. The reaction was stopped by heat-inactivation at 95 °C for 5 min. The precipitated proteins were removed by centrifugation. Forty  $\mu$ L of the supernatant fluid was combined with 40  $\mu$ L of internal standard (IS) solution. As internal standard cXMP was used at a concentration of 200 ng/mL when determining the turnover of all MgNTPs except for MgXTP. When the Michaelis-Menten kinetic of MgXTP was determined, 200 ng/mL cIMP was applied as IS. Determination of cNMP concentration was performed as described in *quantitation of cyclase reactions*.

Cyclase assays with Sf9-membrane preparations were conducted with a protein amount of 40 µg protein per tube, 5 mM Mg<sup>2+</sup>, 1 mM EDTA, 37.5 mM TRIS-HCl pH 7.5, 10 µM GTPγS, 100 µM forskolin in a total volume of 50 µL. Cyclase assays with hsAC were conducted using 1 µg hsAC per tube in 50 mM TRIS-HCl pH 7.4, 5 mM Mg<sup>2+</sup>, and 0.1 wt% BSA in a total volume of 50 µL. hsAC was activated by 10 mM Ca<sup>2+</sup>. MgATP, MgCTP, MgGTP, and MgUTP were used at a concentration of 100 µM. The temperature was set to 37 °C and reaction times were 60 min. The reaction was stopped by 95 °C for 5 min and precipitates removed by centrifugation. Measurement of cNMP amounts was performed as described in *quantitation of cell extracts* and values given as means ± SEM from n = 6.

#### 4.3.4. Cell Culture

HL-60 cells were grown in suspension in RPMI 1640 medium (PAA Laboratories, Pasching, Austria) with 10% (v/v) heat-inactivated and steril-filtered horse serum (Sigma-Aldrich Chemie), 1% (v/v) L-glutamine with penicillin/streptomycin (100x) (PAA Laboratories) and 1% (v/v) MEM-NEAA (100x) (PAN Biotech, Aidenbach, Germany) at 7% (v/v) CO<sub>2</sub> and 37 °C in a humidified atmosphere. Cells were kept at a density of 0.25-1.0 x 10<sup>6</sup> cells/mL.

J774 murine macrophages were grown adherently in RPMI 1640 medium (PAA Laboratories) with 10% (v/v) heat-inactivated and steril-filtered fetal bovine serum (PAN Biotech), 1% (v/v) L-glutamine with penicillin/streptomycin (100x) (PAA Laboratories) and 1% (v/v) Sodium pyruvate (100x) (PAN Biotech) at 5% (v/v) CO<sub>2</sub> and 37 °C in a humidified atmosphere. Cells were kept at a density of 0.4-1.0 x 10<sup>6</sup> cells/mL in T175 tissue flasks (Greiner Bio-one, Frickenhausen, Germany) with 30 mL medium.

For treatment with holo-CyaA toxins and a combination of PA and EF, J774 cells were transferred to a sterile Nunclon 6-well dish à 9.6 cm<sup>2</sup> (Fisher Scientific, Schwerte, Germany) at a concentration of 7.5 x 10<sup>5</sup> cells/well in 1.5 mL medium. Prior to holo-CyaA treatment, HL-60 cells were treated with 1.25% (v/v) DMSO (Sigma-Aldrich Chemie) for 96 hours to induce granulocytic differentiation. HL-60 cells were transferred to a 24-well dish à 1.9 cm<sup>2</sup> with 1.0 x 10<sup>6</sup> cells/well in 1 mL medium. CyaA-wt was added at concentrations of 1 µg/mL and 10 µg/mL to culture medium, the AC defective mutant CyaA-mut was used as negative control at a concentration of 10 µg/mL. CyaA-wt and CyaA-mut were stored at -80°C in 8 M urea buffer. Therefore, an additional negative control with equal amounts of 8 M urea buffer alone was used. PA and EF were applied in a ratio of 7:3 and added to J774 cells at a concentrations of 2.3 µg/mL and 1 µg/mL, respectively. The cells were processed after 15, 30, 45, 60, 120, and 240 min of incubation, respectively, as described in *extraction of cNMPs from cells*.



#### 4.3.5. Extraction of cNMPs from Cells

HL-60 cells were transferred to 1.5 mL tubes on crushed ice (4 °C) and centrifuged at 4 °C at 4.000 x g. The medium was removed and discarded. The extraction mixture was acetonitrile/methanol/water (40/40/20, v/v/v). Threehundred µL of extraction mixture was added to the cell pellet and cells were resuspended to quench metabolism and initiate extraction process followed by a 15 min incubation step at 4 °C. The cell suspension was then heated to 95 °C for 15 min. After cooling, the suspension was centrifuged at maximum speed (20.000 x g) for 5 min. Extraction of the resulting pellet was repeated once and the supernatant fluids combined in a 2 mL tube. The solvent was then evaporated to dryness at 40 °C und a gentle stream of nitrogen gas. The residue was resuspended in 150 µL of water under vigorous mixing and centrifuged at full speed to remove insoluble precipitates.

Medium was removed from J774 cells on ice and 300 µL of ice-cold extraction mixture was added. Cells were scraped from the surface and the suspension was transferred to 1.5 mL cups on ice and incubated for 15 min. All further steps correspond to the work-up of HL-60 cells. cNMPs were determined from three independent experiments as described in *quantitation of cell extracts*.

#### 4.3.6. RNA-Extraction

J774 cells ( $7.5 \times 10^5$  cells) were transferred to 6-well plates treated with the stimuli CyaA-wt, CyaA-mut, Bt<sub>2</sub>cAMP, Bt<sub>2</sub>cCMP, cAMP, and cCMP. RNA was extracted for microarray and real-time-PCR analysis. Plates were placed on ice and medium was removed. Cells were washed twice with ice-cold phosphate buffer saline (PBS) solution. PBS was obtained by 1:10 dilution of Dulbecco's PBS 10 x without Ca, Mg (PAA Laboratories). Then, 750 µL PBS was added, the cells were removed from the dish and placed into 1.5 mL tubes. A second step using 500 µL PBS was added and the suspensions were combined. Cells were centrifuged at 3.000 x g and PBS removed thoroughly. The cell pellet was frozen at -80 °C until RNA was extracted by NucleoSpin RNA II kit from Macherey-Nagel (Düren, Germany). The extraction was carried out according to the manufacturer's instructions. The RNA content was determined by a Nanodrop 1000 Spectrometer from Thermo Scientific (Wilmington, DE, USA).

#### 4.3.7. Microarray-Based mRNA Expression Analysis

The Whole Mouse Genome Oligo Microarray (Agilent Technologies, Santa Clara, CA, USA) used in this study contains 45018 oligonucleotide probes covering the entire murine

transcriptome. Synthesis of cRNA was performed with the Quick Amp Labeling kit, one color (Agilent Technologies) according to the manufacturer's recommendations. cRNA fragmentation, hybridization and washing steps were also carried-out exactly as recommended by One-Color Microarray-Based Gene Expression Analysis Protocol V5.7 (see [http://www.chem.agilent.com/en-US/Search/Library/\\_layouts/Agilent/PublicationSummary.aspx?whid=55389&liid=3855](http://www.chem.agilent.com/en-US/Search/Library/_layouts/Agilent/PublicationSummary.aspx?whid=55389&liid=3855) for details). Slides were scanned on the Agilent Micro Array Scanner G2565BA at two different PMT settings (100% and 5%) to increase the dynamic range of the measurements (extended dynamic range mode). Data extraction was performed with the Feature Extraction Software V9.5.3.1 by using the recommended default extraction protocol file: GE2-v5\_95\_Feb07.xml.

Processed intensity values of the green channel (gProcessedSignal or gPS) were globally normalized by a linear scaling approach: All gPS values of one sample were multiplied by an array-specific scaling factor. This scaling factor was calculated by dividing a reference 75<sup>th</sup> percentile value (set as 1500 for the whole series) by the 75<sup>th</sup> percentile value of the particular microarray (Array *i* in the formula shown below). Accordingly, normalized gPS values for all samples (microarray data sets) were calculated by the following formula:

$$\text{normalized } gPS_{\text{Array } i} = gPS_{\text{Array } i} \times (1500 / 75^{\text{th}} \text{ percentile}_{\text{Array } i})$$

A lower intensity threshold was defined as 1% of the reference 75<sup>th</sup> percentile value (= 15). All of those normalized gPS values that fell below this intensity border, were substituted by the respective surrogate value of 15.

Ratios of relative mRNA expression from two biologically independent replicates were calculated using excel macros.

#### 4.3.8. Real-Time PCR (RT-PCR)

cDNA was obtained by mixing 1 µg RNA, Oligo(dT)<sub>18</sub> primer, random hexamer primer, RiboLock RNase inhibitor, 10 mM dNTP Mix, water, and RevertAid M-MuLV Reverse Transcriptase from Fermentas (St. Leon-Rot, Germany) according to the manufacturer's instructions. The mixture was incubated 10 min at 25 °C and afterwards heated to 37 °C for 1 hour.

Primer pairs were purchased from Eurofins MWG Synthesis (Ebersberg, Germany). The expression levels were normalized to the house-keeping gene actin using a TaqMan probe and a TagMan Gene Expression Master Mix by Applied Biosystems (Foster City, CA, USA). A temperature profile of 95 °C for 10 min followed by 40 cycles of 10 s 95 °C and 60 s 60 °C was applied. All other genes were assayed in a 20 µL batch composed of 10 µL Fast Sybr Green Master Mix (2x Mix) (Applied Biosystems), which includes AmpliTaq® Fast DNA

Polymerase, Sybr Green I dye, deoxynucleotides and a passive internal standard reference based on proprietary Rox™ dye, 7 µL water, 2 µL cDNA and 1 µL (= 10 pmol) primer-mixture in MicroAmp 96-well reaction plates covered by MicroAMP Optical Adhesive Film from Applied Biosystems. A non-template control was conducted as negative control. A temperature profile of 95 °C for 20 s for activation of polymerase followed by 40 cycles of denaturation at 95 °C for 3 s and annealing and extension at 60 °C for 30 s was applied. The experiment was performed in a Step One Plus Real-Time PCR System from Applied Biosystems.

Threshold  $C_T$  values for each individual PCR products were calculated by use of the instrument's software, and  $C_T$  values obtained were normalized by subtracting the  $C_T$  values obtained for  $\beta$ -actin. The resulting  $\Delta C_T$  values were then used to calculate relative changes of mRNA expression as ratio  $R$  of mRNA expression of stimulated to unstimulated cells according to the following equation:

$$R = 2^{-[\Delta C_T(\text{stimulated}) - \Delta C_T(\text{unstimulated})]}$$

CyaA-wt and CyaA-mut-treated cells were normalized to cells treated with buffer; Bt<sub>2</sub>cAMP and Bt<sub>2</sub>cCMP-treated cells were referred to cells treated with sodium butyrate, and cAMP and cCMP-treated cells were corrected using results from cells treated with water. RT-PCR was performed with  $n = 4$  and values given as mean  $\pm$  SEM.

#### 4.3.9. Quantitation of Cyclase Reactions

The chromatographic separation of cAMP, cCMP, cUMP, cIMP, and cTMP and the IS cXMP was performed on a LC-10ADVP HPLC system (Shimadzu, Kyoto, Japan) equipped with a binary pump system. A combination of Supelco Column Saver (2.0 µm filter, Supelco Analytical, Bellefonte, CA, USA), Security Guard Cartridge (C18, 4 x 2 mm) in an Analytical Guard Holder KJO-4282 (Phenomenex, Aschaffenburg, Germany) and an analytical NUCLEODUR C18 Pyramid RP column (50 x 3 mm, 3 µm particle size, Macherey-Nagel) temperature controlled by a convenient HPLC column oven at 25 °C was used.

Eluent A consisted of 5 mM ammonium acetate and 0.1% (v/v) acetic acid in water and eluent B was methanol. The injection volume was 50 µL and the flow rate was 0.4 mL/min throughout the chromatographic run. Eluent A (100%) was used from 0 to 5 minutes followed by a linear gradient from 100% A to 70% A until 9 min. Eluent A (70%) was kept until 11 min and re-equilibration of the column at 100% A was achieved from 11 to 15 min. The retention times of analytes were as follows: cAMP: 9.7, cCMP: 5.0, cIMP: 8.7, cTMP: 8.8, cUMP: 7.9 and cXMP: 8.4 min.

The analyte detection was performed on an API 2000 triple quadrupole mass spectrometer (Applied Biosystems) using selected reaction monitoring (SRM) analysis in positive ionization mode. The following SRM transitions using a dwell time of 40 ms were detected: cAMP: +330/136; cCMP: +306/112; cIMP: +331/137; cTMP: +305/127; cUMP: +307/97; cXMP: + 347/153. The mass spectrometer parameter were as follows: ion source voltage: 5500 V, temperature: 350 °C, curtain gas: 40 psi, collisionally activated dissociation (CAD) gas: 5 psi.

The chromatographic separation of cGMP using cXMP as IS and cXMP using cIMP as IS was performed on a Series 200 HPLC system (Perkin Elmer Instruments, Norwalk, CT, USA) equipped with a binary pump system and a 250 µL syringe. A combination of Supelco Column Saver (2.0 µm filter, Supelco Analytical, Bellafonte, CA, USA), Security Guard Cartridge (C18, 4 x 2 mm) in an Analytical Guard Holder KJO-4282 (Phenomenex) and an analytical NUCLEODUR C18 Pyramid RP column (50 x 3 mm, 3 µm particle size, Macherey-Nagel) temperature controlled by a HPLC column oven at 25 °C, was used.

Eluent A consisted of 5 mM ammonium acetate and 0.1% (v/v) acetic acid in water and eluent B was methanol. The injection volume was 50 µL and the flow rate was 0.4 mL/min throughout the chromatographic run. Eluent A (100%) was used from 0 to 5 min followed by a linear gradient from 100% A to 70% A until 9 min. Eluent A (70%) was kept until 11 min and re-equilibration of the column at 100% A was achieved from 11 to 16 min. The retention times of analytes was as follows: cGMP: 8.0, cXMP: 8.5 and cIMP: 8.7 min.

The analyte detection was performed on an API 3000 triple quadrupole mass spectrometer (Applied Biosystems) using selected reaction monitoring (SRM) analysis in positive ionization mode. The following SRM transitions using a dwell time of 40 ms were detected: cGMP: +346/152; cIMP: +331/137; cXMP: +347/153. The mass spectrometer parameter were as follows: ion source voltage: 5500 V, temperature: 350 °C, nebulizer gas: 6 psi, curtain gas: 15 psi, CAD gas: 10 psi.

#### 4.3.10. Quantitation of Cell Extracts

Due to interferences of cell matrix components with the HPLC methods described in *quantitation of cyclase reaction*, the separation method was revised and improved in order to obtain good chromatographic separation without interference of matrix peaks. The chromatographic separation was performed on an Agilent 1100 Series HPLC system (Agilent Technologies) equipped with a binary pump system with 100 µL syringe size. A combination

of Supelco Column Saver (2.0  $\mu\text{m}$  filter, Supelco Analytical), Security Guard Cartridge (C18, 4 x 2 mm) in an Analytical Guard Holder KJO-4282 (Phenomenex) and an analytical Zorbax Eclipse XDB-C16 column (50 x 4.6 mm, 1.8  $\mu\text{m}$  particle size, Agilent Technologies), temperature controlled by a HPLC column oven at 25 °C was used.

Eluent A consisted of 50 mM ammonium acetate and 0.1% (v/v) acetic acid in a methanol/water mixture (5/95 v/v) and eluent B was 50 mM ammonium acetate and 0.1% (v/v) acetic acid in a methanol/water mixture (95/5 v/v). The injection volume was 30  $\mu\text{L}$  and the flow rate was 0.4 mL/min throughout the chromatographic run. A linear gradient from 100% A to 50% A was applied between 0 to 5 min followed by re-equilibration of the column at 100% A from 5 to 8 min. The retention times of analytes was as follows: cAMP: 6.3, cCMP: 3.4; cGMP: 5.3, cIMP: 5.2, cTMP: 5.4, cUMP: 4.5, and cXMP: 2.7 min. No IS was used due to several reasons: First, cXMP elutes very early in chromatographic separation and is, therefore, not suited for the analytes eluting later in the chromatographic run. Second, cXMP might have been an endogenous nucleotide. Third, other substances like deuterated cNMPs suitable to act as IS were not available in 100% purity resulting in a non-negligible contamination of the samples.

The analyte detection was performed on an AP Sciex QTRAP 5500 triple quadrupole mass spectrometer (Applied Biosystems) using SRM analysis in positive ionization mode. The following SRM transitions using a dwell time of 40 ms were detected: cAMP: +330/136; cCMP: +306/112; cGMP: +346/152; cIMP: +331/137; cTMP: +305/127; cUMP: +307/97; cXMP: +347/153. The mass spectrometer parameter were as follows: ion source voltage: 5500 V, temperature: 600 °C, curtain gas: 30 psi, CAD gas: 9 psi.

#### 4.3.11. Analysis of Data

Analysis of data was performed with GraphPad Prism 5.00 for Windows from GraphPad Software (San Diego, CA, USA, [www.graphpad.com](http://www.graphpad.com)). Mean and error as SEM were calculated from at least three replicates. Kinetics were fitted by non-linear enzyme kinetic fit Michaelis-Menten calculating  $k_{\text{cat}}$  and  $K_{\text{M}}$ -values including errors. The substrate saturation curves with XTP and TTP showing substrate inhibition were analyzed by non-linear enzyme kinetic fit substrate inhibition.

## 4.4. Results

### 4.4.1. Nucleotidyl Cyclase Activity of CyaA-N and EF

For the determination of NC activities a highly sensitive HPLC-MS/MS method was employed separating seven cyclic nucleotides (cAMP, cCMP, cGMP, cIMP, cUMP, cTMP, cXMP, for structures see Fig. 4.1.) on a RP column by a binary gradient employing 5 mM ammonium acetate, 0.1 vol% acetic acid in water and methanol. The detection and quantitation of all cNMPs is carried out by tandem MS analysis monitoring SRMs specific for each cNMP (for detailed description see Chapter 4.3.9.). A typical chromatogram is depicted in Fig. 4.2.

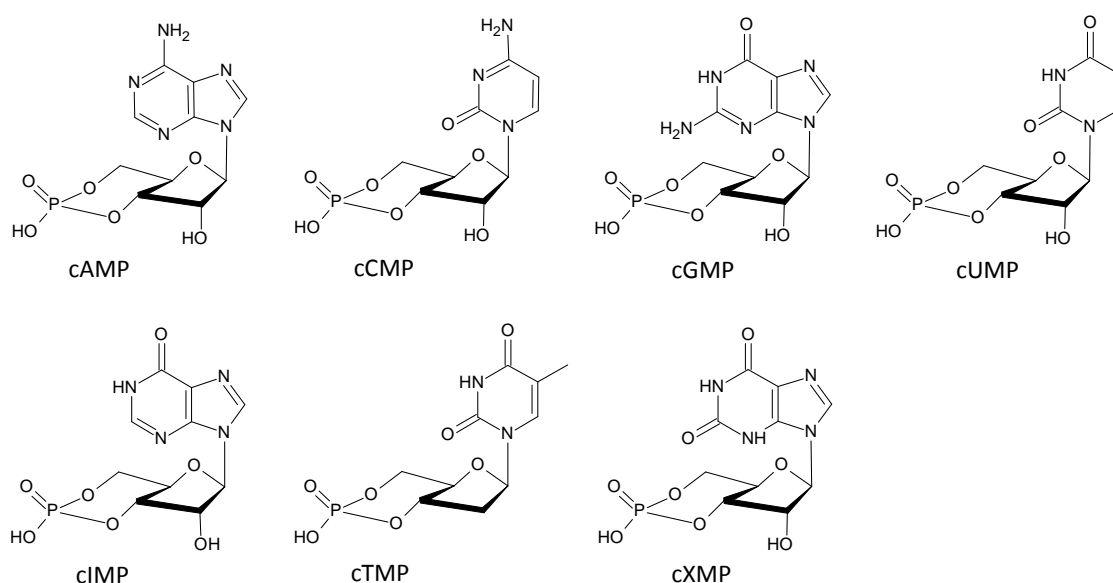


**Fig. 4.1.** Chemical structures of cyclic nucleotides analyzed in HPLC-MS/MS assays

This method was used to determine Michealis-Menten kinetics of full-length EF and the catalytically active domain of CyaA, CyaA-N, in substrate saturation experiments. Substrate specificities of purified enzymes in presence of  $Mg^{2+}$ , the physiological cation, were established. The calibration curves of cNMPs and the corresponding kinetics of CyaA and EF are depicted in Fig. 4.3. and Fig. 4.4 and  $k_{cat}$  and  $K_M$  values are summarized in Table 4.1.

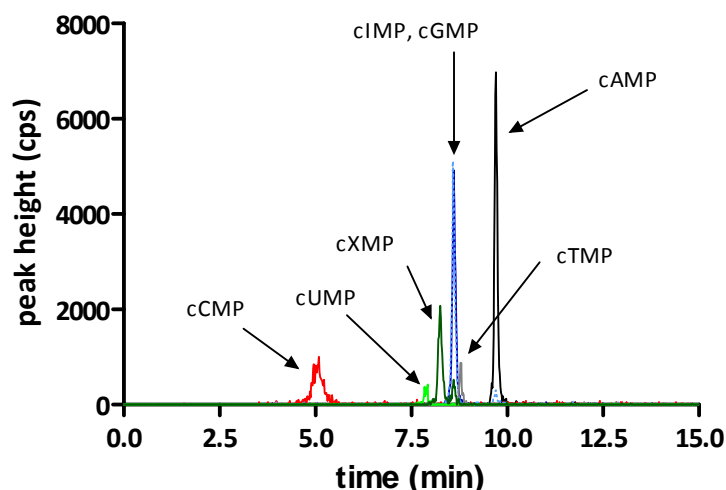


**Fig. 4.2.** Chromatogram of cNMP separation of a standard mixture with 256 ng/mL. Analyte peaks are detected at the following retention times: cCMP (red): 5.0, cUMP (light green): 7.9, cXMP (olive): 8.4, cIMP (cyan): 8.6, cGMP (dark blue): 8.7, cTMP (grey): 8.8, and cAMP (black): 9.7 min. Although peaks coincide, the identity of cNMPs is ascertained by SRM.

**Table 4.1.** Kinetic data of substrate saturation experiments with CyaA-N and EF

|    | CyaA-N                                     |                                      | n | EF  |                                      |
|----|--|--------------------------------------|---|---|--------------------------------------|
|    | $K_M$ ( $\mu\text{M}$ )                    | $k_{\text{cat}}$ ( $\text{s}^{-1}$ ) |   | $K_M$ ( $\mu\text{M}$ )                               | $k_{\text{cat}}$ ( $\text{s}^{-1}$ ) |
| AC | $171 \pm 22.8$                             | $1156 \pm 50$                        | 3 | $78.1 \pm 8.7$  | $524 \pm 14$                         |
| CC | $475 \pm 139$                              | $3.83 \pm 0.54$                      | 6 | $367 \pm 116$   | $1.95 \pm 0.26$                      |
| UC | $599 \pm 59$                               | $0.17 \pm 0.009$                     | 3 | $792 \pm 299$   | $0.31 \pm 0.07$                      |
| IC | $329 \pm 44$                               | $0.043 \pm 0.002$                    | 3 | $507 \pm 108$   | $0.065 \pm 0.007$                    |
| GC | $191 \pm 25$                               | $0.043 \pm 0.002$                    | 3 | $85 \pm 13$   | $0.0024 \pm 9\text{E-}5$             |
| TC | $19 \pm 5$                                 | $0.008 \pm 0.0003$                   | 3 | -   | -                                    |
|    | $K_i$ ( $\mu\text{M}$ ) = $1332 \pm 365$ * |                                      |   |   |                                      |
| XC | $37 \pm 7$                                 | $0.0077 \pm 0.0007$                  | 6 | $161,700 \pm 5.3\text{E}7$ <sup>a</sup>               | $1.02 \pm 335$ <sup>a</sup>          |
|    | $K_i$ ( $\mu\text{M}$ ) = $309 \pm 57$ *   |                                      |   | $K_i$ ( $\mu\text{M}$ ) = $0.03 \pm 8$ <sup>a,*</sup> |                                      |

<sup>a</sup> data-fit ambiguous, \*  $K_i$  for substrate inhibition

In fact, both CyaA-N and EF exhibited CC activity, but  $k_{\text{cat}}$  values were approximately 300 times lower than for AC activity. Both toxins also produced cUMP, cGMP, cIMP and cXMP at very low catalytic rates. cTMP production could only be detected in CyaA-N. XTP and TTP both are substrate and inhibitor at the same time.

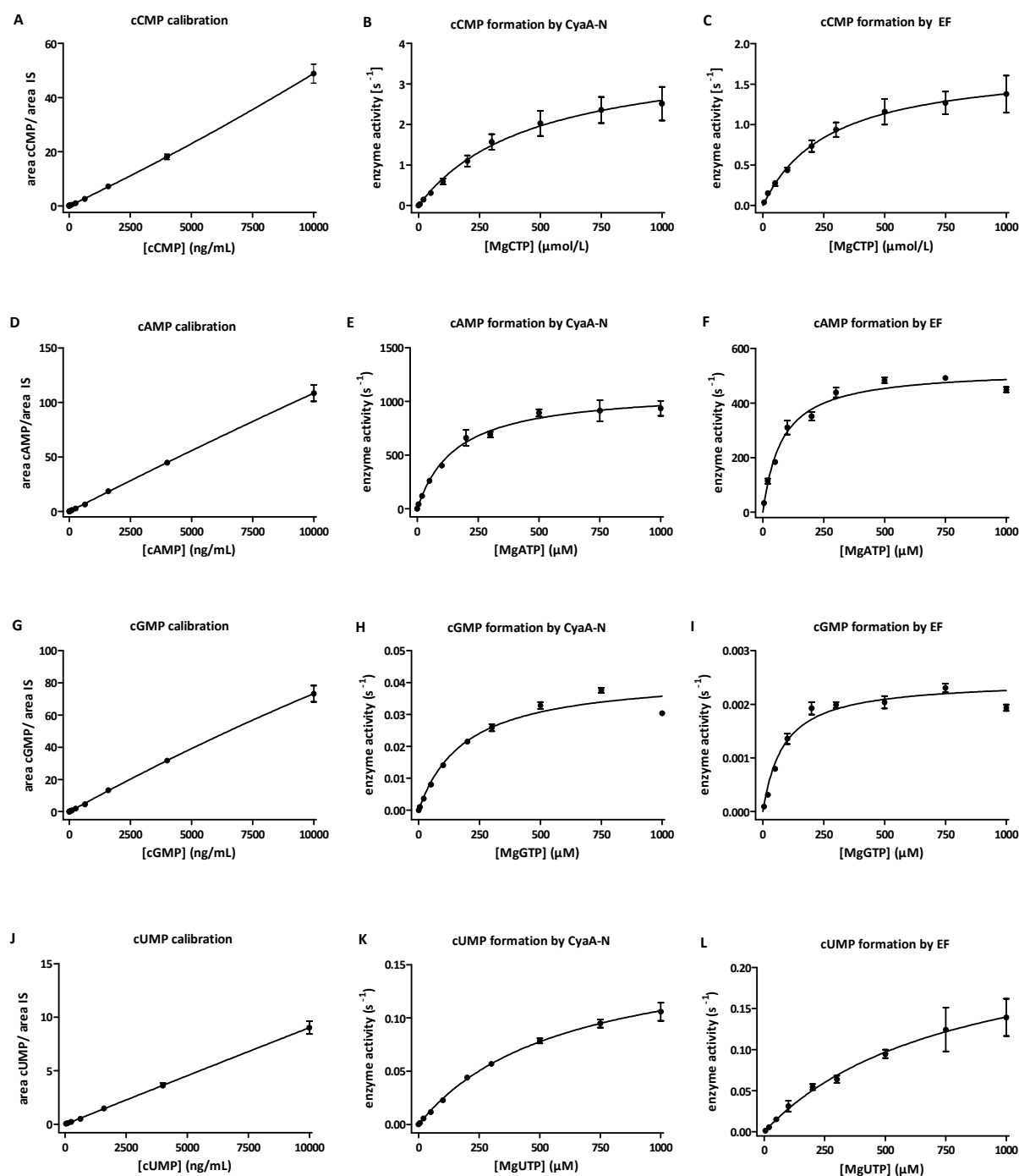


**Fig. 4.3.** Calibration curves of cNMPs and corresponding substrate saturation experiments with CyaA-N and EF, respectively. **A-C** cCMP calibration and CTP saturation, **D-F** cAMP calibration and ATP saturation, **G-I** cGMP calibration and GTP saturation and **J-L** cUMP calibration and UTP saturation.



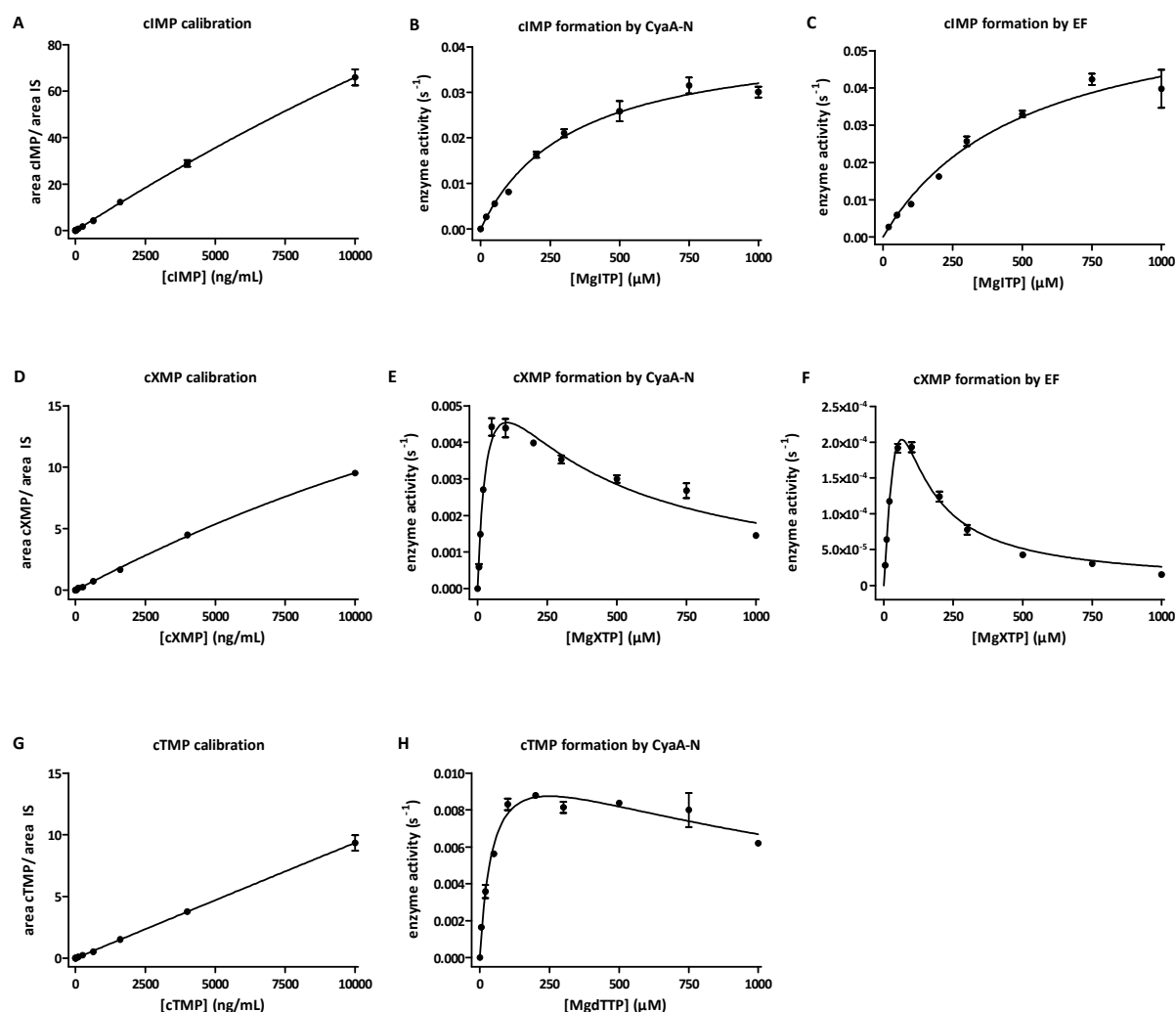


**Fig. 4.4.** Calibration curves of cNMPs and corresponding substrate saturation experiments with CyaA-N and EF, respectively. **A-C** cIMP calibration and ITP saturation, **D-F** cXMP calibration and XTP saturation, **G-H** cTMP calibration and TTP saturation. cTMP formation was only detected in CyaA-N but not in EF.

Fragmentation spectra of standard cCMP and cUMP and samples from an EF assay were recorded in order to ensure the identity of these cyclic nucleotides. The mass spectrum of cCMP shows signals from protonated cCMP ( $m/z = 306.00$  Da) and from the protonated cytosine base ( $m/z = 112.08$  Da). SRM of the  $m/z$  transition of 306.00 to 112.08 Da proofed the production of cCMP (see Fig. 4.5.). In case of cUMP, mass signals resulted from protonated cUMP ( $m/z = 307.08$  Da), the protonated uracil base ( $m/z = 112.92$  Da) and a not entirely identified fragment presumably containing phosphate ( $m/z = 97.08$ ). As the signal of the protonated uracil base is quite weak, the detection and quantitation of cUMP was achieved by the SRM 307/97.

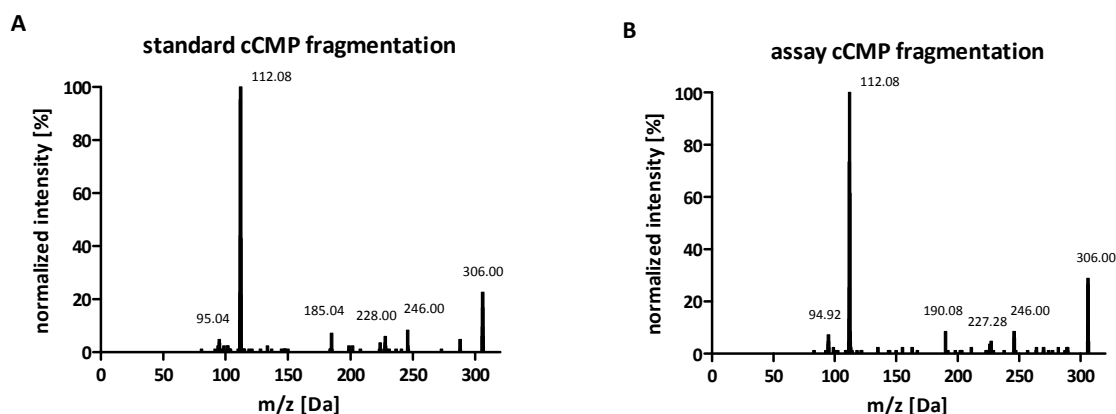


**Fig. 4.5.** Comparison of fragmentation patterns of **A** standard cCMP and **B** cCMP produced in a substrate saturation assay with EF and the substrate CTP. The patterns resemble one another very closely and provide evidence, that actually cCMP is produced in this assay.

#### 4.4.2. Effects of CyaA Holotoxins and EF in Intact Cells

It was demonstrated that both AC toxins produce other cyclic nucleotides than cAMP *in vitro*. To answer the question whether AC toxins increase cNMP levels other than cAMP in living systems, the effects of CyaA on murine J774 macrophages and granulocytic differentiated human leukemia HL-60 cells were investigated. For these experiments a cell-permeable CyaA holoenzyme, CyaA-wt, and a catalytically inactive but cell-permeable mutant, CyaA-mut, was used.

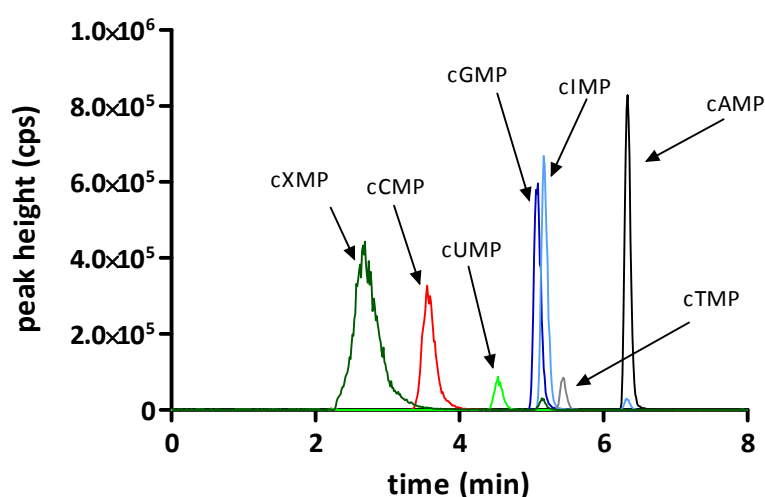


**Fig. 4.6.** Chromatographic separation of a standard mixture of cNMPs with 102 ng/mL by the HPLC-MS/MS method used for cell extracts. Retention times of analytes were as follows: cCMP (red): 3.4, cUMP (light green): 4.5, cXMP (olive): 2.7, cIMP (cyan): 5.2, cGMP (dark blue): 5.3, cTMP (grey): 5.5, and cAMP (black): 6.4 min

For these experiments, a new chromatographic method was developed due to interferences of cell matrix with the detection of cNMPs. A RP-column with smaller particle

size (3 → 1.8  $\mu\text{m}$ ) was used and the molarity of eluents was set from 5 to 50 mM ammonium acetate still containing 0.1 vol% acetic acid. Eluent A was 50 mM  $\text{NH}_4\text{OAc}$ , 0:1 vol% HAc in methanol/water (5/95 v/v) and eluent B 50 mM  $\text{NH}_4\text{OAc}$ , 0:1 vol% HAc in methanol/water (95/5 v/v). The chromatography was shortened from 15 to eight minutes (see Fig. 4.6.). The detection of cNMPs was performed on an extremely sensitive QTRAP 5500 system. An IS was omitted due to the fact that no suitable IS was available: cXMP eluted too early in chromatography and might have been an endogenous nucleotide itself and isotopically labeled cNMPs were only available at 98% purity resulting in considerable contamination of samples (for details see Chapter 4.3.10.).

In these experiments we surprisingly detected not only endogenous cAMP and cGMP but also cCMP and cUMP in both cell types. Remarkably, cCMP and cUMP levels were comparable to cGMP levels, making those nucleotides “common” rather than “rare” as they range in a physiologically relevant region (see Fig. 4.7. and 4.8.). Nevertheless, the endogenous levels of cNMPs in J774 and HL-60 cells differ approximately by a factor of two, with HL-60 cells showing lower cNMP concentration. In HL-60 cells, cCMP concentrations were above the detection limit but below the lower limit of quantitation (LLOQ).

CyaA-wt induced rapid and massive cAMP increases (~100-fold) in both cell types. Strikingly, CyaA-wt caused a delayed but substantial cCMP increase in J774 macrophages (~200-fold) and a less pronounced cCMP accumulation (~10-fold) in HL-60 cells. In J774 cells the cCMP levels reached roughly 10% of the cAMP levels. In addition to increases in cCMP a smaller and even further delayed cUMP increase was detected in J774 macrophages only, whereas no change in cGMP could be detected in both cell lines. The effects of CyaA-wt on cNMP levels were specific since the catalytically inactive CyaA-mut did not cause any significant changes in cNMP levels (see Fig. 4.7. and 4.8.). The cNMP increases were observed in the absence of any PDE inhibitor, and surprisingly, the global PDE inhibitor 3-isobutyl-methyl-xanthine (IBMX, 100  $\mu\text{M}$ ) had virtually no effect on cyclic nucleotide accumulation.

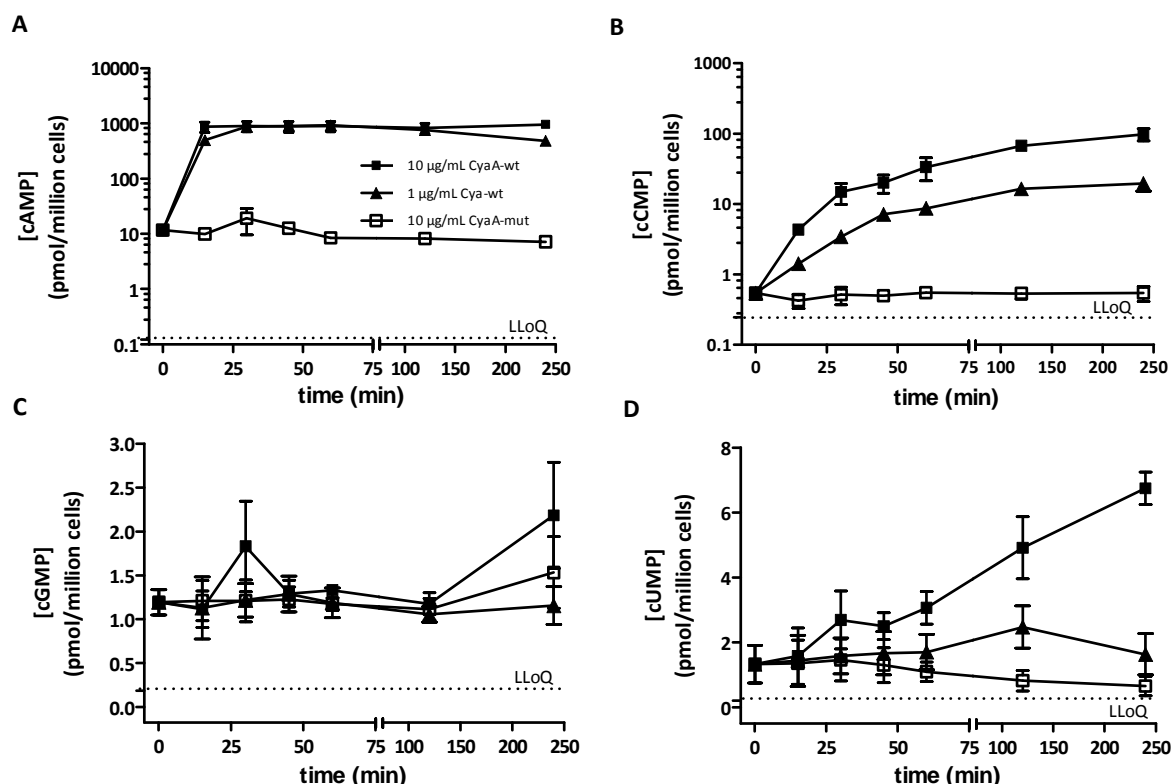


**Fig. 4.7.** cNMP accumulation in J774 cells after CyaA treatment. After treatment of J774 cells with 10 µg/mL CyaA-wt (■), 1 µg/mL CyaA-wt (▲) and 10 µg/mL CyaA-mut (□) **A** cAMP, **B** cCMP, **C** cGMP, and **D** cUMP concentrations were determined by HPLC-MS/MS. LLoQ depicts the lower limit of quantitation.

To obtain insights into the signalling cascade initiated by CyaA, microarray studies of mRNA levels in J774 macrophages were performed. CyaA-wt induced the expression of most genes to a much larger extent than the cell-permeable dibutyryl-cAMP (Bt<sub>2</sub>cAMP), suggestive for an additional role of cAMP-independent mechanisms. A correlation of expression levels demonstrates the difference in expression levels (see Fig. 4.9.) Among the upregulated genes were FOS (role in cell proliferation and differentiation)<sup>37</sup>, COX2 (role in inflammation)<sup>38</sup>, Nr4a2 (member of the steroid-thyroid hormone receptor superfamily with role in cell survival)<sup>39</sup>, Pscdbp (cytohesin 1-interacting protein with role in cell adhesion)<sup>40</sup>, Vegfa (member of PDGF/VEGF growth factor family with role in vascular permeability and angiogenesis)<sup>41</sup> and CD83 (role in B cell maturation and activation)<sup>42</sup>, all fitting to roles in host defence and inflammation.

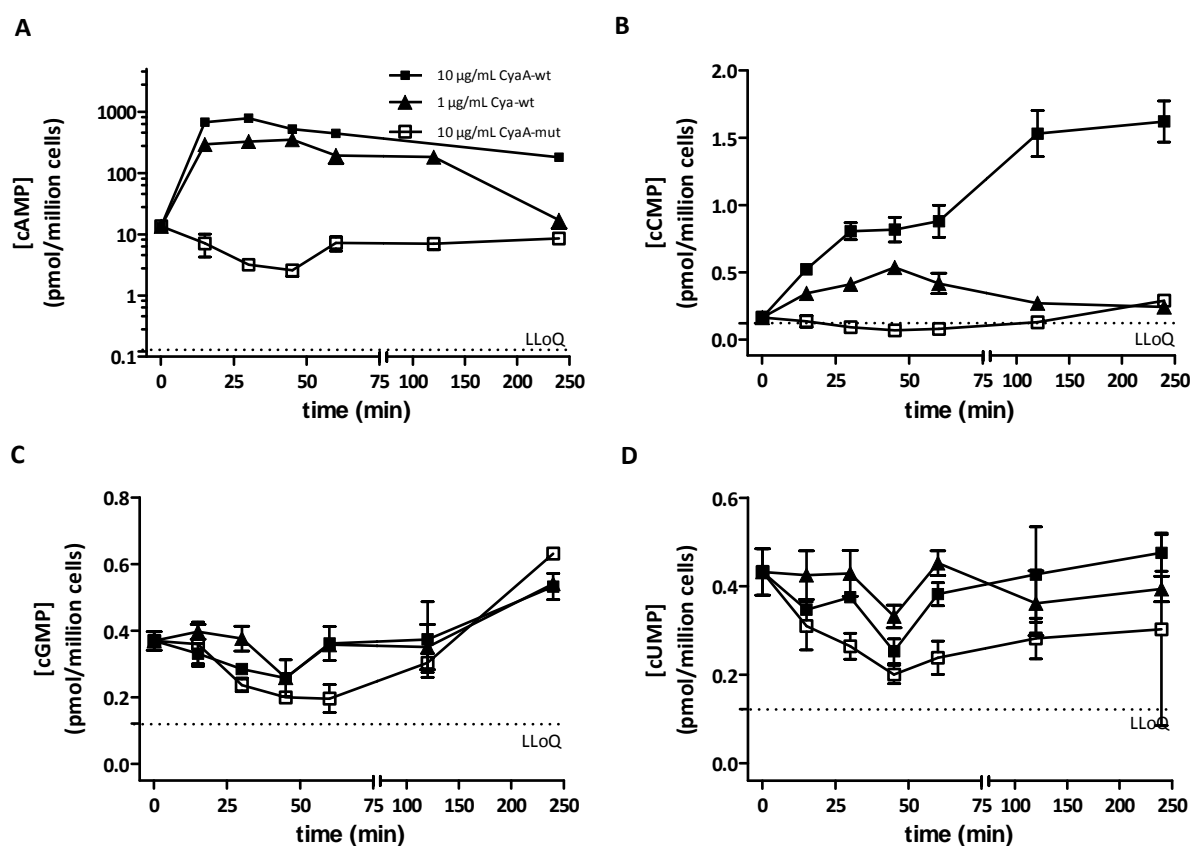


**Fig. 4.8.** cNMP accumulation in HL-60 cells after CyaA treatment. After treatment of HL-60 cells with 10 µg/mL CyaA-wt (■), 1 µg/mL CyaA-wt (▲) and 10 µg/mL CyaA-mut (□) **A** cAMP, **B** cCMP, **C** cGMP, and **D** cUMP concentrations were determined by HPLC-MS/MS. LLOQ depicts the lower limit of quantitation

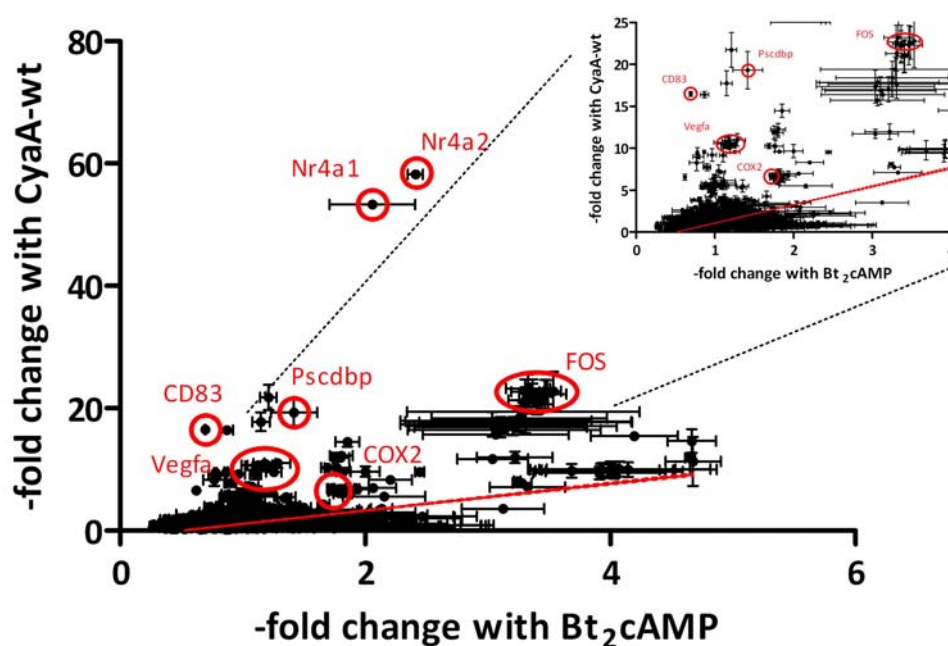


**Fig. 4.9.** Correlation of changes in mRNA expression levels when J774 cells are treated with CyaA-wt and Bt<sub>2</sub>cAMP. Prominent outliers were highlighted and analyzed by RT-PCR.

The effects of CyaA on gene expression were cNMP-mediated since the catalytically inactive CyaA-mut showed only negligible effect on mRNA expression levels. In contrast to the robust effects of Bt<sub>2</sub>cCMP on vascular relaxation and platelet aggregation reported<sup>43</sup>, this nucleotide showed little effects on gene expression as was true for cCMP and cAMP. For J774 macrophages, there are two explanations for these data. First, cCMP may act as modulator of cAMP action on gene expression rather than inducing prominent effects itself, or second, cCMP is compartmentalized in living cells and the addition of Bt<sub>2</sub>cCMP does not deliver cCMP where it has effects *in vivo*. The enhanced expression of the genes mentioned before was confirmed by RT-PCR experiments (see Fig. 4.10.).

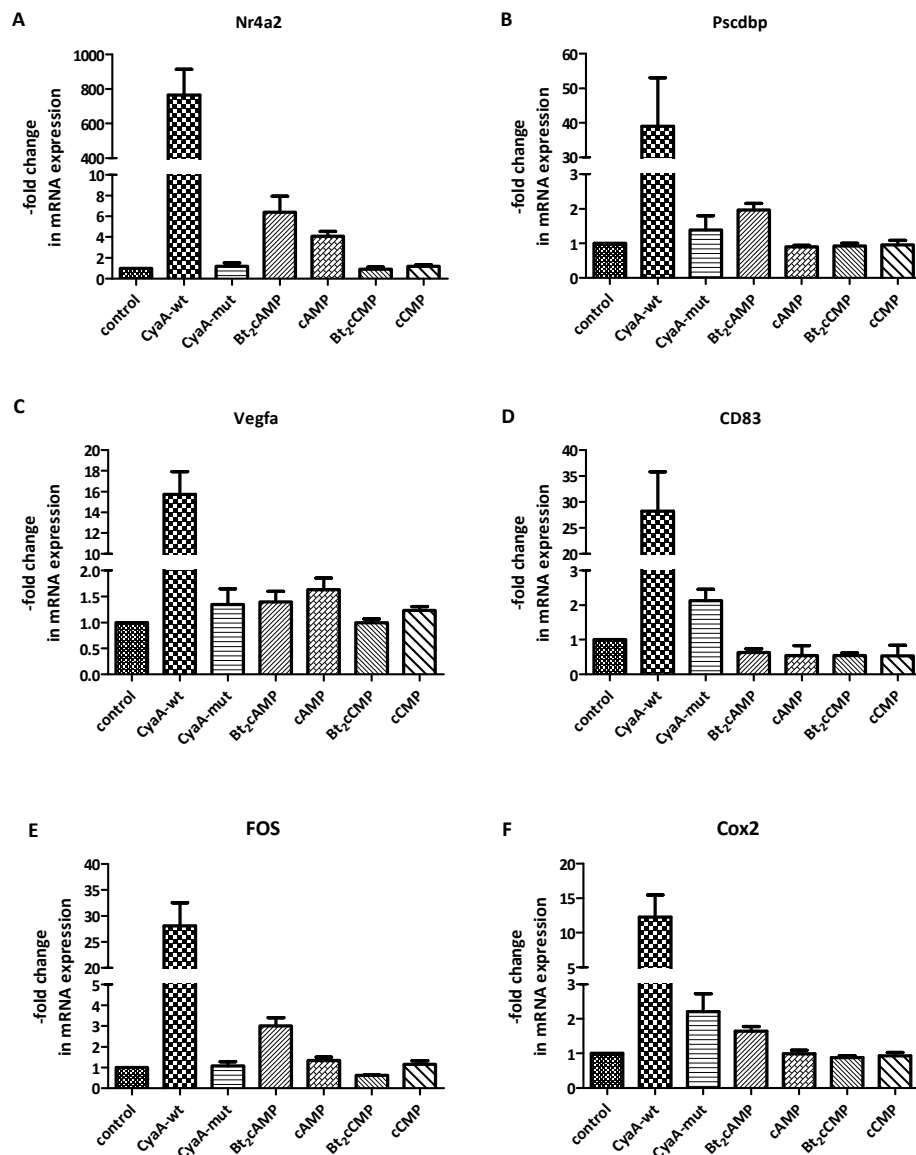


**Fig. 4.10.** Changes in mRNA expression levels on RT-PCR basis. Treatment with CyaA-wt induces massive changes in mRNA expression. In contrast, Bt<sub>2</sub>cAMP shows less effect on gene expression levels supporting the assumption that cAMP is not the only agent influencing changes in mRNA expression.

Additionally, we examined the effects of EF on cNMP accumulation in J774 macrophages. In general, it is assumed that EF needs PA for cell entry forming the holotoxin ETX.<sup>22</sup> Surprisingly, EF alone increased cAMP levels in J774 cells without the need of PA, indicating a PA-independent mechanism of cell entry. However, EF alone did not increase cCMP levels, but required the presence of PA for cCMP accumulation (see Fig. 4.11.). No increases of cGMP and cUMP were detected, neither with EF nor with ETX. EF was less effective at increasing cAMP- and cCMP-levels in J774 macrophages than CyaA, though.

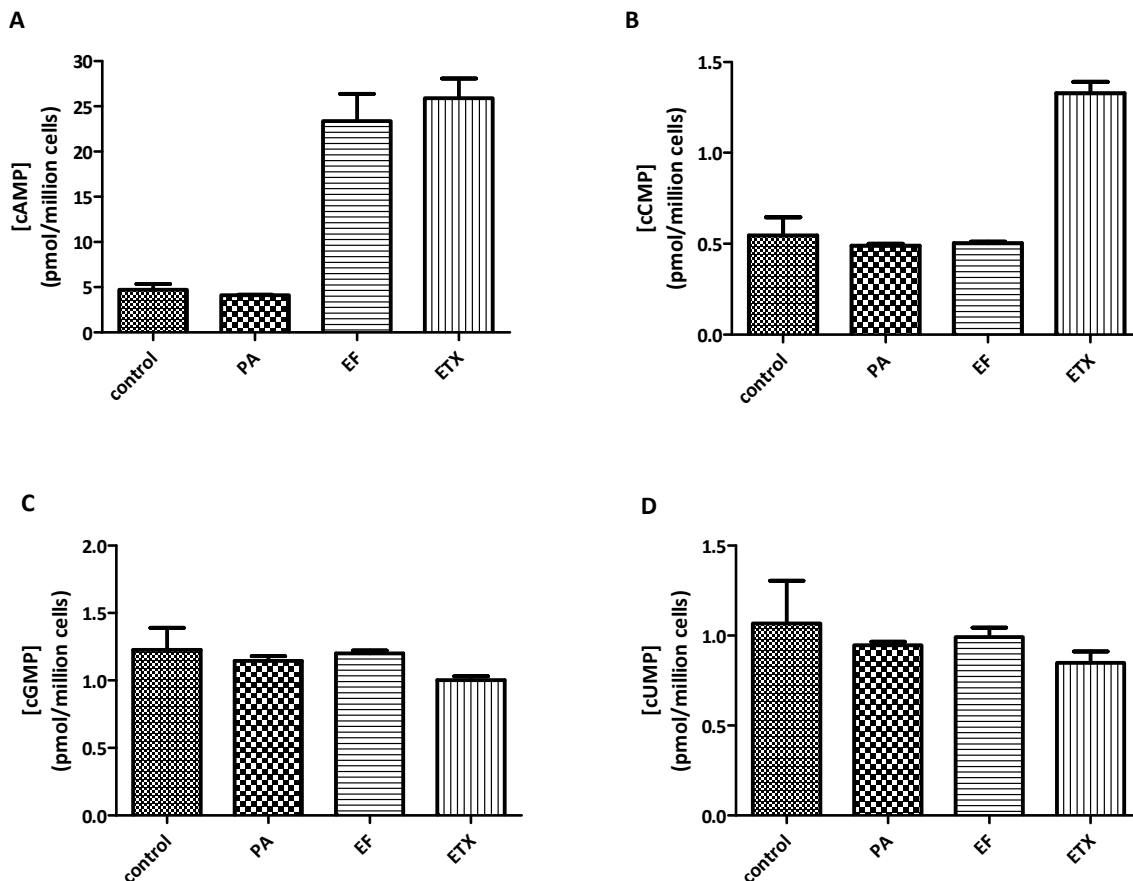


**Fig. 4.11.** cNMP concentrations in pmol/million cells after treatment of J774 cells for two hours with EF, PA and ETX. **A** cAMP concentration increases both with EF alone and ETX, whereas **B** cCMP only accumulates in the presence of ETX. **C** cGMP- and **D** cUMP-levels did not change after toxin treatment.

The function of the nucleotides cCMP and cUMP in living cells is not known, but initial experiments ( $n = 1$ ) with J774 macrophages at different cell densities per square centimeter show different cNMP concentrations per million cells indicating a possible role of cCMP and cUMP in cell growth (see Fig. 4.12.). However, there are no target genes or proteins identified, yet.

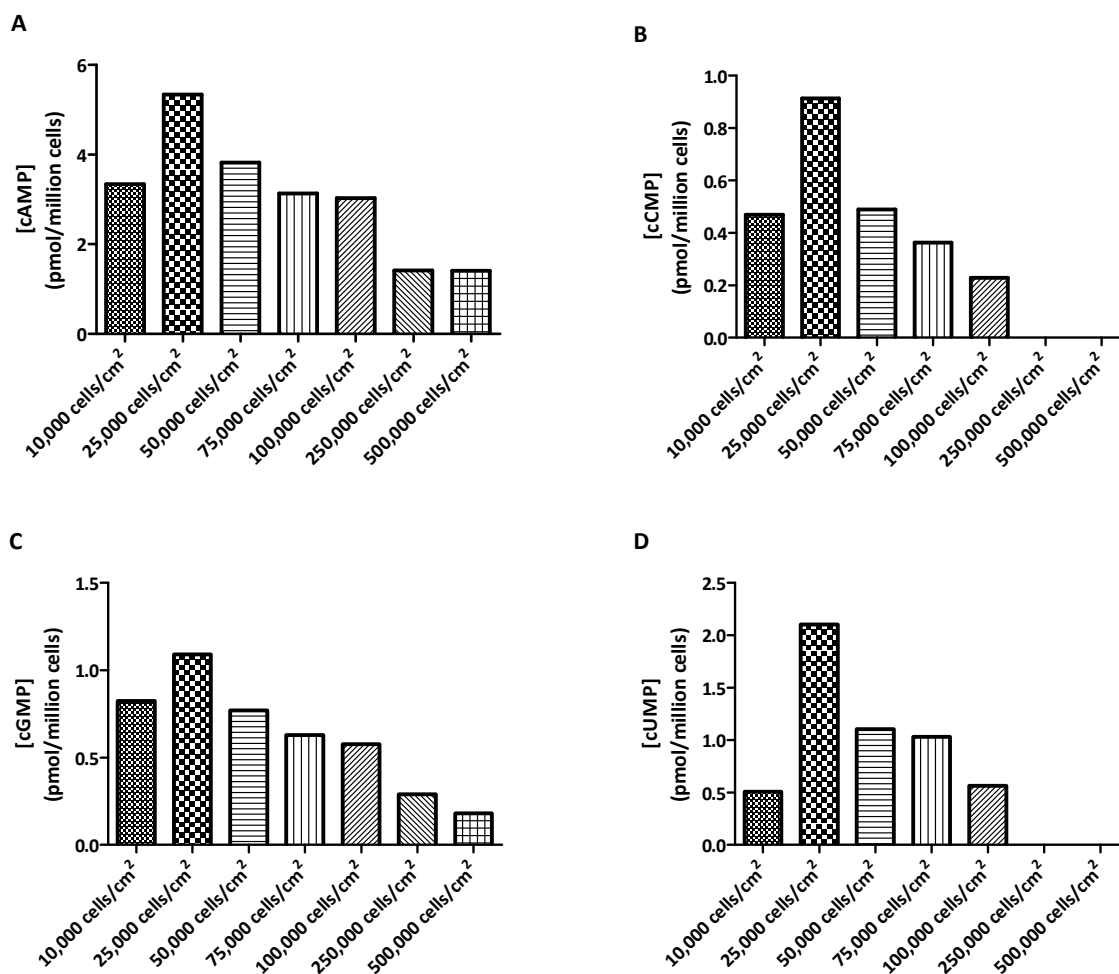


**Fig. 4.12.** Cyclic nucleotide concentrations in pmol/million cells according to cell density.

#### 4.4.3. cCMP Formation by Mammalian ACs

The identification of endogenous cCMP and cUMP in phagocytes raises the question which mammalian enzymes generate those cNMPs. Previous studies showed broad base-specificity in mACs and sGC regarding inhibitor affinity<sup>32</sup>, and demonstrated that sGC possesses UC activity assessed by a radiometric assay.<sup>33</sup> Therefore, the substrate-specificity of three representative mAC isoforms AC 1, AC 2 and AC 5 in Sf9 insect cell membranes and hsAC was assessed using the HPLC-MS/MS method developed for cell extracts.

mACs and C1:C2 were fully activated by 5'-[γ-thio]triphosphate and the diterpene forskolin and hsAC was activated by  $\text{Ca}^{2+}$ . Overexpression of ACs 1, 2 and 5 substantially increased the formation of cAMP and cCMP above Sf9-background, with no effect on cGMP formation (see Table 4.2.). Thus, various mammalian ACs synthesize cCMP at very low rates, approximately 0.1 % of cAMP formation rates.



**Table 4.2.** cNMP formation of mammalian ACs at reaction times of one hour.

|                   | cNMP formation [pmol/mg protein/h] |           |              |               |
|-------------------|------------------------------------|-----------|--------------|---------------|
|                   | cAMP                               | cGMP      | cCMP         | cUMP          |
| Sf9 mock-infected | 9,600 ± 3,500                      | 20 ± 8.8  | 0.88 ± 0.3 * | n.d.          |
| AC 1              | 35,200 ± 9,700                     | 17.5 ± 5  | 3.25 ± 1     | 0.38 ± 0.38 * |
| AC 2              | 31,250 ± 9,000                     | 16.5 ± 5  | 4.13 ± 0.75  | n.d.          |
| AC 5              | 64,000 ± 15,700                    | 14.75 ± 5 | 6.13 ± 2.5   | n.d.          |
| human sAC         | 542,000 ± 93,000                   | 200 ± 50  | 200 ± 30     | 1,250 ± 550   |

\* only detected in one of six experiments. n.d.: not detected

If cCMP concentrations in intact cells arose from mACs, an increase in cCMP concentration should be achieved by stimulation with FSK<sup>2</sup> or the  $\beta$ -adrenoceptor agonist isoproterenol<sup>44</sup>. However, no change in cNMP concentrations could be detected.

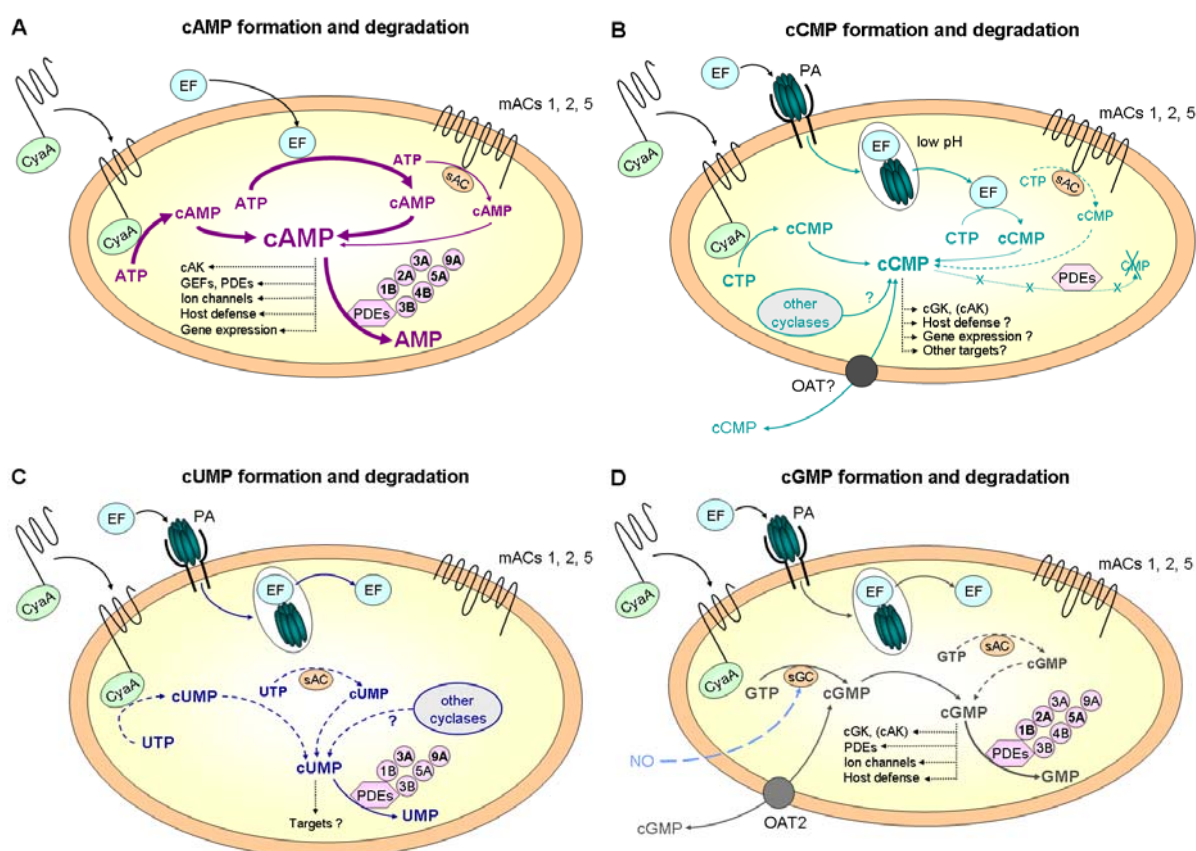
The very low cCMP synthesis rates of known mammalian ACs *in vitro* are in contrast to the relatively high cCMP concentrations in macrophages. Moreover, the PDE inhibitor IBMX did not enhance cCMP increases in intact cells upon treatment with CyaA-wt. Astonishingly, Bt<sub>2</sub>cCMP effectively activates cGMP-dependent protein kinase-regulated cell functions in vascular smooth muscle and platelets despite low affinity of this kinase for cCMP, indicative for substantial cCMP accumulation.<sup>43</sup>

Furthermore, a number of representative purified and defined PDE isoforms (1B, 2A, 3A, 3B, 4B, 5A, and 9A) were examined for cCMP hydrolyzing activity. Strikingly, none of the PDEs studied hydrolyzed cCMP, even after an exceedingly long incubation time of 24 h.<sup>27</sup> Thus, the prominent functional effects of Bt<sub>2</sub>cCMP on vascular smooth muscle relaxation and platelet aggregation<sup>43</sup> as well as the prolonged cCMP accumulation in phagocytes without IBMX are readily explained by hydrolysis-resistance of cCMP.

## 4.5. Discussion

In this work we present novel, highly sensitive and specific HPLC-MS/MS methods that strikingly identified cCMP as endogenous nucleotide in intact cells and its accumulation by the action of the “AC” toxins EF and CyaA *in vivo*. Specific retention times in HPLC-chromatography, fragmentation patterns and SRM analysis further confirm the actual identity of cCMP. The catalytic activity of AC toxins as well as of mammalian ACs are not restricted to ATP turnover. EF and CyaA produce all cNMPs examined in this study with the

exception of cTMP in case of EF *in vitro*. hsAC shows cAMP, cCMP and cUMP formation, whereas mACs seem to be restricted to AC and very low CC activity.



**Scheme 4.1.** depicts ways of cNMP accumulation in cells, points of interaction and known or proposed physiological effects for **A** cAMP, **B** cCMP, **C** cUMP and **D** cGMP.

To better understand cCMP formation by the toxins EF and CyaA molecular dynamics studies based on crystal structures of both toxins<sup>45,46</sup> were performed in a collaboration with Prof. Dr. Stefan Dove (Department of Medicinal and Pharmaceutical Chemistry II, University of Regensburg) (see Fig. 4.13.). The docking studies were performed with the molecular modeling suite SYBYL 7.3 on a Silicon Graphics Octane workstation. ATP and CTP were manually docked to both enzymes. Models were refined with the AMBER\_F99 force field.<sup>47</sup>

The catalytic sites of both toxins are spacious cavities located at the interface of two structural domains, C<sub>A</sub> and C<sub>B</sub>. An alignment of the catalytic sites of both enzymes, performed by superposition of the backbone atoms of 15 amino acids surrounding the ligands (rms distance 1.22 Å), illustrates the close correspondence. 14 of the 15 amino acids are identical, only Thr 548 in EF is replaced by Val 271 in CyaA.

The position of two Mg<sup>2+</sup> ions, one coordinated by two aspartates and one histidine, the other by the α-, β- and γ-phosphates of NTPs, indicates two-metal-ion catalysis starting with nucleophilic attack of the deprotonated 3'-oxygen on the α-phosphorus. The 3'-endo

conformation of the ribosyl moiety facilitates the attack by direct coordination of the 3'-oxygen by the metal and by activation of one water molecule by a histidine residue leading to deprotonization of 3'-OH. The binding modes of ATP and CTP are very similar with respect to the phosphate chain and ribosyl moiety. The amino groups of adenine and cytosine form the same two hydrogen bonds with the backbone oxygens of two threonine residues, and the ring planes are aligned with the side chain of an asparagine. However, the van der Waals surface of ATP is by  $\sim 22 \text{ \AA}^2$  larger than the CTP surface. In the presence of  $\text{Mn}^{2+}$  MANT-CTP is an approximately 6-fold more potent EF inhibitor than its ATP analogue.<sup>26</sup> A reason for the higher affinity may be a water molecule in an ideal position where it forms three hydrogen bonds, bridging the cytosine oxygen with the side chains of arginine and glutamate.

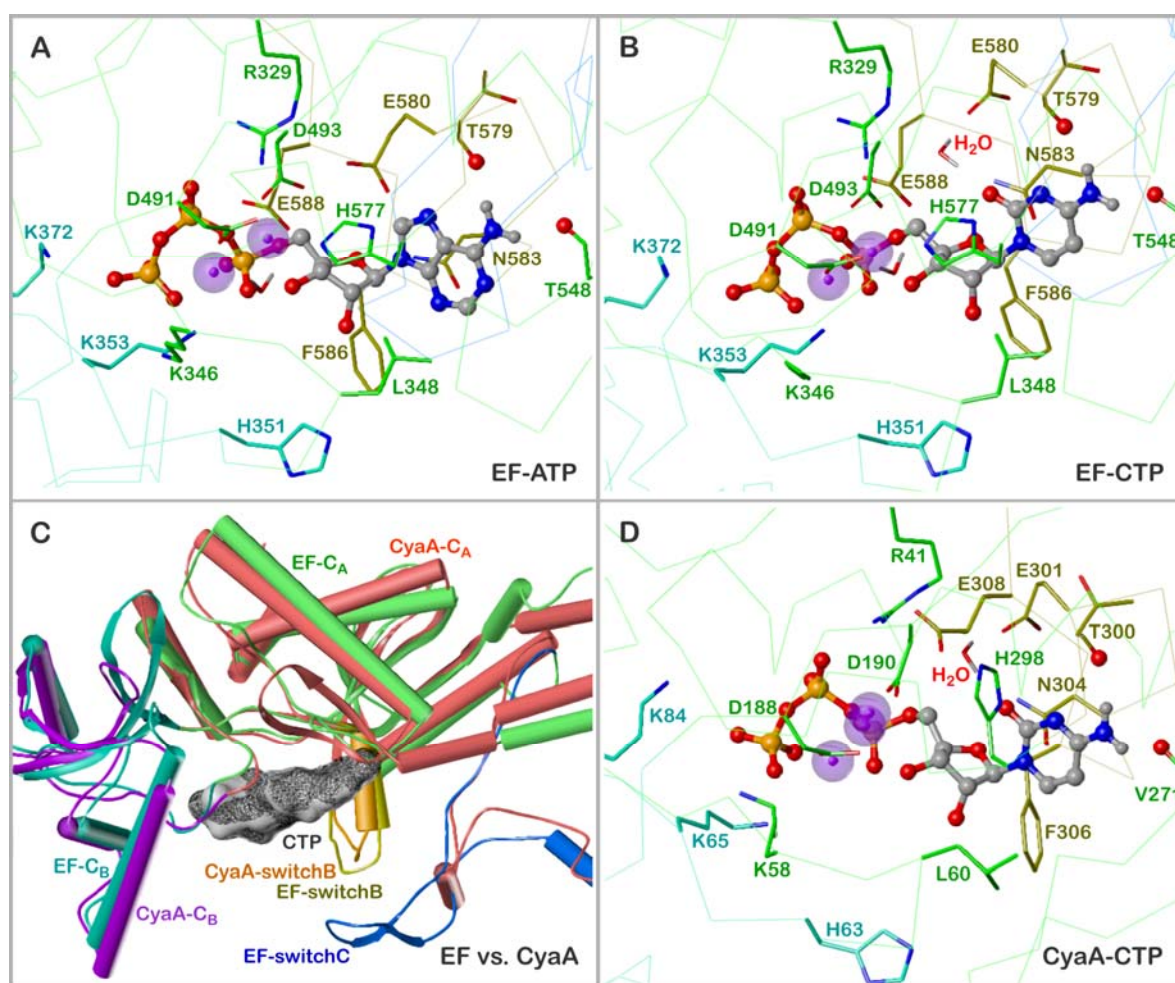


**Fig. 4.13.** Model of the interaction of EF and CyaA with ATP and CTP constructed by Prof. Dr. Stefan Dove. Colors of atoms, unless otherwise indicated: P – orange, O – red, N – blue, C, H – grey,  $\text{Mg}^{2+}$  – purple spheres. **A** Interaction of EF with ATP. **B** Interaction of EF with CTP. **C** Alignment of the nucleotide binding sites of EF and CyaA in complex with CTP (represented as MOLCAD surfaces, bound to EF – black lines, bound to CyaA – grey opaque). Enzyme models: cylinders – helices, ribbons –  $\beta$ -sheets, tubes – loops, EF: domain  $C_A$  – green, domain  $C_B$  – greenblue, switch B – yellow, switch C – blue; CyaA: domain  $C_A$  – apricot, domain  $C_B$  – purple, switch B – orange. **D** Interaction of CTP with CyaA. In panels **A**, **B** and **D**, the side chains of the amino acids of the binding sites are drawn as sticks and labeled. The backbone oxygen atoms suggested to form hydrogen bonds with the amino groups of ATP and CTP are marked as balls.

Microarray studies and RT-PCR have not revealed any target genes, yet. A reason for that may be synergistic effects of cAMP and cCMP or the compartmentalization of cCMP in cells that cannot be mimicked by the addition of cell-permeable cCMP analogues. Nevertheless, initial experiments with J774 cells cultured at different densities in cell culture dishes may hint at a role of cCMP and cUMP in cell growth.

This study does not exclude the possibility that other known ACs or GCs may display distinct CC activities nor the existence of an unknown specific CC. Similar considerations apply for PDEs. As known so far, cCMP is resistant to hydrolysis by PDEs raising the question for termination of biological actions by cCMP. This may happen *via* transport processes of cCMP into extracellular space by cyclic nucleotide efflux pumps or organic anion transporters.<sup>48,49,50</sup> As a result of such mechanism, cCMP should also be detectable in the extracellular space. In fact, another cyclic nucleotide, cGMP, was first detected in urine.<sup>49,51</sup>

A serendipitous side aspect of this cCMP research project was the identification of cUMP as endogenous nucleotide in cells and UC activity in EF, CyaA and hsAC. The kinetics of CC- and UC- activity of AC toxins are different regarding distinct cCMP and cUMP accumulation in intact cells, indicating diversely compartmentalized CTP- and UTP pools differentially accessible for EF and CyaA. Furthermore, different cell types show a distinct cNMP accumulation profile possibly due to variable compartmentalization of NTPs. This is evidenced by the discriminative effects of CyaA-wt on J774 and HL-60 cells.

This work opens new fields of research in an area plagued by artifacts, unconfirmed data and scepticism. Main objectives for the future remain to identify target genes and proteins and possible undiscovered enzymes with specific CC and cCMP-PDE activities. Further alternatives are synergistic effects of cCMP together with cAMP or cGMP enhancing or reducing their biological mode of actions. Scheme 4.1. summarizes our current knowledge on synthesis, degradation and mechanism of action of cNMPs. Furthermore, proposed mechanisms like the efflux of cCMP by transporters are indicated. Nevertheless, cCMP and cUMP generation, termination and signalling remain by and large a black box which may turn out as treasure chest for understanding of cellular events in future.

## 4.6. References

- <sup>1</sup> Sunahara RK, Taussig R (2002) Isoforms of mammalian adenylyl cyclase: multiplicities of signaling, *Mol Interv* **2**, 168-184
- <sup>2</sup> Sadana R, Dessauer CW (2008) Physiological roles for G protein-regulated adenylyl cyclase isoforms: insights from knockout and overexpression studies, *Neurosignals* **17**, 5-22

- <sup>3</sup> Defer N, Best-Belpomme M, Hanoune J (2000) Tissue specificity and physiological relevance of various isoforms of adenylyl cyclase, *Am J Physiol Renal Physiol* **279**, F400-F416
- <sup>4</sup> Sunahara RK, Dessauer CW, Gilman AG (1996) Complexity and diversity of mammalian adenylyl cyclases, *Annu Rev Pharmacol Toxicol* **36**, 461-480
- <sup>5</sup> Krauss G (2003) Biochemistry of signal transduction and regulation, 3<sup>rd</sup> Completely Revised Edition, Wiley-VCH Weinheim, 231-236
- <sup>6</sup> Kots AY, Martin E, Sharina IG, Murad F (2009) A short history of cGMP, guanylyl cyclases, and cGMP-dependent protein kinases, *HHHW Schmidt, F Hofman, J-P Stasch: cGMP: Generators, Effectors and Therapeutic Implications Handbook of Experimental Pharmacology* **191**, Springer-Verlag Berlin-Heidelberg, 1-14
- <sup>7</sup> Dessauer CW (2009) Adenylyl cyclase-A-kinase anchoring protein complexes: the next dimension in cAMP signaling, *Mol Pharmacol* **76**, 935-941
- <sup>8</sup> Antoni FA (2000) Molecular diversity of cyclic AMP signalling, *Front Neuroendocrin* **21**, 103-132
- <sup>9</sup> Conti M, Beavo J (2007) Biochemistry and physiology of cyclic nucleotide phosphodiesterases: essential components in cyclic nucleotide signaling, *Annu Rev Biochem* **76**, 481-511
- <sup>10</sup> Newton RP, Hakeem NA, Salvage BJ, Wassenaar G, Kingston EE (1988) Cytidylate cyclase activity: identification of cytidine 3',5'-cyclic monophosphate and four novel cytidine cyclic phosphates as biosynthetic products from cytidine triphosphate, *Rapid Commun Mass Spectrom* **2**, 118-126
- <sup>11</sup> Cech SY, Ignarro LJ (1977) Cytidine 3',5'-monophosphate (cyclic CMP) formation in mammalian tissue, *Science* **198**, 1063-1065
- <sup>12</sup> Cheng Y-C, Bloch A (1978) Demonstration, in leukemia L-1210 cells, of a phosphodiesterase acting on 3':5'-cyclic CMP but not on 3':5'-cyclic AMP or 3':5'-cyclic GMP, *J Biol Chem* **253**, 2522-2524
- <sup>13</sup> Helfman DM, Katoh N, Kuo JF (1984) Purification and properties of cyclic CMP phosphodiesterase, *Adv Cyclic Nucleotide Protein Phosphorylation Res* **16**, 403-416
- <sup>14</sup> Cailla HL, Roux D, Delaage M, Goridis C (1978) Radioimmunological identification and measurement of cytidine 3',5'-monophosphate in rat tissue, *Biochem Biophys Res Commun* **85**, 1503-1509
- <sup>15</sup> Newton RP (1993) Contributions of fast-atom bombardment mass spectrometry to studies of cyclic nucleotide biochemistry, *Rapid Commun Mass Spectrom* **7**, 528-537
- <sup>16</sup> Newton RP, Groot N, van Geyschem J, Diffley PE, Walton TJ, Bayliss MA, Harris FM, Games DE, Brenton AG (1997) Estimation of cytidylyl cyclase activity and monitoring of side-

- product formation by fast-atom bombardment mass spectrometry, *Rapid Commun Mass Spectrom* **11** 189-194
- <sup>17</sup> Bond AE, Dudley E, Tuytten R, Lemi  re F, Smith CJ, Esmans EL, Newton RP (2007) Mass spectrometric identification of Rab23 phosphorylation as a response to challenge by cytidine 3',5'-cyclic monophosphate in mouse brain, *Rapid Commun Mass Spectrom* **21**, 2685-2692
- <sup>18</sup> Ding S, Bond AE, Lemi  re F, Tuytten R, Esmans EL, Brenton AG, Dudley E, Newton RP (2008) Online immobilized metal affinity chromatography/mass spectrometric analysis of changes elicited by cCMP in the murine brain phosphoproteome, *Rapid Commun Mass Spectrom* **22**, 4129-4138
- <sup>19</sup> Ervens J, Seifert R (1991) Differential modulation by *N*<sup>4</sup>,2'-*O*-dibutyryl cytidine 3':5'-cyclic monophosphate of neutrophil activation, *Biochem Biophys Res Commun* **174**, 258-267
- <sup>20</sup> Gaion RM, Krishna G (1979) Cytidylate cyclase: possible artifacts in the methodology, *Science* **203**, 672-673
- <sup>21</sup> Gaion RM, Krishna G (1979) Cytidylate Cyclase: the product isolated by the method of Cech and Ignarro is not cytidine 3',5'-monophosphate, *Biochem Biophys Res Commun* **86**, 105-111
- <sup>22</sup> Mock M, Fouet A (2001) Anthrax, *Annu Rev Microbiol* **55**, 647-671
- <sup>23</sup> Ladant D, Ullmann A (1999) *Bordetella pertussis* adenylate cyclase: a toxin with multiple talents, *Trends Microbiol* **7**, 172-176
- <sup>24</sup> Galley J, Vincent M, de la Sierra IML, Munier-Lehmann H, Renouard M, Sakamoto H, B  rzu O, Gilles AM (2004) Insight into the activation mechanism of *Bordetella pertussis* adenylate cyclase by calmodulin using fluorescence spectroscopy, *Eur. J Biochem* **271**, 821-833
- <sup>25</sup> G  ttle M, Dove S, Steindel P, Shen Y, Tang W-J, Geduhn J, K  nig B, Seifert R (2007) Molecular analysis of the interaction of *Bordetella pertussis* adenylyl cyclase with fluorescent nucleotides, *Mol Pharmacol* **72**, 526-535
- <sup>26</sup> Taha HM, Schmidt J, G  ttle M, Suryanarayana S, Shen Y, Tang W-J, Gille A, Geduhn J, K  nig B, Dove S, Seifert R (2009) Molecular analysis of the interaction of anthrax adenylyl cyclase toxin, edema factor, with 2'(3')-*O*-(*N*-(methyl)anthraniloyl)-substituted purine and pyrimidine nucleotides, *Mol Pharmacol* **75**, 693-703
- <sup>27</sup> Spangler CM, G  ttle M, Reinecke D, Ladant D, Tang W-J, Kees F, Schlossmann J, Sandner P, Dove S, Kaefer V, Seifert R, Cytidylyl cyclase activity of bacterial and mammalian “adenylyl” cyclases, *submitted*
- <sup>28</sup> Voth DE, Hamm EE, Nguyen LG, Tucker AE, Salles II, Ortiz-Leduc W, Ballard JD (2005) *Bacillus anthracis* oedema toxin as a cause of tissue necrosis and cell type-specific cytotoxicity, *Cell Microbiol* **7**, 1139-1149

- <sup>29</sup> Shen Y, Lee Y-S, Soelaiman S, Bergson P, Lu D, Chen A, Beckingham K, Grabarek Z, Mrksich M, Tang W-J (2002) Physiological calcium concentrations regulate calmodulin binding and catalysis of adenylyl cyclase exotoxins, *EMBO J* **21**, 6721-6732
- <sup>30</sup> Gopalakrishna R, Anderson WB (1982) Calcium(2+)-induced hydrophobic site on calmodulin: application for purification of calmodulin by phenyl-sepharose affinity chromatography, *Biochem Biophys Res Commun* **29**, 830-836
- <sup>31</sup> Gille A, Seifert R (2003) 2'(3')-O-(N-Methylantraniloyl)-substituted GTP Analogs: A novel class of potent competitive adenylyl cyclase inhibitors, *J Biol Chem* **278**, 12672-12679
- <sup>32</sup> Gille A, Lushington GH, Mou TC, Doughty MB, Johnson RA, Seifert R (2004) Differential inhibition of adenylyl cyclase isoforms and soluble guanylyl cyclase by purine and pyrimidine nucleotides, *J Biol Chem* **279**, 19955-19969
- <sup>33</sup> Suryanarayana S, Göttle M, Hübner M, Gille A, Mou TC, Sprang SR, Richter M, Seifert R (2009) Differential inhibition of various adenylyl cyclase isoforms and soluble guanylyl cyclase by 2',3'-O-(2,4,6-trinitrophenyl)-substituted nucleoside 5'-triphosphates, *J Pharmacol Exp Ther* **330**, 687-695
- <sup>34</sup> Karimova G, Fayolle C, Gmira S, Ullmann A, Leclerc C, Ladant D (1998) Charge-dependent translocation of *Bordetella pertussis* adenylate cyclase toxin into eukaryotic cells: implication for the *in vivo* delivery of CD8+ T-cell epitopes into antigen-presenting cells, *Proc Natl Acad Sci USA* **95**, 12532-12537
- <sup>35</sup> Preville X, Ladant D, Timmerman B, Leclerc C (2005) Eradication of established tumors by vaccination with recombinant *Bordetella pertussis* adenylate cyclase carrying the human papillomavirus 16 E7 oncoprotein, *Cancer Research* **65**, 641-649
- <sup>36</sup> Ladant D, Glaser P, Ullmann A (1992) Insertional mutagenesis of *Bordetella pertussis* adenylate cyclase. *J Biol Chem* **267**, 2244-2250
- <sup>37</sup> Durchdewald M, Angel P, Hess J (2009) The transcription factor Fos: a Janus-type regulator in health and disease, *Histol Histopathol* **24**, 1451-1461
- <sup>38</sup> Mitchell JA, Warder TD (2006) COX isoforms in the cardiovascular system: understanding the activities of non-steroidal anti-inflammatory drugs, *Nat Rev Drug Discov* **5**, 75-86
- <sup>39</sup> Pols TW, Bonta PI, de Vries CJ (2007) Nr4a nuclear orphan receptors: protective in vascular disease?, *Curr Opin Lipidol* **18**, 515-520
- <sup>40</sup> Heufler C, Ortner D, Hofer S (2008) Cybr, CYTIP or CASP: an attempt to pinpoint a molecule's functions and names, *Immunobiology* **213**, 729-732
- <sup>41</sup> Cuevas I, Boudreau N (2009) Managing tumor angiogenesis: lessons from VEGF-resistant tumors and wounds, *Adv Cancer Res* **103**, 25-42
- <sup>42</sup> Breloer M, Fleischer B (2008) CD83 regulates lymphocyte maturation, activation and homeostasis, *Trends Immunol* **29**, 186-194

- <sup>43</sup> Desch M, Schinner E, Hofmann F, Seifert R, Schlossmann J, Cyclic cytidine 3',5'-monophosphate (cCMP) signals *via* cGKI, *submitted*
- <sup>44</sup> Oner SS, Kaya AI, Onar HO, Ozcan G, Ugur O (2010) Beta2-adrenoceptor, Gs and adenylyl cyclase coupling in purified detergent-resistant, low density membrane fractions, *Eur J Pharmacol* **630**, 42-52
- <sup>45</sup> Shen Y, Zhukovskaya NL, Guo Q, Florián J, Tang W-J (2005) Calcium-independent calmodulin binding and two-metal ion catalytic mechanism of anthrax edema factor, *EMBO J* **24**, 929-941
- <sup>46</sup> Guo Y, Shen Y, Lee YS, Gibbs CS, Mrksich M, Tang W-J (2005) Structural basis for the interaction of *Bordetella pertussis* adenylyl cyclase toxin with calmodulin, *EMBO J* **21**, 3190-3201
- <sup>47</sup> Cornell WD, Cieplak P, Bayly CI, Gould IR, Merz KM, Ferguson DM, Spellmeyer DC, Fox T, Caldwell JW, Kollman PA (1995) A second generation force field for the simulation of proteins, nucleic acids, and organic molecules, *J Am Chem Soc* **117**, 5179-5197
- <sup>48</sup> Guo Y, Kotova E, Chen Z-S, Lee K, Hopper-Borge E, Belinsky MG, Kruh GD (2003) MRP8, ATP-binding cassette C11 (ABCC11), is a cyclic nucleotide efflux pump and a resistance factor for fluoropyrimidines 2',3'-dideoxycytidine and 9'-(2'-phosphonylmethoxyethyl) adenine, *J Biol Chem* **278**, 29509-29514
- <sup>49</sup> Cropp CD, Komori T, Shima JE, Urban TJ, Yee SW, More SS, Giacomini KM (2008) Organic anion transporter 2 (SLC22A7) is a facilitative transporter of cGMP, *Mol Pharmacol* **73**, 1151-1158
- <sup>50</sup> Anzai N, Kanai Y, Endou H (2006) Organic anion transporter family: current knowledge, *J Pharmacol Sci* **100**, 411-426
- <sup>51</sup> Schmidt PM (2009) Biochemical detection of cGMP from past to present: an overview, *HHHW Schmidt, F Hofman, J-P Stasch: cGMP: Generators, Effectors and Therapeutic Implications Handbook of Experimental Pharmacology* **191**, Springer-Verlag Berlin-Heidelberg, 195-228



## 5. Summary

### 5.1. Summary in English

The adenylyl cyclase (AC) toxins EF and CyaA contribute to the pathogenity and mortality of anthrax and whooping cough caused by *Bacillus anthracis* and *Bordetella pertussis*, respectively. In both diseases a “point-of-no-return”, despite antibiotic treatment, is described, attributable to the action of bacterial toxins. Additionally, a number of antibiotic-resistant strains is known. Therefore, inhibitors of bacterial toxins would mitigate the course of disease and increase survival rates.

A luminescence-based AC assay was developed as screening tool for AC toxin inhibitors. The assay proved to be fast and inexpensive and no work-up steps like chromatography are needed. It is performed in 96-well plates, and therefore is suitable for high-throughput screening. The luminescent complex TbNflx responds to changes in analyte concentrations immediately, and hence allows monitoring of real-time enzyme kinetics.

The full characterization of CyaA and EF *in vitro* and *in vivo* improves our knowledge of intracellular mechanisms upon infection and leads to a better understanding of disease courses. Thus, substrate-specificity of both toxins was explored *in vitro* and CyaA and EF show turnover of ATP, CTP, UTP, GTP, ITP and XTP. Cytidylyl cyclase activity was determined to be approximately 300 times lower than AC activity. To answer the question whether AC toxins increase cNMP levels other than cAMP *in vivo*, the effects of AC toxins on two different cell systems were tested.

Here, endogenous cCMP and cUMP was identified in HL-60 and J774 cells by a highly specific and sensitive HPLC-MS/MS method. Additionally, we demonstrated the accumulation of cCMP after toxin treatment. However, cCMP research was plagued by methodological problems in the past. Therefore, doubts about the identity of cCMP were addressed by chromatographic separation with specific retention times and the identification of nucleotides by specific mass transitions from protonated cNMP to the protonated base.

To identify a potential source of endogenous cCMP and cUMP in cells, mammalian ACs were analyzed for cytidylyl and uridylyl activity. Membrane-bound ACs indeed produce cCMP in very small amounts, whereas soluble AC produces cCMP as well as cUMP. The existence and formation of cCMP and cUMP in living systems led us to possible biological actions of these cNMPs. In microarray and RT-PCR experiments no significant change in mRNA expression upon addition of cCMP and the cell permeable derivative Bt<sub>2</sub>cCMP could

be detected. However, the increase in mRNA expression levels by CyaA could not be explained by the action of cAMP alone.

Therefore, a number of questions remain to be solved: Does cCMP only display synergistic effects, enhancing or reducing the actions of the already known second messengers cAMP or cGMP? Is cCMP compartmentalized in cells and has only impact on mRNA expression in these compartments? Are there target proteins for cCMP? Is there a specific CC or does endogenous cCMP amount from already known mACs? Is there another mAC not explored in this work that synthesizes cCMP with high catalytic activity? And last but not least, how is the action of cCMP terminated? In conclusion, this work opens a new field of research in an area troubled with artifacts and unconfirmed data.

## 5.2. Summary in German

Die Adenylyl Zyklase (AC) Toxine EF und CyaA tragen zur Pathogenität und Mortalität von Anthrax und Keuchusten bei. Diese Krankheiten werden von *Bacillus anthracis* und *Bordetella pertussis* verursacht. Bei beiden Krankheiten wurde trotz antibiotischer Behandlung ein "Point-of-no-return" beschrieben. Dieser wird durch das Wirken von bakteriellen Toxinen verursacht. Zusätzlich sind bereits einige Stämme beider Erreger bekannt, die Antibiotikaresistenzen aufweisen. Inhibitoren, die auf bakterielle Toxine wirken, würden deshalb den Verlauf der Krankheit mildern und die Überlebenschancen erhöhen können.

Ein lumineszenzbasierter AC Assay wurde für das Screening von Inhibitoren für AC-Toxine entwickelt. Der Assay hat sich als schnell und günstig erwiesen und kann in 96-well Platten durchgeführt werden. Aufarbeitungsschritte wie chromatographische Trennungen sind überflüssig. Dieser Assay eignet sich daher zur Anwendung im Hochdurchsatz-Screening. Außerdem spricht der lumineszente TbNflx Komplex sofort auf Änderungen der Analytkonzentrationen an und erlaubt damit die Durchführung von Echtzeitkinetiken dieser Toxine.

Die komplette Charakterisierung von CyaA und EF *in vitro* und *in vivo* erweitert unsere Kenntnisse über intrazelluläre Mechanismen bei einer Infektion und führt zu einem besseren Verständnis des Krankheitsverlaufs. Deswegen wurde die Substratspezifität beider Toxine *in vitro* untersucht. Dabei zeigen sowohl CyaA als auch EF Umsatz von ATP, CTP, UTP, GTP, ITP und XTP. Die Cytidylyl Zyklase Aktivität beider Toxine liegt ca. um den Faktor 300 niedriger als die AC-Aktivität. Daraus ergab sich die Frage, ob diese Toxine abgesehen von der cAMP-Konzentration auch die Konzentration anderer cNMPs *in vivo* erhöhen können.

Die Auswirkung der AC Toxine auf zwei unterschiedliche Zellsysteme wurde daher untersucht.

Dabei wurden sowohl cCMP als auch cUMP als endogene Nukleotide in HL-60- und J774-Zellen mit Hilfe einer hochspezifischen und –sensitiven HPLC-MS/MS-Methode identifiziert. Zusätzlich konnten wir die Anreicherung von cCMP nach Toxinbehandlung nachweisen. Die cCMP-orschung war jedoch in der Vergangenheit mit massiven methodischen Problemen belastet. Um Zweifel an der Identität von cCMP auszuräumen, wurde die chromatographische Analyse mit spezifischen Retentionszeiten und die Identifizierung von Nukleotiden mit Hilfe von Massenübergängen vom protonierten Nukleotid zur protonierten Base herangezogen.

Zur Bestimmung einer möglichen Quelle von endogenem cCMP und cUMP in Zellen wurde die Cytidylyl und Uridylyl Zyklase Aktivität von Mammalia-ACs bestimmt. Membrangebundene ACs produzieren sehr kleine Mengen an cCMP, während lösliche AC sowohl cCMP als auch cUMP erzeugt. Die Existenz und Produktion von cCMP und cUMP in lebenden Systemen führte uns zur Frage möglicher biologischer Effekte dieser cNMPs. In Microarray- und RT-PCR Untersuchungen konnte keine signifikante Änderung der mRNA Expression durch Behandlung der Zellen mit cCMP und dem zellpermeablen Derivat Bt<sub>2</sub>cCMP festgestellt werden. Dennoch kann der Anstieg der mRNA-Expression, der durch CyaA verursacht wird, nicht allein durch die Wirkung von cAMP erklärt werden.

Durch die Ergebnisse dieser Arbeit ergeben sich zahlreiche Fragen: Verursacht cCMP nur synergistische Effekte und verstärkt oder reduziert es dabei die Wirkung von bekannten sekundären Botenstoffen wie cAMP und cGMP? Ist cCMP auf verschiedene Zellkompartimente verteilt und hat nur dort Effekte auf die mRNA-Expression? Gibt es Zielproteine für cCMP? Gibt es eine spezifische CC oder entsteht das endogene cCMP durch die bekannten mACs und sAC? Gibt es eine mAC, die hier nicht untersucht wurde, die cCMP mit hoher katalytischer Aktivität bildet? Und nicht zuletzt, wie wird cCMP in der Zelle inaktiviert? Abschließend kann man festhalten, dass diese Arbeit ein neues Forschungsgebiet eröffnet in einem Bereich, der von Artefakten und unbestätigten Daten beherrscht war.

## 6. Curriculum Vitae

### Personal Information

---

Name: Corinna Maria Spangler  
Date of Birth: 09<sup>th</sup> February, 1982  
Place of Birth: Deggendorf

### Education

---

02/2009 – present Continuation **PhD thesis** at the Institute of Pharmacology, Hannover Medical School  
Supervisors: Prof. Dr. Roland Seifert, Prof. Dr. Otto S. Wolfbeis  
10/2006 – 01/2009 **PhD thesis** at the Institute of Analytical Chemistry, Chemo- and Biosensors and the Institute of Pharmacology and Toxicology, University of Regensburg  
10/2001 – 09/2006 **Diploma in Chemistry**, University of Regensburg  
Diploma Thesis at the Institute of Analytical Chemistry, Chemo- and Biosensors (Supervisor: Prof. Dr. Otto S. Wolfbeis): “Synthesis of New Reagents for the Fluorescence Derivatisation of Thiols”  
09/2003 – 03/2004 **Erasmus Student**, University of Aberdeen, Scotland, UK  
Student Exchange  
06/2001 **Graduation from High School**, Gymnasium Vilshofen

### Professional Qualification

---

Advanced Courses in Pharmacology:

“Methoden zur Analyse G-Protein-gekoppelter Rezeptoren”, Mainz 2010  
“Moderne Massenspektrometrie in Pharmakologie und Toxikologie”, Mainz 2010  
“Tiermodelle in der Pharmakologischen Forschung”, Mainz 2009  
“Arzneimittelinteraktionen, -metabolismus und -transport”, Mainz 2009

Advanced Training “Umgang mit offenen radioaktiven Stoffen”, Regensburg 2007

Advanced Training “Gentechnische Sicherheit für Projektleiter und Beauftragte für Biologische Sicherheit nach § 15 GenTSV”, Hannover 2009

Proof of Competence “Amtlicher Sachkundenachweis im Umgang mit Gefahrstoffen gemäß § 5 ChemVerbotsV”

## 7. Abstracts and Publications

Parts of this thesis or related studies were published or presented as posters or short lectures.

### Original Publications

**Corinna M. Spangler**, Martin Göttle, Daniel Reinecke, Daniel Ladant, Wei-Jen Tang, Frieder Kees, Jens Schlossmann, Peter Sandner, Tung-Chung Mou, Stefan Dove, Volkhard Kaever, Roland Seifert, Cytidylyl and uridylyl cyclase activity of bacterial and mammalian adenylyl cyclases, *submitted*

Christian Spangler, **Corinna M. Spangler**, Michael Spoerner, Michael Schäferling (2009) Kinetic determination of the GTPase activity of Ras proteins by means of a luminescent terbium complex, *Anal Bioanal Chem* **394**, 989-996

**Corinna M. Spangler**, Christian Spangler, Martin Göttle, Yuequan Shen, Wei-Jen Tang, Roland Seifert, Michael Schäferling (2008) A fluorimetric assay for real-time monitoring of adenylyl cyclase activity based on terbium norfloxacin, *Anal Biochem* **381**, 86-93

### Review Articles

**Corinna M. Spangler**, Michael Schäferling, Luminescent Chemical and Physical Sensors Based on Lanthanide Complexes, *P. Hänninen, H. Härmä: Springer Series on Fluorescence Vol 7: The Luminescence of Lanthanides: Spectroscopy, Materials, Bioanalytical Implications*, Springer-Verlag, Berlin Heidelberg, *invited review*

**Corinna M. Spangler**, Christian Spangler, Michael Schäferling (2008) Luminescent lanthanide complexes as probes for the determination of enzyme activity, *Ann NY Acad Sci* **1130**, 138-148

## Short lectures

**Corinna M. Spangler**, Daniel Ladant, Wei-Jen Tang, Volkhard Kaefer, Roland Seifert (2010) Nucleotidyl cyclase activity of bacterial exotoxins CyaA and EF and its impact on cellular cyclic nucleotide levels, *51. Jahrestagung der Deutschen Gesellschaft für Experimentelle und Klinische Pharmakologie und Toxikologie (DGPT)*, Mainz

**Corinna M. Spangler**, Christian Spangler, Michael Schäferling, Roland Seifert (2008) Fluorimetric assay for adenylyl cyclase activity, *49. Jahrestagung der Deutschen Gesellschaft für Experimentelle und Klinische Pharmakologie und Toxikologie (DGPT)*, Mainz

## Poster presentations

**Corinna M. Spangler**, Bettina Wilhelm, Heike Burhenne, Kerstin Rauch, Roland Seifert, Volkhard Kaefer (2009) Sensitive assay for the detection of cyclic nucleotides by mass spectrometry, *4<sup>th</sup> International Conference on cGMP Generators, Effectors and Therapeutic Implications*, Regensburg

**Corinna M. Spangler**, Christian Spangler, Roland Seifert, Michael Schäferling (2008) A fluorimetric assay for adenylyl cyclase activity facilitating real-time enzyme kinetics and high throughput screening, *Symposium on "Signaltransduktion: Innovative Quelle für die Pharmakologie"*, Hannover

Christian Spangler, **Corinna M. Spangler**, Michael Spoerner, Michael Schäferling (2008) Probing the GTPase activity of Ras proteins by means of luminescent lanthanide complex terbium-norfloxacin, *8<sup>th</sup> International Symposium on Luminescence Spectroscopy*, Bologna, Italy

**Corinna M. Spangler**, Christian Spangler, Roland Seifert, Michael Schäferling (2007) Luminescent probes for nucleoside phosphates and their application to the determination of adenylyl cyclase activity, *10th Conference on Methods and Applications of Fluorescence: Spectroscopy, Imaging and Probes*, Salzburg, Austria

## Eidesstattliche Erklärung

Ich erkläre hiermit an Eides statt, dass ich die vorliegende Arbeit ohne unzulässige Hilfe Dritter und ohne Benutzung anderer als der angegebenen Hilfsmittel angefertigt habe; die aus anderen Quellen direkt oder indirekt übernommenen Daten und Konzepte sind unter Angabe des Literaturzitats gekennzeichnet. Weitere Personen waren an der inhaltlich materiellen Herstellung der vorliegenden Arbeit nicht beteiligt. Insbesondere habe ich hierfür nicht die entgeltliche Hilfe eines Promotionsberaters oder anderer Personen in Anspruch genommen. Niemand hat von mir weder unmittelbar noch mittelbar geldwerte Leistungen für Arbeiten erhalten, die im Zusammenhang mit dem Inhalt der vorgelegten Dissertation stehen. Die Arbeit wurde bisher weder im In- noch im Ausland in gleicher oder ähnlicher Form einer anderen Prüfungsbehörde vorgelegt.

Hannover, den \_\_\_\_\_

\_\_\_\_\_  
Corinna Spangler